

Aus der Medizinischen Klinik und Poliklinik IV

Klinik der Universität München

Direktor: Prof. Dr. med. Martin Reincke

**Differential roles of HMGB1 in myeloid cells versus tubular epithelial cells in  
the healthy or postischemic kidney**

Dissertation

zum Erwerb des Doktorgrades der Humanbiologie

an der Medizinischen Fakultät der

Ludwig-Maximilians-Universität zu München

vorgelegt von

**Zhibo Zhao**

Aus Datong, China

2022

**Mit Genehmigung der Medizinischen Fakultät  
der Universität München**

Berichterstatter: Prof. Dr. med. Hans-Joachim Anders

Mitberichterstatter: PD Dr. Gerald Bastian Schulz

Mitberichterstatter: Prof. Dr. Peter Weyrich

Dekan: Prof. Dr. med. Thomas Gudermann

Tag der mündlichen Prüfung: 14.07.2022

**TABLE OF CONTENTS**

Declaration of academic honesty.....	vi
Zusammenfassung.....	vii
Summary.....	IX
1 Introduction.....	1
1.1 Acute kidney injury and chronic kidney disease.....	1
1.2 Acute tubular necrosis.....	4
1.2.1 Oxidative stress.....	4
1.2.2 Damage-associated molecular patterns.....	5
1.2.3 Innate and adaptive immune response in acute tubular necrosis.....	7
1.2.4 Tissue regeneration.....	9
1.2.5 Pharmacologic treatment for acute kidney injury.....	9
1.3 High mobility group box 1.....	10
1.3.1 Structure of high mobility group box 1.....	10
1.3.2 HMGB1 as a damage-associated molecular pattern.....	11
1.3.3 HMGB1 and tissue regeneration.....	12
1.3.4 HMGB1 and gene transcription.....	13
1.3.5 HMGB1 as a therapeutic target.....	14
1.4 HMGB1 in kidney parenchymal cells.....	15
1.5 HMGB1 in myeloid cell-derived cells.....	16
2 Hypotheses.....	19
3 Material and Methods.....	20
3.1 Reagents.....	20
3.2 Instruments.....	22
3.3 Transgenic mice.....	23
3.4 Animal studies.....	24
3.5 Unilateral ischemia-reperfusion surgery.....	25
3.6 Experimental design of animal studies.....	26
3.7 Blood sampling and creatinine measurement.....	27
3.8 Measurement of glomerular filtration rate.....	28
3.9 Immunohistochemistry.....	28
3.10 Periodic acid Schiff and Sirius red staining.....	29
3.11 Immunofluorescence.....	29
3.12 RNA isolation and quantitative Real-time PCR and endpoint PCR.....	30
3.12.1 Total RNA isolation.....	30
3.12.2 RNA reverse transcription.....	30

3.12.3	Quantitative Real-time PCR .....	31
3.12.4	Oligonucleotide primers used for endpoint PCR and quantitative RT-PCR .....	31
3.12.5	Endpoint PCR for LysMCre and HMGB1 transgene.....	33
3.12.6	Pax8rtTA,TetOCre genotyping .....	35
3.13	Bone marrow mononuclear cell isolation and cell culture .....	35
3.14	Renal primary murine tubule isolation and tubular cell culture .....	36
3.15	Primary human kidney cell culture .....	36
3.16	Preparation of kidney mononuclear cells for flow cytometry .....	36
3.17	Preparation of spleen B cells and T cells .....	38
3.18	Protein isolation and Western blot .....	38
3.19	HMGB1 Elisa kits .....	39
3.20	Lactate dehydrogenase cell death assay and cell viability assay.....	39
3.21	Time-lapse imaging.....	39
3.22	Phagocytosis of monocyte-derived macrophages.....	40
3.23	Statistics.....	40
4	Results.....	41
4.1	HMGB1 in myeloid cells mitigates postischemic kidney injury .....	41
4.1.1	Selective HMGB1 deletion in myeloid cells.....	41
4.1.2	Myeloid cell-derived HMGB1 attenuates acute kidney injury .....	43
4.1.3	Myeloid cell-derived HMGB1 protects resident dendritic cell from death .....	45
4.1.4	HMGB1 in myeloid cells determines the phenotype of infiltrating dendritic cells .....	47
4.1.5	HMGB1 in myeloid cells ameliorates AKI-CKD transition .....	50
4.2	HMGB1 in tubular epithelial cells contributes to postischemic kidney injury .....	53
4.2.1	Ablation of HMGB1 in Pax8-positive tubular cells.....	53
4.2.2	Nuclear HMGB1 in Pax8-positive tubular cells has no substantial effect on postischemic acute kidney injury.....	54
4.2.3	HMGB1 in Pax8-positive tubular cells contributes to AKI-CKD transition .....	57
4.2.4	Endogenous HMGB1 in Pax8-positive tubular cells as a late mediator contributes to tubular cell damage .....	60
4.3	Targeting HMGB1 with inhibitors attenuates kidney injury in postischemic kidneys .....	62
4.3.1	Preemptive HMGB1 blockage with glycyrrhizic acid or ethyl pyruvate attenuates postischemic acute kidney injury .....	63



4.3.2	Preemptive treatment with HMGB1 inhibitors attenuates chronic kidney disease in postischemic kidneys .....	66
4.3.3	Delayed treatment of HMGB1 inhibitors still contributes to tissue healing in the recovery phase after ischemia .....	69
5	Discussion .....	72
5.1	Myeloid cell-derived HMGB1 attenuates kidney injury in renal IRI .....	72
5.2	Tubular cell-derived HMGB1 contributes to kidney injury .....	74
5.3	Targeting HMGB1 as a danger signal protects against tissue injury .....	75
5.4	HMGB1 location and function .....	76
6	References .....	82
7	Acknowledgement .....	96

### **Declaration of academic honesty**

I hereby declare that all of the present work embodied in this thesis was carried out by me from 10/2017 until 07/2021 under the supervision of Prof. Dr. Hans Joachim Anders, Nephrologisches Zentrum, Medizinische Klinik und Poliklinik IV, Innenstadt Klinikum der Universität München. This work has not been submitted in part or full to any other university or institute for any degree or diploma.

Part of the work has been accepted as an abstract at the International Society of Nephrology (ISN) World Congress of Nephrology 2021.

Part of the work has been accepted as an abstract at the European Renal Association-European Dialysis and Transplant Association (ERA-EDTA) Congress 2021.

Date: 14.07.2022

Signature:

Place: Munich, Germany

Zhibo Zhao

### Zusammenfassung

HMGB1 als Damage-Associated Molecular Pattern (DAMP), das von nekrotischen Zellen und aktivierten Immunzellen freigesetzt wird, löst die Infiltration von Immunzellen aus und trägt zur Nierenschädigung in postischämischen Nieren bei. Das Targeting von HMGB1 mit zellspezifischem HMGB1-Mangel oder Antagonisten könnte bei postischämischen Nieren vor Nierenschäden schützen. Hier habe ich zwei transgene Mäuselinien etabliert: MLys-HMGB1-Mäuse mit HMGB1-Mangel in myeloischen Zellen und Pax8-HMGB1-Mäuse mit induzierbarem HMGB1-Mangel in Pax8-positiven Tubuluszellen. Um zu testen, ob HMGB1 in myeloischen Zellen und Tubuluszellen eine Nierenschädigung fördert, habe ich die Wirkung eines HMGB1-Mangels in myeloischen Zellen oder Pax8-positiven Tubuluszellen auf akute Nierenschädigung (AKI) und das Fortschreiten einer chronischen Nierenschädigung (CKD) als Folge einer einseitigen renalen Ischämie-Reperfusionsschädigung untersucht (IRI). Außerdem untersuchte ich die Wirkung von HMGB1-Antagonisten auf den renalen Zellschutz bei postischämischer Nierenschädigung.

Wir hatten die Hypothese aufgestellt, dass HMGB1 aus Myeloidzellen die Nierenschädigung in postischämischen Nieren verschlimmert. Die Deletion von endogenem HMGB1 in myeloischen Zellen reduziert die Entzündungsreaktion in postischämischen Nieren. Ich beobachtete jedoch eine verschlimmerte AKI bei MLys-HMGB1-Knockout-Mäusen, die mit weniger renalen residenten DCs und mehr infiltrierenden Monozyten-abgeleiteten Makrophagen während der renalen IRI verbunden war. Der verstärkte Zelltod und die Nierenschädigung trugen zur Rekrutierung peripherer Leukozyten bei, was bei AKI weitere Zellschäden und Gewebeschädigungen hervorrief. Darüber hinaus modulierte endogenes HMGB1 in myeloischen Zellen den Phänotypen infiltrierender dendritischer Zellen und Makrophagen, was zur Heilung des Nierengewebes in der Erholungsphase beitragen kann. Somit verbesserte endogenes HMGB1 in myeloischen Zellen die AKI und verhinderte eine postischämische CKD.

Wir hatten die Hypothese aufgestellt, dass nukleäres HMGB1 in Pax8-positiven Tubuluszellen zu Tubulusschäden bei Ischämie beiträgt. Meine Daten zeigten, dass tubulär abgeleitetes endogenes HMGB1 als später Mediator zur Nierenschädigung in postischämischen Nieren beitrug. HMGB1-Mangel erleichtert das Fortschreiten von Fibrose und CKD, aber nicht von AKI in postischämischen Nieren. HMGB1-Knockout-

Tubuluszellen zeigten zu einem späten Zeitpunkt eine abgeschwächte Wasserstoffperoxid (H<sub>2</sub>O<sub>2</sub>)-induzierten Zellschädigung. Somit trug nukleäres HMGB1 in Tubuluszellen als später Mediator zum Übergang von AKI zu CKD in postischämischen Nieren bei.

Freigesetztes HMGB1 wirkt wahrscheinlich als Gefahrensignal bei Nierenschäden in postischämischen Nieren. Die HMGB1-Antagonisten mit Glycyrrhizinsäure oder Ethylpyruvat wurden verwendet, um die extrazelluläre HMGB1-Freisetzung während einer postischämischen Nierenschädigung zu blockieren. Die HMGB1-Inhibitoren senkten die Plasmaspiegel von HMGB1 und Kreatinin und verbesserten glomerulären Filtrationsrate (GFR) nach AKI und den Übergang zur CKD bei postischämischen Nieren. HMGB1-Inhibitoren können in der Erholungsphase an der Gewebeheilung teilnehmen. HMGB1-Antagonisten verbesserten in vitro den H<sub>2</sub>O<sub>2</sub>-induzierten Zelltod sowohl in primären murinen tubulären Zellen als auch in kultivierten humanen primären Nierenzellen. Somit könnte HMGB1 als therapeutisches Ziel dienen, um Nierenschäden in postischämischen Nieren zu verhindern.

Zusammenfassend lässt sich sagen, dass freigesetztes HMGB1 an einer Nierenschädigung bei postischämischen Nieren beteiligt war, was ein therapeutisches Ziel zum Schutz vor Nierenschäden bei renaler IRI darstellen könnte. Der Beitrag von endogenem HMGB1 zur Nierenschädigung hängt jedoch von der Zelllinie ab. Von Myeloidzellen abgeleitetes HMGB1 verbessert die Nierenschädigung, und von den Nierentubuli abgeleitetes HMGB1 ist an der Gewebeschädigung bei renaler IRI beteiligt. Somit hängt die Rolle von HMGB1 vom Ort und der Zelllinie ab, was die schädliche oder vorteilhafte Wirkung auf eine Nierenschädigung bestimmen kann.

### Summary

HMGB1 as a damage-associated molecular pattern (DAMP) released from necrotic cells and activated immune cells triggers the infiltration of immune cells and contributes to kidney injury in postischemic kidneys. Targeting HMGB1 with cell-specific HMGB1 deficiency or antagonists may protect against kidney injury in postischemic kidneys. Here I established two transgenic mice lines: MLys-HMGB1 mice with HMGB1 deficiency in myeloid cells and Pax8-HMGB1 mice with inducible HMGB1 deficiency in Pax8-positive tubular cells. To test if HMGB1 promotes kidney injury, I studied the effect of HMGB1 deficiency in myeloid cells or Pax8-positive tubular cells on acute kidney injury (AKI) and progression of chronic kidney injury (CKD) as a consequence of renal unilateral ischemia-reperfusion injury (IRI). In addition, I investigated the effect of HMGB1 antagonists on renal cellular protection in postischemic kidney injury.

We had hypothesized that myeloid cell-derived HMGB1 aggravates kidney injury in postischemic kidneys. Deletion of endogenous HMGB1 in myeloid cells ameliorates the inflammatory response in postischemic kidneys. However, I observed aggravated AKI in MLys-HMGB1 knockout mice, which was associated with less renal resident DCs and more infiltrating monocyte-derived macrophages during renal IRI. The aggravated cell death and kidney injury contributed to the recruitment of peripheral leukocytes, which further provoked more cellular damage and tissue injury in AKI. In addition, endogenous HMGB1 in myeloid cells modulated the phenotype of infiltrating dendritic cells and macrophages, which may contribute to renal tissue healing in the recovery phase. Thus, endogenous HMGB1 in myeloid cells ameliorated AKI and prevented postischemic CKD.

We had hypothesized that nuclear HMGB1 in Pax8-positive tubular cells contributes to tubular damage under ischemia. My data showed that tubular-derived endogenous HMGB1 as a late mediator contributed to kidney injury in postischemic kidneys. HMGB1 deficiency ameliorated the progression of fibrosis and CKD but not AKI in postischemic kidneys. HMGB1 knockout tubular cells showed attenuated hydrogen peroxide (H<sub>2</sub>O<sub>2</sub>)-induced cellular damage at a late time point. Thus, nuclear HMGB1 in tubular cells as a late mediator contributed to the transition of AKI to CKD in postischemic kidneys.

Released HMGB1 likely acts as a danger signal during kidney injury in postischemic kidneys. I administrated HMGB1 antagonists with glycyrrhizic acid or ethyl pyruvate to block extracellular HMGB1 release during postischemic kidney injury. My data showed HMGB1 inhibitors decreased plasma levels of HMGB1 and creatinine with better outcomes of glomerular filtration rate (GFR) in AKI, and prevent the transition of AKI to CKD in postischemic kidneys. HMGB1 inhibitors may participate tissue healing in the recovery phase. HMGB1 antagonists ameliorated H<sub>2</sub>O<sub>2</sub>-induced cell death in both primary murine tubular cells and cultured human primary renal cells *in vitro*. Thus, HMGB1 could serve as a therapeutic target to prevent kidney injury in postischemic kidneys.

In conclusion, released HMGB1 participated in kidney injury in postischemic kidneys, which may represent a therapeutic target to protect against kidney injury in renal IRI. However, the contribution of endogenous HMGB1 to kidney injury depends on cell lineage. Myeloid cell-derived HMGB1 ameliorates kidney injury, and renal tubular-derived HMGB1 participates in tissue injury in renal IRI. Thus, the role of HMGB1 depends on the location and cell lineage, which may determine the detrimental or beneficial effect to kidney injury.

## **1 Introduction**

### **1.1 Acute kidney injury and chronic kidney disease**

The functional unit of the kidney is the nephron. The nephron is constituted of a renal corpuscle and a renal tubule. The renal corpuscle contains a glomerulus and an encompassing Bowman's capsule (Fig 1). The renal tubule extends from the capsule, followed by the proximal tubule, loop of Henle, distal tubule, and collecting duct system. Every nephron segment is composed of cells that are suitable to perform specific transport functions. The nephrons are essential in regulating body volumes and fluid osmolality, acid-base balance, and the electrolyte balance. In addition, the nephrons produce and excrete metabolic products such as urea, uric acid, creatinine, and products of hemoglobin metabolism and hormones.

More than 850 million people suffer from kidney disease worldwide, a number increasing every year. Kidney disease covers a broad spectrum of diseases with diverse causes, from acute kidney injury (AKI) to chronic kidney disease (CKD). AKI, also named acute kidney failure, is defined by a sudden loss of kidney function within a few hours or a few days. Triggers of AKI include dehydration, sepsis, nephrotoxic drugs, especially following cardiovascular surgery, and contrast agents. According to the Kidney Disease Improving Global Outcomes (KDIGO) Clinical Practice Guideline, AKI is defined as an increase of creatinine by 0.3 mg/dl or  $\geq 26 \mu\text{mol/l}$  within 48h, and/or rise of creatinine by 1.5 times from baseline within 7 days, and/or decrease of urine output  $< 0.5 \text{ ml/kg/h}$  for more than 6 h [1]. The measurements of creatinine and increased blood urea nitrogen (BUN) indicate the decline of renal function. Another measurement of kidney function is glomerular filtration rate (GFR). In clinical practice, creatinine clearance or estimated creatinine clearance based on serum creatinine level is applied to measure GFR. The decline of GFR results in the retention of nitrogenous wastes and an increase of creatinine and BUN [2]. The filtration and excretion of nitrogenous waste products serve as crucial factors for kidney function. Impaired filtration and excessive production of nitrogenous waste products define AKI. AKI is pathologically characterized by tubular cell damage, inflammation, and vascular dysfunction [3]. In clinical practice, AKI is not easily detectable with no apparent early symptoms, which may be a principal cause to prevent further CKD and deaths. CKD is described as abnormalities of kidney function and loss of nephrons, which presents for more than 3 months with reduction of estimated glomerular filtration rate ( $\text{eGFR} <$

60 ml/min per 1.73 m<sup>2</sup>), increased urine albumin excretion ( $\geq 30$  mg/g or 3 ng/mmol creatinine), or both [4]. Pathological abnormalities of the kidney lead to decreased GFR. The kidney biopsy of pathologically evidenced CKD is characterized by glomerular sclerosis, tubular atrophy, and interstitial fibrosis [5]. The pathologic damage of CKD results in irreversible loss of nephrons. The progressive loss of nephrons in CKD ultimately leads to end-stage renal disease (ESRD), which demands kidney transplantation therapy for survival.



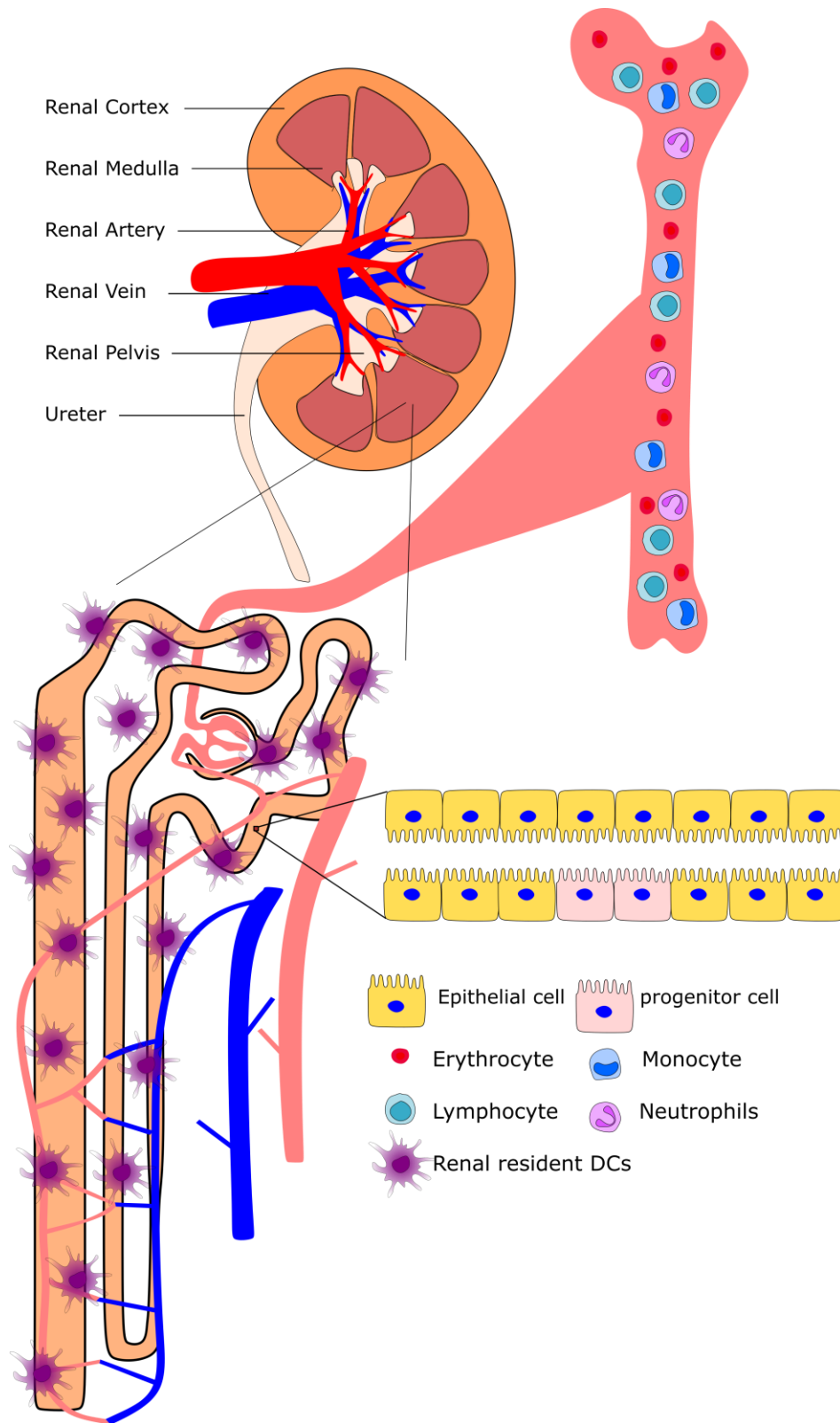


**Fig 1. Anatomy of human kidney.** The nephron is the kidney's central structural and functional unit consisting of a corpuscle and a renal tubule. The tubule prolongs from the capsule, surrounded by the peritubular capillaries, where the primary filtrate from peripheral blood flows with filtration, absorption, secretion, and excretion. The renal resident DCs localize in the renal nephrons, representing antigen-presenting, phagocytic, and innate immune response in renal physiological and pathological conditions.

### 1.2 Acute tubular necrosis

Acute tubular necrosis (ATN) describes the death of tubular cells that form the tubules of the kidneys. ATN is a common cause of AKI and includes postischemic AKI, cisplatin nephrotoxicity, contrast-induced renal dysfunction, and delayed graft function [6-9]. ATN is related with oxidative stress, the release of damage-associated molecular patterns (DAMPs) and an immune response. Mitochondrial dysfunction promotes oxidative stress, in turn, oxidative damage elicits mitochondrial permeability transition, which aggravates in ATN [10]. Oxidative stress also promotes the recruitment of immune cells [11]. In addition, DAMPs, passively released from necrotic cells, activate pattern recognition receptors (PRRs) on infiltrated immune cells and tissue resident cells, which triggers the pro-inflammatory response and accelerates ATN [12, 13].

#### 1.2.1 Oxidative stress

Oxidative stress describes the imbalance between the generation of reactive oxygen species (ROS) and the detoxification processes that counteract the constant generation of ROS. The excessive of oxidative stress may contribute to ROS-induced cell death. Mitochondria can produce a low level of ROS under physiological conditions, but ROS accumulate under pathological conditions [14]. The generated ROS disrupts mitochondrial function during renal ATN, which results in kidney cell injury [11, 15]. Thus, ROS are considered a critical factor in the progression of cellular injury in both vascular endothelial cells and renal tubular epithelial cells [16].

Renal ischemia-reperfusion injury (IRI) involves temporary ischemia following reperfusion of blood and oxygen. Ischemia occurs from the sudden blockage of the blood flow from the peripheral circulation to the kidney. Kidney IRI is inevitably accompanied with injury and death of renal tubular epithelial cells under hypoxia-induced oxidative stress [17]. Renal IRI changes mitochondrial oxidative phosphorylation and ATP depletion, resulting in the production of excessive ROS [17]. ROS mediates tissue parenchymal cell death. The proximal tubules are more sensitive to oxidative stress under ischemia [18]. It takes immense consumption of oxygen to produce ATP for supporting the active transport in tubular epithelial cells. Also, proximal tubules cannot synthesize glutathione for producing antioxidants to protect against ROS [19, 20]. ROS activation results in apoptotic cell death by activating of caspases pathway [21]. The accumulation of ROS also induces ATN with the

association of poly(ADP-ribose) polymerase (PARP-1) [22, 23]. Another source of ROS comes from the infiltrated leukocytes in renal inflammatory diseases. The released pro-inflammatory chemokines and cytokines from parenchymal and endothelial cells trigger the recruitment of circulation leukocytes, which prolongs oxidative stress upon renal IRI, resulting in kidney cell apoptosis and necrosis [24].

### **1.2.2 Damage-associated molecular patterns**

DAMPs encompass a group of intracellular molecules released from necrotic cells [25]. The released DAMPs as danger signals activate PRRs, which are expressed on leukocytes and all renal cells [26]. Certain DAMPs participate in kidney injury via PRRs-induced regulated necrosis, including necroptosis, necrosis, and pyroptosis (Fig 2). For example, histones elicit toxic effects on renal parenchymal cells and vascular endothelial cells via PRRs [27, 28]. In addition, DAMPs promote the activation and infiltration of immune cells. The activated immune cells contribute to the release of DAMPs through inflammasome-induced pyroptosis [26]. The DAMPs released from necrotic tubular cells and activated immune cells further contribute to kidney inflammation. Tissue inflammation induced by DAMPs triggers additional kidney cell death such as necroptosis [29]. The autoamplification loop of cell necrosis and inflammatory response referred to as necroinflammation, which amplifies local inflammation and tissue injury, eventually leads to organ failure [26].

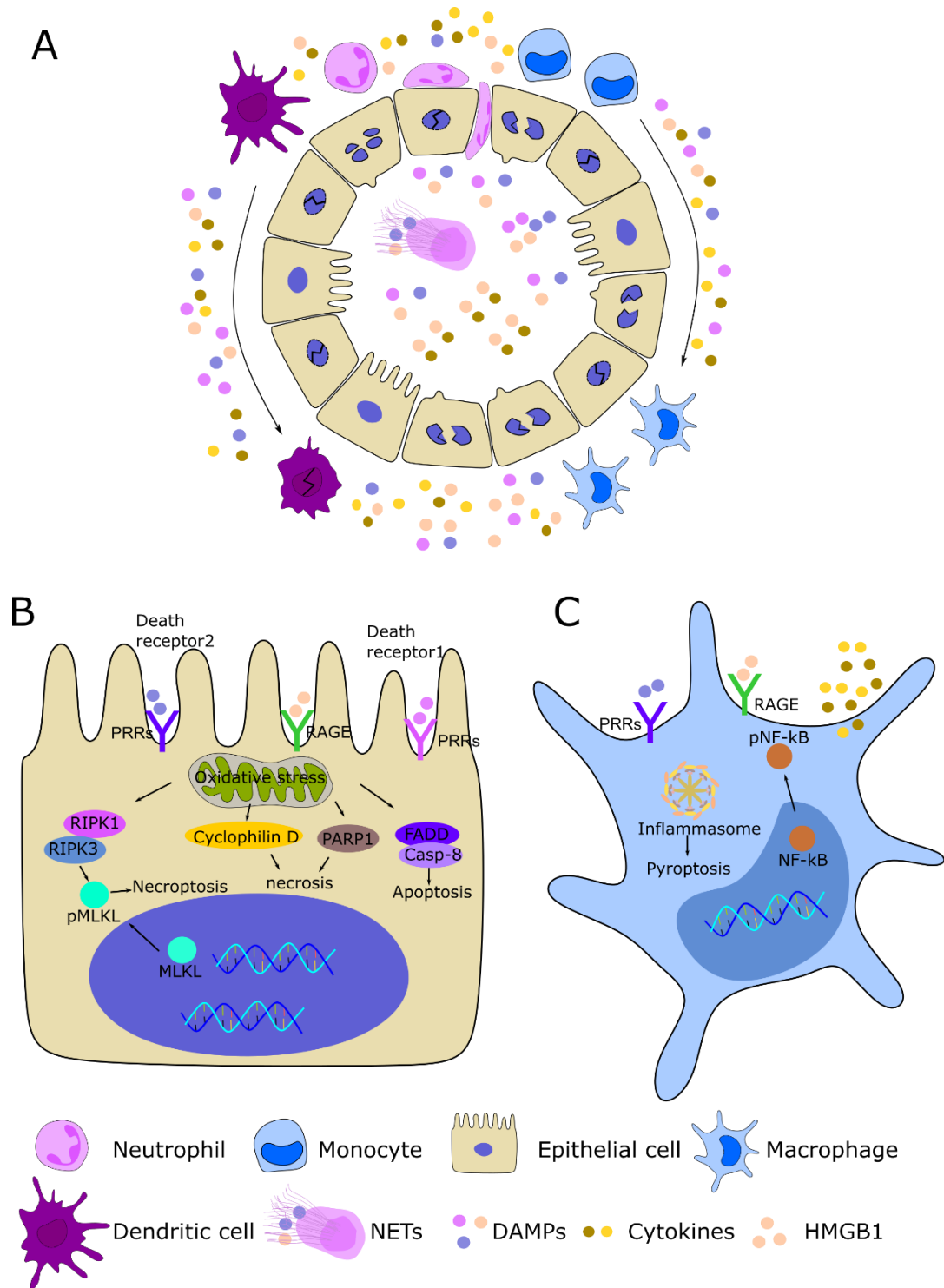


**Fig 2. Damage-associated molecular patterns in the cellular signaling pathway.** (A) Renal resident tubular epithelial cells undergo regulated necrosis with the release of DAMPs to the extracellular space. DAMPs trigger the migration of neutrophils and monocytes/macrophages. (B) DAMPs interact with different receptors to trigger RIPK1/MLKL-mediated necroptosis [30, 31], cyclophilin D-mediated [3, 32] or PARP1-mediated necrosis [23, 33], and caspase-induced apoptosis [34]. (C) DAMPs promote inflammasome activation and subsequent pyroptosis of macrophages with the release of cytokines acting as alarmins.

### **1.2.3 Innate and adaptive immune response in acute tubular necrosis**

ATN promotes inflammatory response with the involvement of immune cells, including resident mononuclear phagocytes such as resident DCs, and the influx of peripheral immune cells such as neutrophils, monocytes, macrophages, dendritic cells, and lymphocytes [35]. The progressing of infiltrated immune cells contributes to different phases of kidney injury, including neutrophil-driven tissue injury in the early injury phase, pro-inflammatory macrophage-induced kidney dysfunction in the late injury phase, anti-inflammatory-mediated functional recovery in the recovery phase, and immunity-supported wound healing as a long-lasting response [36].

Resident DCs do not derive from monocytes in steady state but originate from classical DCs (pre-cDCs) and plasmacytoid DCs (PDC). The derivation from the lineage of hematopoietic stem cells (HSCs) are replaced continually from extrarenal DC precursors [37-39]. The common precursor (MPD) in bone marrow differentiates into common DC precursor (CDP) [39]. Pre-classical DCs (pre-cDCs) and plasmacytoid DCs (PDC) derive from CDP traffic to lymphoid and non-lymphoid organs to produce resident DCs [40]. Thus, kidney resident DCs are part of the myeloid lineage. Data showed that CX<sub>3</sub>CR1<sup>+</sup> DCs co-express the markers CD11c, high major histocompatibility complex class II (MHCII), F4/80, and FcR, which comprise the majority of the mononuclear phagocyte system in the healthy kidney [41].

Kidney resident DCs establish an extensive network in the entire kidney. Kidney resident DCs can mount the vital immune defense against infections in initiating and propagating inflammation for host defense [42]. In addition, kidney resident DCs participate in tissue regeneration and fibrogenesis in CKD [42]. Renal DCs respond to the sterile danger signals with antigen presentation and phagocytosis to participate in the clearance of DAMPs. Meanwhile, kidney DCs recruit peripheral immune cells to enhance inflammatory responses in the early injury phase [43]. In the recovery phase, resident DCs modulate the phenotype switch from M1 (pro-inflammatory) macrophages to M2 (anti-inflammatory) macrophages, which promote renal fibrogenesis and tubule regeneration [44, 45]. For example, renal DCs mediate the Wnt signaling pathway and TLR4-induced IL22 accelerate tubule regeneration in the recovery phase [45, 46].

Neutrophils are the first immune response to inflammatory pathologies. Upon pathogen infection, neutrophils expel chromatin into the extracellular space with nuclear, granular, and cytoplasmic proteins referred to as neutrophil extracellular traps (NETs). NET formation serves as a host defense of pathogen fixation and killing but also occurs in sterile inflammation [47]. For example, neutrophils release NETs during regulated necrosis [28]. Neutrophils rapidly respond to AKI and are the principal inflammatory mediators of the innate immune response in the early injury phase [48]. Circulating neutrophils attach to the kidney endothelium and initiate inflammation-mediated tissue damage in the early reperfusion phase. Subsequently, DAMPs released from the damaged tissue cells contribute to the formation NETs [28]. The localization of neutrophils in injured kidneys and NET formation result in kidney inflammation and amplify kidney injury and even contribute to remote organ damage [28].

Macrophages and peripheral DCs follow after immigration of neutrophils, which is mediated by interaction of CCR2 and CX<sub>3</sub>CR1 with their respective chemokine ligands [49]. During ATN, peripheral monocytes and common progenitor cells differentiate to different types of macrophages, such as M1 macrophages and M2 macrophages. The polarization of macrophages from M1-like to M2-like phenotypes depends from changes of local inflammatory micromilieu to an anti-inflammatory response [36]. Heterogeneous phenotypes of macrophages contribute to the injured kidney at different reperfusion phases. The pro-inflammatory macrophages produce cytokines and chemokines, which induce tissue cell damage in the early injury phase [50]. The anti-inflammatory macrophages elicit the anti-inflammatory response with IL-4 and IL-10 [51], which are related to tissue healing and repair in the recovery phase.

Peripheral DCs are crucial motivators of the innate immune response and orchestrate inflammation in ATN. Infiltration of circulating DCs has a deleterious effect on ischemia AKI. Deletion of peripheral DCs reduces the production of inflammatory cytokines, immune cell infiltration, and tissue cell death in renal IRI [52]. The phenotypes change from a pro-inflammation to an anti-inflammation, which modulates peripheral DCs function at the recovery phase. For example, the anti-inflammatory DCs start to increase the production of IL10 along the co-expression of F4/80 and CD11c. Deletion of CD11c<sup>+</sup>F4/80<sup>+</sup> DCs impairs the recovery of kidney function. Adoptive transfer of extra CD11c<sup>+</sup> cells reverses this process [44].

T cell migration is essential both in the early injury phase and in the recovery phase in kidney IRI. The recruitment of CD4<sup>+</sup> T cells has been observed in postischemic kidneys at the early phase [53]. However, the ablation of T cells and B cells did not protect from postischemic kidney injury. In turn, adoptive transfer of B cells and T cells protects from kidney injury in renal IRI [54].

### **1.2.4 Tissue regeneration**

DAMPs contribute to re-epithelialization and extracellular matrix remodeling. DAMPs can accelerate tubular progenitor cell regeneration [25]. For example, TLR2-agonistic DAMPs promote clonal expansion and differentiation of tubular progenitor cells [55, 56]. In addition, TLR4-agonistic DAMPs mediate activation and phenotypes changing of renal resident DCs with the release of IL-22, which accelerates tubule re-epithelialization [46]. Blockage of TLR4 in the recovery phase reduces tubule regeneration [46]. Besides, DAMPs trigger tubular epithelial cell proliferation and the secretion of extracellular matrix, which is involved in the TGF- $\beta$  receptor-dependent mesenchymal transition of renal epithelial cells [25].

### **1.2.5 Pharmacologic treatment for acute kidney injury**

Many agents have been employed for the treatment of AKI. Oxidative stress is one cause of AKI. Oxidative stress of kidney endothelial and epithelial cells under ischemia contributes to cell death and tissue injury. Damaged tissue elicits accumulation of oxidative stress, which promotes mitochondrial dysfunction and ATP depletion in AKI [57]. Antioxidant agents have therapeutic potential to protect against AKI. For example, an antioxidant to renal proximal tubular cells prevented renal tubular damage and the migration of leukocytes [58].

DAMPs released from necrotic cells promote the infiltration of immune cells and regulated necrosis in AKI. Circulation DAMPs promote neutrophil-mediated inflammatory response and tissue damage [59]. Targeting DAMPs as danger signals may ameliorate leukocyte infiltration-associated inflammatory response and tissue injury. For instance, histones as one of the cytotoxic DAMPs contribute to the NET formation and ATN. Pretreatment with anti-histone IgG prevents ischemia-induced NET formation and kidney failure [28]. Targeting DAMPs as danger signals may prevent the propagation of oxidative stress-induced regulated cell death and protect from kidney injury in AKI.

Inflammation is one of the therapeutic targets for AKI. Anti-inflammatory agents and inhibitors of leukocyte infiltration can suppress the inflammatory response and attenuate the consequences of AKI [60]. For example, pro-inflammatory cytokines tumor necrosis factor (TNF $\alpha$ ) and interleukin 6 (IL6) contribute to the kidney dysfunction in renal IRI. Treatment with an anti-TNF $\alpha$  antibody or an anti-IL6 antibody reduced inflammation-mediated kidney dysfunction caused by ischemia [61, 62]. Also, cell adhesion molecules such as P-selectin and intracellular adhesion molecule-1 (ICAM-1) prompt the recruitment of leukocytes and inflammatory response. Administration of P-selectin inhibitor prevents kidney injury in renal IRI. Treatment of anti-ICAM-1 prior to ischemia limits inflammation-induced renal injury [63, 64].

### **1.3 High mobility group box 1**

Extracellular high mobility group box 1 (HMGB1) acts as a DAMP and contributes to the inflammatory response and kidney injury in AKI. Regulated necrosis promotes the release of HMGB1 into extracellular space [65, 66]. Targeting HMGB1 with inhibitors or cell-specific HMGB1 deficiency may have a protective effect on kidney injury. Here I introduce the role of HMGB1 to my topic.

#### **1.3.1 Structure of high mobility group box 1**

HMGB1 belongs to HMGB proteins. It is encoded by the HMGB1 gene, and localizes to chromosome 13 in humans and chromosome 5 in mice. HMGB1, a highly abundant protein, which bind to chromatin, not only to DNA minor grooves to bend DNA but also to distorted DNA to unwind nucleosomes [67]. Vertebrate HMGB1 includes 216 amino acids with tandem HMG-box domain (box A, box B) and an acidic C-terminal tail (Fig 3). HMG-boxes are identified by their abundance, function, and DNA specificity. HMG-box A (amino acid 7 to 78) interacts with DNA to bend and distort DNA helix. HMG-box B (amino acid 95 to 163) is responsible for combination with HMGB1 receptors, including Toll-like receptors (TLRs) and advanced glycation end-products (RAGE) [68]. Both HMG-box A and HMG-box B contribute to cytokine release in inflammatory diseases [69].



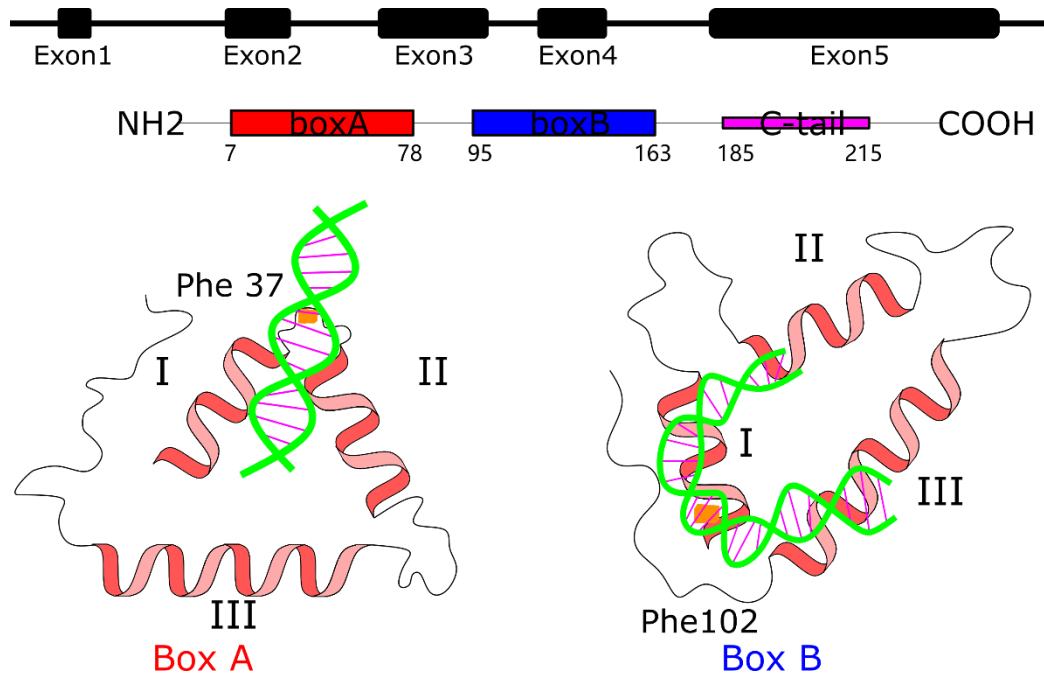


**Fig 3. The structure of murine HMGB1** (Original image from M. Štros [70] with modification). Murine HMGB1 protein has 216 amino acids, including Box A (red) domain and Box B (blue) domain, and an acidic C tail of amino acids. Each box of HMGB1 consists of three  $\alpha$ -helices. A hydrophobic wedge of residues phe37 intercalate into Box A, while residues phe102 locate at Box B. Phe 37 and phe 102 can bind to linker DNA to bend and kink DNA. The acidic C tail of HMGB1 is composed of consecutive runs of Glu/Asp residues. There are two NLS (nuclear localization sequences) located at Box A (aa27-aa43) and acidic C terminal (aa178-aa184), respectively, which contributes to the localization of HMGB1 in the nucleus.

### 1.3.2 HMGB1 as a damage-associated molecular pattern

HMGB1 as a danger signal contributes to necroinflammation, because HMGB1 released from necrotic tissue cells triggers the migration of immune cells. Also, activated immune cells release HMGB1 to the extracellular space, which promotes the inflammatory response. HMGB1 released from necrotic tissue cells and activated immune cells should both aggravate parenchymal cell damage and tissue injury [71, 72].

So far, several mouse models have been elucidated the role of HMGB1 in acute inflammatory disease. IRI is one of the most studied mice models to illuminate the function of HMGB1 in activating the innate immune response. Renal IRI promotes an elevated serum protein level of HMGB1. The increased HMGB1 promoted the recruitment of neutrophils and monocytes to the injured kidney at the early injury phase [73]. For example, HMGB1 as a DAMP contributes to neutrophils infiltration and amplified NET formation [74, 75]. In addition, HMGB1 as a danger signal contributes

to an inflammatory response by activating inflammasome-induced pyroptosis in both endothelial cells and activated macrophages [76, 77]. HMGB1 prompts the release of chemokines and cytokines from both activated immune cells and tissue parenchymal cells. For example, HMGB1 induces cytokine release from innate immune cells [78]. In addition, HMGB1 promotes the expression of adhesion molecules such as vascular cell adhesion protein 1 (VCAM-1), ICAM-1, cytokines, and the release of chemokines from endothelial cells via interacting with RAGE, resulting in the activity of the NF- $\kappa$ B signaling pathway, which is associated with the B-box of HMGB1 [79]. Administration of anti-HMGB1 antibody before or soon after renal IRI reduced the production of pro-inflammatory factors, such as TNF $\alpha$ , IL6, and MCP1 in mRNA level [80].

In addition to the role of HMGB1 in acute inflammatory disease, HMGB1 also mediates chronic inflammation. For example, HMGB1 involves in the pathogenesis of rheumatoid diseases. Serum HMGB1 level was elevated in rheumatoid arthritis patients [81]. The decreased anti-inflammation activation was linked to the elevated level of HMGB1 in patients with rheumatoid arthritis, which implies the extent of chronic inflammatory disease [82].

### **1.3.3 HMGB1 and tissue regeneration**

C-X-C chemokine receptor type 4 (CXCR4) is known as a multi-chemokines receptor, which links to CXCL12 chemotactic activity. Post-translational modification of reduced HMGB1 can coordinate the interaction with CXCL12, which function as a heterocomplex. HMGB1-CXCL12 complex can bind to CXCR4, which participates in tissue healing and regeneration via propagation of progenitor cells [83-85].

Receptor for advanced glycation end-products (RAGE) is referred to as a pattern recognition receptor, which was characterized as the first receptor of HMGB1 [86, 87]. Amino acids in C terminal of HMGB1 are responsible for RAGE binding. HMGB1 interacts with its receptors RAGE and CXCR4, which promotes the undifferentiated tissue cells and progenitor cells to do proliferation and regeneration [84]. Meanwhile, HMGB1 induces recruitment and proliferation of vessel-associated stem cells via interacting with its receptor RAGE, participating in tissue regeneration [88]. In addition, HMGB1 orchestrates tissue repair and healing by switching macrophages toward a

tissue-healing phenotype and activating the proliferation of progenitors and vascular stem cell migration [89].

### **1.3.4 HMGB1 and gene transcription**

Nuclear HMGB1 contributes to the bending of DNA to condensed chromatin, meanwhile unpacks DNA to modulate gene transcription and interaction with other proteins [70]. Normally, HMGB1 binds to the linker region of nucleosomal DNA to destabilize nucleosome structure [90], which promotes a shift of bending DNA to exposure the binding region of the nucleosome for binding with transcriptional factors. DNA bending and unwinding from HMGB1 provide the possibility for transcriptional factors to bind specific DNA sequences [70]. HMGB1 is associated with a bulk of regulators of transcriptional factors, including p53, Hox transcriptional factors, and steroid hormone receptors [91-93]. HMGB1 can modulate chromatin structural changes, which results in the nucleosome sliding, accompanied by detaching the histone H1 from the chromosome, promoting the DNA bending and activation of gene transcription in chromatin remodeling [70] (Fig 4). Data showed HMGB1 knockout elevates gene expression associated with glycolysis and lipid metabolic as well as downregulated genes response to hypoxia [94].

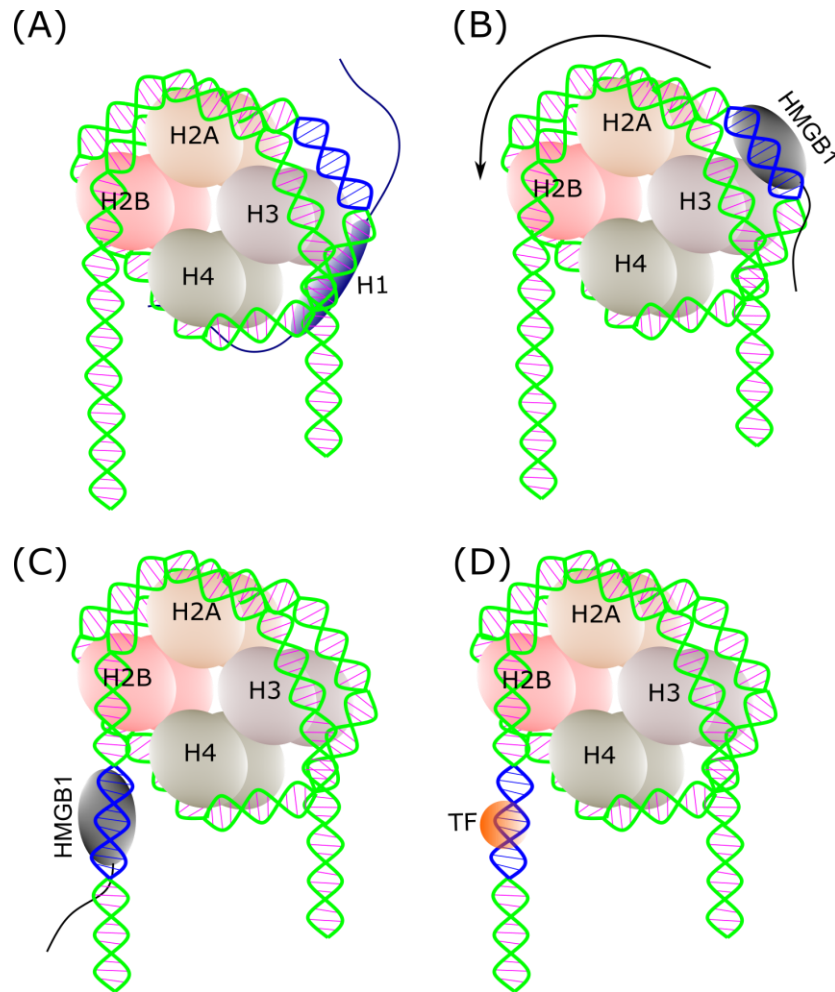


**Fig 4. HMGB1 regulates transcriptional factor expression.** (A) Nucleosome spiral around the histone octamer when histone H1 binds at the entry sites of the nucleosome. (B) HMGB1 can bind to the sequence-specific sites of the nucleosome. However, the binding of histone H1 and HMGB1 is mutually exclusive. Thus, HMGB1 binding to specific sequences replaces the binding of histone H1. The acidic C tail of HMGB1 facilitates the binding of histone H1 to the nucleosome. (C) HMGB1 binds at the nucleosome to bend or distort DNA, followed by the propagation of DNA around the histone octamer, resulting in the exposure of sequence-specific sites of the nucleosome. (D) Transcriptional factors access to the sequence-specific binding sites with the dissociation of HMGB1 from the nucleosome.

### 1.3.5 HMGB1 as a therapeutic target

HMGB1 as a late mediator in lethal bacterial endotoxin toxicity and septic patients showed a high serum level of HMGB1, considered to be a therapeutic target for investigation, identified firstly in 1999 [95]. SIRT1 interacts with HMGB1 at the deacetylated lysine sites, which prohibits the acetylation of HMGB1, subsequently suppressing the inflammatory response in sepsis-correlated acute kidney injury [96]. An anti-HMGB1 antibody attenuates glomerulonephritis and proteinuria in lupus-like disease mice [97]. In human patients, data showed that serum antibodies of systemic

lupus erythematosus patients were anti-HMGB1 positive compared with controls [98]. Researchers depicted a bulk of antagonists of HMGB1 as potential therapeutic agents for HMGB1-related diseases [99]. The application of HMGB1 antagonists on clinical trials represents a promising approach for HMGB1-associated renal pathological diseases.

### **1.4 HMGB1 in kidney parenchymal cells**

In renal IRI, the outer medulla of kidney nephron is more vulnerable to ischemia, endothelial cell dysfunction, and tubular epithelial cell damage in the S3 segment [100]. The tight junctions of endothelial cells are susceptible to ischemia [101, 102]. Ischemia induces renal endothelial cell damage. The damaged endothelial cells lose the integrity of their barrier function, which contributes to the infiltration of immune cells. In addition, tubular cells challenged with ischemia progress to regulated necrosis with the release of DAMPs to extracellular space. HMGB1 as a DAMP may trigger apoptosis and regulated cell death in parenchymal cells. For example, HMGB1 triggers neuronal cell death in a dose-dependent manner [103]. HMGB1 induces cell necrosis by a RIPK3-dependent manner in hepatocytes [104]. The regulated necrosis and apoptosis of renal tubular cells, which are recognized as pathological factors in AKI [3].

Oxidative stress plays a crucial role in the regulation of HMGB1 biology. Ischemic-induced oxidative stress boosts the activation and post-translational modification of HMGB1, resulting in modified-HMGB1 shuttling from nucleus to the cytoplasm even extracellular matrix, which contributes to inflammatory response and cellular damage [105]. For example, oxidized HMGB1 released to extracellular space promotes pro-inflammatory response in kidney diseases [106]. HMGB1 promotes tissue endothelial cell death and vascular inflammation by binding to RAGE in tissue IRI [107]. HMGB1 promotes the pro-inflammatory chemokines and cytokines expression such as TNF $\alpha$ , IL-8, monocyte chemotactic protein-1 (MCP-1) through interacting with the receptor of RAGE in human microvascular endothelium [108]. HMGB1 promotes tubular epithelial cell death with the upregulated release of cytokines and chemokines through the TLR4 pathway [73]. In tubulointerstitial cells, HMGB1 as an inflammatory mediator promotes the construction of profibrotic cytokines and epithelial-mesenchymal transition by the receptor of RAGE in kidney and lung fibrosis [109-111].

Non-conditional HMGB1 knockout mice die shortly after birth because of decreased glucocorticoid receptors and the inability to use glycogen [112, 113]. Both ablations of endogenous and exogenous HMGB1 in mice destroy preimplantation embryo development in mice [114]. However, data implied that specific HMGB1 ablation in the liver and heart did not affect autophagy and mitochondrial function in physiological conditions [115]. HMGB1 knockout in specific tissue cells has been applied on tissue disease models. Tissue-specific HMGB1 knockout mice show different phenotypes in various mice models. For example, HMGB1 deficiency in the pancreas renders the pancreas more vulnerable to acute pancreatitis due to nuclear catastrophe with more nucleosome release [116]. Hepatocyte-specific HMGB1 knockout mice exacerbate liver IRI with increased cell death because of greater DNA damage and decreased chromatin accessibility [117]. However, a conditional HMGB1 knockout in hepatocytes attenuates tissue injury by reducing neutrophils infiltration and inflammatory response in liver IRI [112]. In addition, down-regulation of nuclear HMGB1 by siRNA ameliorates tissue damage by reducing its extracellular release in liver IRI [118].

Tissue-specific nuclear HMGB1 knockout may result in DNA damage and nucleosome release under pathological conditions. Conditional and inducible knockout of HMGB1 in tissue-specific cell may maintain its functional role but decrease the release of extracellular HMGB1, which prevents HMGB1-induced pro-inflammatory response, resulting in the protective effect of tissue injury.

### **1.5 HMGB1 in myeloid cell-derived cells**

Myeloid cells originate from bone marrow progenitors derived from hematopoietic stem cells [119]. The differentiation of myeloid cells to different lineages is influenced by granulocyte-macrophage colony stimulating factor (GM-CSF), colony-stimulating factor 1 (CSF-1), and FMS-like related tyrosine kinase 3 ligand (Flt3L) [120]. Peripheral myeloid cells are rapidly recruited to local tissues in sterile inflammatory disease, thereby participates in the innate immune response. Myeloid cells distribute in local organ tissues, which function as a tissue-dependent immune system. Here I introduce the innate immune response involving HMGB1 in murine disease models.

Neutrophils recruited to injured tissue contribute to tissue damage associated with HMGB1-induced NET release and acute inflammation [28, 74]. For instance, keratinocyte HMGB1 mediates neutrophil infiltration and NET formation. Keratinocyte

HMGB1-deficient mice display less formation of NETs in a skin wound-healing model [121]. In addition, TLR2-, TLR4- and TLR9-mediated HMGB1 induce neutrophil recruitment and NET formation. Inhibition or knockout of TLR2, TLR4 or TLR9 protects from inflammatory response and tissue injury by reducing of NET formation [74, 122]. Thus, HMGB1 can interact with different receptors, which may mediate the formation of NETs, resulting in the inflammatory response and tissue damage.

HMGB1 triggers the activation and immigration of monocytes/macrophages, which participates in pro-inflammatory response [123]. When activated monocytes and macrophages undergo pyroptosis, post-translational modifications of HMGB1 occur, which modulate the shuttling of modified HMGB1 from the nucleus to the cytoplasm even the extracellular space [124]. Released HMGB1 enhances the monocyte/macrophage-driven inflammatory response. Targeting the translocation and released HMGB1 from macrophages may ameliorate the inflammatory response in kidney disease. In addition, HMGB1 triggers macrophage phenotypes change from pro-inflammatory response to anti-inflammatory response with binding to RAGE receptor [123]. The anti-inflammatory macrophages contribute to tissue regeneration and wound healing in the recovery phase [125].

DCs maturation or surface antigen expression is associated with the extracellular HMGB1 [126-129]. For example, the release of HMGB1 mediates the maturation and upregulation of DC surface markers such as CD86, CD80, CD83 by RAGE receptor [130]. HMGB1 induced the maturation of DCs via its B-box domain, which mediated the secretion of pro-inflammatory cytokines [131]. In addition, infiltrated peripheral DCs modulate CD8<sup>+</sup> T cells activation [132]. DCs maturation controls the activation of T lymphocytes, which represents a compensated evolutionary mechanism [133]. Renal DCs participates in ischemic AKI. Depletion of DCs has a protective effect on kidney injury [134, 135]. However, in a study of kidney transplantation, renal IRI is associated with the loss of graft-kidney DCs and progression of peripheral DCs and regulator T cells, which implies the protective effect of renal DCs [136].

Myeloid cell-derived HMGB1 deficiency are more sensitive to endotoxin shock, accompanied by more macrophage cell death. Lack of HMGB1 in macrophages reduces the process of autophagic flux, which results in apoptosis of macrophages in bacterial infection [137]. For example, researchers established Vav1-Cre transgenic mice with HMGB1 deficiency in hematopoietic cells, which was confirmed by loss of

HMGB1 in bone marrow, spleen, and F4/80-positive hepatic macrophages [112]. Ablation of HMGB1 did not affect LPS-induced apoptosis and inflammation, but was associated with an increased LPS-related mortality [112]. However, the contribution of myeloid cell-derived HMGB1 to tissue sterile inflammation is unknown. Myeloid cell-derived HMGB1 contribute to recruitment of immune cells and promote inflammatory response. Depletion of HMGB1 in myeloid cells may ameliorate inflammatory response and inflammation-induced tissue injury.

In summary, many studies characterized targeting extracellular HMGB1 as a danger signal in organ injury and inflammatory diseases such as sepsis and rheumatoid arthritis [65, 138, 139]. However, the contribution of endogenous HMGB1 from myeloid cells and resident tissue cells and the release of HMGB1 from different cell types in kidney disease remains elusive. Animal models are commonly applied for the research of AKI, CKD, and transition of AKI to CKD as well as evaluating potential therapies. Renal IRI is a widely used model to study renal pathology aspects and test experimental therapeutics *in vivo*. Here I establish two new HMGB1-deficient mouse lines to study how cell-specific HMGB1 ablation in myeloid cells or in Pax8-positive tubular cells regulates kidney injury in postischemic kidneys. Additionally, I target extracellular HMGB1 by inhibiting HMGB1 functions in postischemic kidney injury.



### **2 Hypotheses**

Based on the above introduction, the hypotheses of the thesis are the following:

Myeloid cell-derived HMGB1 aggravates kidney injury in postischemic kidneys. Deletion of endogenous HMGB1 in myeloid cells ameliorates the inflammatory response in postischemic kidneys.

Renal tubular cell-derived HMGB1 contributes to kidney injury in postischemic kidneys. Conditional ablation of endogenous HMGB1 in tubular epithelial cells mitigates the release of HMGB1 with the reduction of DAMP-induced renal cellular damage in postischemic kidneys.

Targeting HMGB1 with inhibitors attenuates kidney injury in postischemic kidneys. Administration of different antagonists of HMGB1 decreases the release of HMGB1 to the extracellular space, which protects from kidney injury in postischemic kidneys.

### 3 Material and Methods

#### 3.1 Reagents

Chemicals and reagents	Company	Cat. number
Anti-HMGB1 antibody	Abcam, Cambridge, United Kingdom	ab18256
Anti-rabbit Alexa Fluor 647, Second antibody	ThermoFisher Scientific	A27040
B cell isolation kit	Miltenyibiotec, Germany	130-090-862
B-actin antibody	Cell Signaling	#4967S
Bovine Serum Albumin	Roche Diagnostics GmbH, Mannheim, Germany	10735086001
BUN kit	Diasys Diagnostic Systems	131019910021
Biocoll separation solution	Biochrom KG, Berlin, Germany	L6113
Cytochalasin D	Sigma-Aldrich, Germany	C8273
Collagenase D	Sigma-Aldrich, Germany	11088866001
Creatinine kit	Diasys Diagnostic Systems	117119910026
CD45 microbeads	Miltenyibiotec, Germany	130-052-301
DMEM medium	Gibco/ThermoFisher, UK	21885-025
Dextran	Sigma Aldrich, Germany	31392
Doxycycline Hyclate USP	Fagron	803781
D(+)-Saccharose	ROTH	200-334-9
Epithelial growth factor	Sigma Aldrich, Germany	SRP3196
Ethyl pyruvate	Sigma-Aldrich, Germany	E47808
Fc block	Biolegend, Inc.	101302
Fetal bovine serum	Biochrom KG, Berlin, Germany	L6113
FITC-sinistrin	Medi Beacon	13109910021
Glycyrrhizic Acid	Sigma-Aldrich, Germany	PHR1516
HMGB1 elisa kit	Cusabio, China	CSB-E08225m

## Material and Methods

---

HEPES	Sigma Life Science, Germany	H3375
Hydrocortisone	Sigma Aldrich, Germany	H0888
Hexanucleotide Mix	Sigma-Aldrich, Germany	11277081001
Hydrogen peroxide solution	Sigma-Aldrich, Germany	H1009
Helix NPTM Green	Biolegend, Inc.	425303
Insulin-Transferrin-Natrim-selenit-Zusatz	Sigma-Aldrich, Germany	11074547001
LDH reagent	Roche	4744926001
LS column	MACS Miltenyibiotec, Germany	130-042-401
MTT labeling reagent	Sigma-Aldrich, Germany	11465007001
Mouse Anti-F4/80 microbeads UltraPure	MACS Miltenyibiotec, Germany	130-110-443
Nonfat dried milk powder	PanReac AppliChem ITW Reagents	A0830,1000
Penicillin-streptomycin	Sigma-Aldrich, Germany	P4333
Precision Plus Protein™ Dual Color Standards	BIO-RAD	#1610374
Pierce™ ECL Western Blotting Substrate	ThermoFisher Scientific, Germany	32109
Potassium chloride	Merck KGaA, Darmstadt, Germany	7447-40-7
Protein Assay Dye Reagent Concentrate	BIO-RAD	#5000006
Percoll	Sigma-Aldrich, Germany	P1644
Protease and phosphatase inhibitors	Thermo Scientific, Germany	A32959
Prostaglandin E1	Sigma Aldrich, Germany	P7527
Paraformaldehyde	Sigma-Aldrich, Germany	158127
Phrodo	Thermo Fisher Scientific, Germany	p35371
Propidium Iodide Solution	Biolegend, Inc.	421301
RIPA buffer	Sigma-Aldrich, Germany	R0278

## Material and Methods

---

Recombinant mouse M-CSF	Biolegend, Inc.	576404
Rnasin and ribonuclease inhibitor	Promega, Germany	N2515
RNA isolation kit	Invitrogen by ThermoFisher Scientific	12183018A
Recombinant mouse GM-CSF	Biolegend, Inc.	576304
Recombinant Mouse HMGB1	Biolegend, Inc.	764006
Strainer (70 µm)	MACS Miltenyibiotec, Germany	130-098-462
Saponin	Sigma-Aldrich, Germany	47036
Superscript <sup>TM</sup> II Reverse Transcriptase	Invitrogen	18064071
T cell isolation kit II	Miltenyibiotec, Germany	130-095-130
Triiodothyronine	Sigma Aldrich, Germany	T6397
Taq DNA Polymerase	Biolabs Inc, New England	M0273E

---

All other reagents are available from Invitrogen, Sigma or Roche.

### 3.2 Instruments

---

Instruments	Equipment	Company
Cell incubators	Type B5060 EC-CO <sub>2</sub>	Heraeus Sepatech, Germany
Fluorescence Microscopes	Leica DMI8	Leica Microsystems, UK
	Nikon Eclipse Ti2	NIKON corporation, Japan
	Nikon DS-Qi2 camera	NIKON corporation, Japan
	Leica DM IL	Leica Microsystems, Germany
ELISA-Reader	Tecan, GENios Plus	Tecan, Crailsheim, Germany
Microscopes	Leica DMRBE	Leica Microsystems, Germany

	Carl Zeiss Digital Camera	Göttingen, DE
Spectrophotometer	Beckman DU® 530	Beckman Coulter, Fullerton, USA
Flow cytometry	FACS Canto II	BD, USA
	FACS Calibur	BD, USA
Centrifuge	Heraeus, Biofuge primo	Kendro Laboratory Products GmbH, Germany
	Heraeus, Minifuge T	VWR International, Germany
	Heraeus, Biofuge A	Sepatech Heraeus Sepatech, Germany
Miniaturized imager device	For GFR measurement	Mannheim Pharma & Diagnostics GmbH
Miniaturized battery	For GFR imager device	Mannheim Pharma & Diagnostics GmbH
PCR cycler	Light Cycler480	Roche Mannheim, Germany
	PCR cycler	Eppendorf, Germany
Other Equipments	Cryostat CM 3000	Leica Microsystems, Bensheim, Germany
	Microtome HM 340E	Microm, Heidelberg, Germany
	Nanodrop	PEQLAB Biotechnology GMBH, Erlangen, Germany
	Homogenizer ULTRA-TURRAX	IKA GmbH, Staufen, Germany

---

### 3.3 Transgenic mice

The transgenic Pax8rTtA,TetOCre,HMGB1 mice were developed on the C57BL/6J background by crossing the Pax8rTtA,TetOCre mice and the HMGB1 flox-flox mice.

The Pax8<sup>rtTA</sup>,TetO<sup>Cre</sup> mice were developed by crossing a Pax8.<sup>rtTA</sup> mice (B6.Cg-Tg(Pax8-rtTA2S<sup>+</sup>M2)1Koes/J and the TetO<sup>Cre</sup> strain B6.Cg-Tg(TetO-Cre)1Jaw/J. HMGB1 flox-flox mice were generated by B6.129P2-Hmgb1<sup><tm1Ttg></sup>, which were obtained from clinic of the LMU, Munich, Germany. The Pax8.<sup>rtTA</sup> mouse and the TetO<sup>Cre</sup> strain were obtained as a gift from Tadatsugu Taniguchi, University of Tokyo, Japan. In floxed HMGB1 gene, loxP was inserted to HMGB1 intron 1 and downstream of exon 4, HMGB1 null allele was the deletion of HMGB1 from exon 2 to exon 4. Pax8<sup>rtTA</sup>,TetO<sup>Cre</sup>,HMGB1 transgene recombination was induced by administration of 2 mg/ml doxycycline hyclate every two days in 5% D(+)-saccharose drinking water for at least three weeks in littermates to induce Cre expression and recombination of the Hmgb1 flox cassette in Pax8-expressing tubular epithelial cells, resulting in an irreversible deletion of HMGB1 in a cell type-specific manner under steady-state conditions. 8- 12-week-old male and female both were for the experiment. Mice with no Pax8 promotor or no Cre recombinase, but homozygous of floxed HMGB1 gene were used for wildtype controls (Pax8-HMGB1 WT). Mice with both heterozygous Pax8 promotor and heterozygous Cre recombinase, and the homozygous of floxed HMGB1 gene were used as Pax8-HMGB1 KO in this study.

The transgenic LysM<sup>Cre</sup>,HMGB1 mice were developed on the C57BL/6J mice by crossing the mice of LysM<sup>Cre</sup> and mice with the homozygous for floxed HMGB1 gene. LysM<sup>Cre</sup> mice obtained from Dr. Irmgard Mausz, Center for Leadership and People Management, Munich, Germany. As described before [137], the establish of LysM<sup>Cre</sup> mice was generated by the Cre gene inserting into the endogenous M lysozyme (LysM) locus. After crossing the LysM<sup>Cre</sup> mice and HMGB1-loxP mice, I established the mouse line with the deletion of HMGB1 gene in myeloid cells. The littermates of 8- 12-week-old were for experiment no matter male or female. Mice with no LysM<sup>Cre</sup> but the homozygous of floxed HMGB1 gene were used as wildtype controls (MLys-HMGB1 WT) and mice with heterozygous LysM<sup>Cre</sup> and the homozygous of floxed HMGB1 gene were used as MLys-HMGB1 KO.

### 3.4 Animal studies

All mice were housed under specific-pathogen-free (SPF) conditions under a 12-h light and dark cycle. Cages, food, nestles, bedding, and water were sterilized by autoclaving before use. Water and standard chow diet (Ssniff, Soest, Germany) were available for the complete duration of the experiments. All experimental procedures

were operated according to the German animal care and ethics legislation and had been approved by the local government authorities.

### 3.5 Unilateral ischemia-reperfusion surgery

Kidney unilateral IRI was conducted as described before [140]. Mice were anesthetized according to the protocol (Table 1). Metamizol was applied before narcosis induction. The mice were maintained in a heating chamber set at 37.0 °C to stabilize body temperature. Every mouse body temperature was recorded by using online rectal temperature monitoring after the onset of complete anesthesia and was persistent until wound closure. Prior to and during surgery, appropriate measures were to be taken to stabilize the body core temperature between 36.5 and 38.5 °C during the procedure. Surgery was performed on a heating plate set at 41 °C. The left renal pedicles were clamped for 17 min with a microaneurysm clamp (Medicon, Tuttlingen, Germany). After clamp removal, the kidney recovery was proved by blood flow with the evidence of returning to its original color. All mice received two drops of 37 °C warm normal saline on the exposed kidney. After kidney repositioning, wounds were closed by using Vicryl sutures for muscular layer and Ethibond sutures for cutaneous layer. Analgesic treatment with buprenorphine was started 30 min prior to narcosis antagonization (Table 1). Sham-operated mice were operated in the same procedure without clamping.

**Table 1.**

Application	Drug	Concentration (mg/kg)	Cat number	Company	Treatment regime
Narcosis	Medetomidine	0.5	07725752	Zoetis	i.p. injection, once prior to surgery, surgical tolerance verified by toe pinching.
	Midazolam	5	4921530	Ratiopharm	
	Fentanyl	0.05	2084366	Janssen-Cilag	
Antagonist	Atipamezol	5	8-00732	CP-Pharma	s.c. injection, once
	Flumazenil	0.1	4470990	Hexal	

Analgesia	Buprenorphine	0.1	01498870	Bayer Vital	i.p. injection, once 30min prior to antagonization, then every 8h for 3 consecutive days
	Metamizol-Natrium 1 H <sub>2</sub> O	200	0731672	Sanofi-Aventis	p.o. application, 5min prior to narcosis induction

---

### 3.6 Experimental design of animal studies

For the transgenic MLys-HMGB1 mice, I performed 17 min unilateral-IRI with the endpoint at day 1, day 10, or day 30 after IR surgery, respectively.

For the transgenic Pax8-HMGB1 mice, I performed 17 min unilateral-IRI with the endpoint at day 7 or day 30 after IR surgery.

The C57BL/6J male mice were purchased from Charles River Laboratories (Sulyfeld, Germany), 8- to 12-weeks-old mice. All mice underwent 17 min unilateral-IRI. For the pretreatment experiment, I did intraperitoneal injection 1 h before IR surgery and daily treatment until day 7 or day 14 with endpoint of day 7 or day 30, respectively. For the delayed treatment experiment, I did intraperitoneal injection from day 3 after IR surgery and daily treatment until day 17, the endpoint is day 30. PBS as control group, Ethyl pyruvate 80 mg/kg or Glycyrrhizic Acid 50 mg/kg as intervention group.

At least four mice per group were measured in each experiment. At the endpoint of the experiment, kidney tissues were harvested after sacrifice by cervical dislocation.



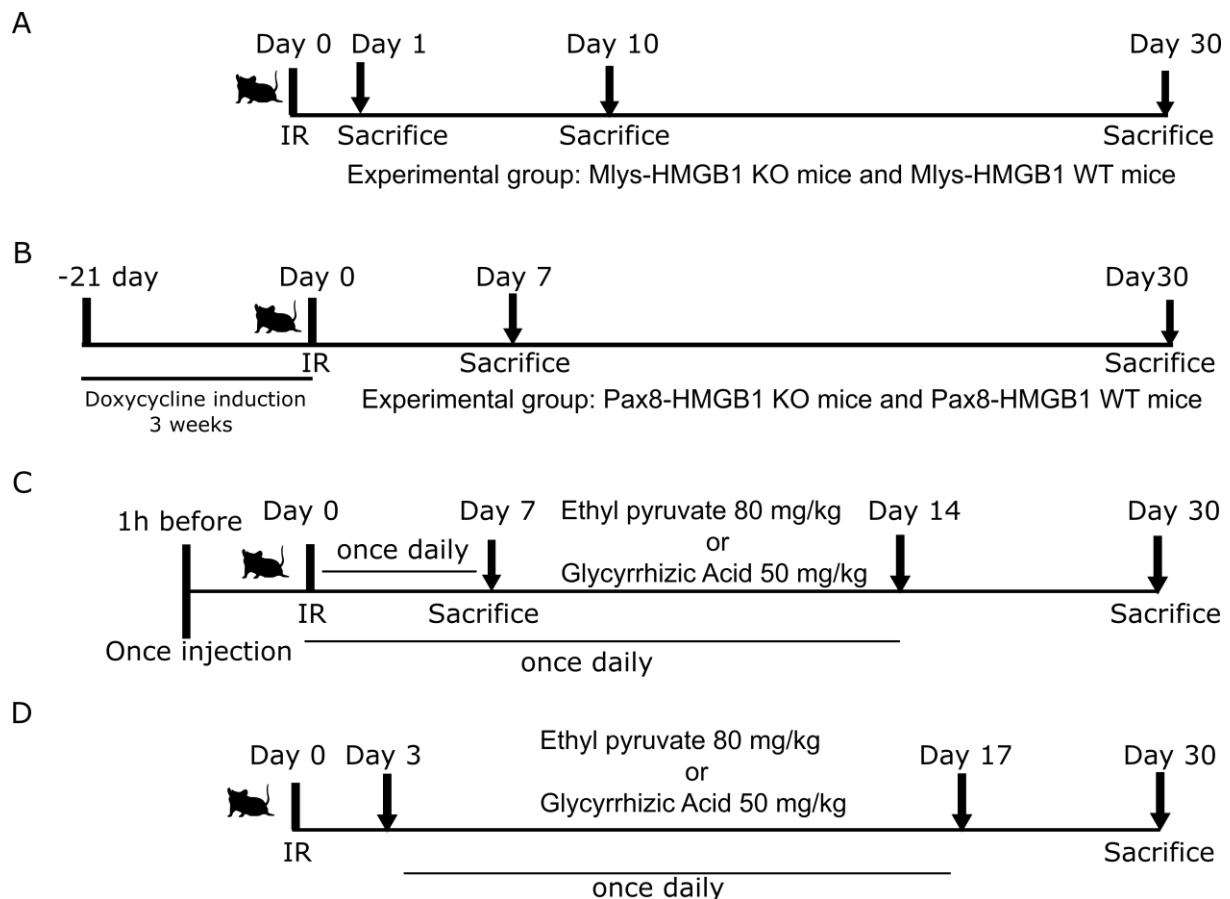


**Fig 5. Schematics of respective experimental designs.** Unilateral-IRI and different endpoint experiment in (A) MLys-HMGB1 mice, (B) Pax8-HMGB1 mice, and (C, D) C57BL/6J mice.

## 3.7 Blood sampling and creatinine measurement

Mouse blood samples were gathered into 1.5 ml Eppendorf tubes containing heparin by using the technique of retro-orbital bleeding, under isoflurane anesthesia with 20% oxygen. Plasma supernatant was collected by centrifuging at 800 rpm for 10 min, and stored at -80 °C for the future.

For creatinine assay: The standard samples were prepared with a gradient concentration. Working mixed reagent (R1:R2=4:1) was offered with the creatinine kit. Firstly, 10  $\mu$ l of plasma sample was added to a 96-well plate. Then, the mixed reagent was added to each well immediately before reading the plate. The absorbance was measured at 492 nm with the kinetics of 60 seconds, 120 seconds, 180 seconds (a1), and 20 min (a2) after the reagent-mixture. The corrected absorbance ( $\Delta a$ ) is samples reading subtract the blank reading. The final concentration of creatinine is based on

the corrected absorbance of standard curve data. Creatinine (mg/dl) =  $\Delta a$  sample/standard \* Concentration of standard (mg/dl)

### 3.8 Measurement of glomerular filtration rate

The measurement of transdermal glomerular filtration rate (GFR) represents the renal function of mice according to the protocol [141]. We use an exogenous GFR tracer of sinistrin conjugated with fluorescein-isothiocyanate (FITC) to measure the excretion kinetics. The FITC-sinistrin is prepared at 30 mg/ml in 0.9% Sodium chloride.

Mice were anesthetized by isoflurane with 20 % oxygen. We set up a GFR device (Medibeacon, Germany) onto the shaved neck to record the excretion kinetics of FITC-sinistrin. Here we used the same size of patches (Medibeacon, Germany), one side stick to the GFR device and the other side attached to the shaved area of the mice. The GFR device was fixed onto the shaved back with hypoallergenic silk tape. You can see the LEDs flashing to start recording and wait for around 10 min for the recording. Then, the FITC-sinistrin was administrated intravenously at the dose of 0.15 mg/g mice of body weight. The measurement period is around 1.5 h. After removing the GFR device, the MPD Lab software (Medibeacon, Germany) was used to analyze the data.

### 3.9 Immunohistochemistry

Kidneys were harvested from experimental mice, fixed in 4% formalin for 24h, then processed to tissue processors (Leica). Paraffin-embedded sections were prepared by slicing the paraffin blocks. De-paraffinization was performed by using xylene for 3 times and each 5 min. Incubation steps performed rehydration with 100% absolute ethanol for 3 times and each 3 min, 95% ethanol for 2 times and each 3 min, 70% ethanol for once and 3 min, followed by washing with PBS for 3 times and 5 min each.

To block endogenous peroxidase, the sections were incubated with 3% H<sub>2</sub>O<sub>2</sub> in methanol for 20 min in the dark, followed by washing with PBS for 3 times and 5 min each. For unmasking of antigen, tissue sections were plunged in 1% antigen unmasking solution and steamed in the microwave for 10 min. After washing, endogenous biotin was blocked by incubation of Avidin (Vector) for 15 min, followed by incubating with biotin (Vector) for a further 15 min. Then sections were incubated with primary antibodies Tamm–Horsfall protein (THP-1) or Lotus tetragonolobus lectin

(LTL) at 4 °C overnight. After washing, sections were incubated with biotinylated secondary antibodies for 30 min, followed by washing with PBS. Then, sections were incubated with substrate solution (ABC solution, Vector) for 30 min. After washing with PBS, sections were rinsed with Tris for 5 min, followed by DAB staining. Then, methyl green (Fluka) was used for counterstaining. Finally, sections were washed with 96 % alcohol to remove excess stain and xylene, mounted with VectaMount (Vector) after drying. THP-1 was quantified with the proportion of THP-1 positive area in medulla, LTL was quantified with the proportion of LTL positive area in cortex.

A TdT-mediated dUTP nick end labeling (TUNEL) assay was used to quantify the nuclear DNA of damaged tubular cells. TUNEL staining was calculated with the mean fluorescence intensity (MFI). Image J software (Imagej.nih.gov) software was used for quantification.

### **3.10 Periodic acid Schiff and Sirius red staining**

Re-hydrated sections were stained with 2% Periodic acid for 5 min followed by washing with distilled water. Then, sections were stained with Schiff solution for 20 min followed by washing with tap water. Counterstaining was carried out with hematoxylin solution for 2 min, followed by washing with tap water. Finally, sections were dipped in 90% alcohol, closed with cover slips after drying. Tubular damage was quantified by assessing the proportion of in the corticomedullary junction that showed cell necrosis, loss of brush border, cast formation, and tubular dilatation. Each parameter was scored from 0 to 2 (0 = no injury, 0.5 = 25% injury, 1 = 50% injury, 1.5 = 75% injury, 2 = 100% injury). The summary was scored from 0 to 8.

Re-hydrated sections were stained with Weigert's haematoxylin for 8 minutes, followed by washing the slides in distilled water. Then the sections were stained with picro-sirius red for one hour, followed by washing with tap water. Finally, sections were dipped in 90% alcohol, closed with cover slips after drying. Kidney fibrosis was quantified by evaluating the percentage of collagen (Red) in tissue sections. Image J software (Imagej.nih.gov) software was used for quantification.

### **3.11 Immunofluorescence**

Cells were seeded in 8-well chambers for the experiment. The slides were incubated with HMGB1 antibody with 1: 200 diluted in blocking buffer (3% BSA, 0.1% saponin in

PBS) at 4 °C overnight, followed by washing with PBS for three times, each for 5 min. Then the slides were incubated with a secondary antibody: anti-rabbit Alexa 647 or anti-rabbit Alexa 555 with 1:100 diluted in blocking buffer (0.1% saponin in PBS) at room temperature for 30 min, followed by washing with PBS three times, 5 min each. Finally, the slides were mounted with DAPI (Vector H-1200) and covered with coverslips. The slides were kept at 4 °C for taking pictures with fluorescence microscopy in the future.

### 3.12 RNA isolation and quantitative Real-time PCR and endpoint PCR

#### 3.12.1 Total RNA isolation

The half of kidney was transferred with forceps to 2 ml lysis buffer with 1% 2-mercaptoethanol in 5 ml Falcons. The samples were kept on ice all the time. Every sample was homogenized once for 20 seconds with Ultra-Turrax on level 4, and centrifuged at 6000 g for 5 min, and then the supernatant was transferred to a clean RNase-free tube. 700 µl sample was taken to homogenate with the same amount of 70% ethanol and mixed thoroughly. Total RNA was isolated by using Qiagen mRNA extraction kit following instructions. The purified RNA was stored at -80 °C for long-term storage.

#### 3.12.2 RNA reverse transcription

RNA samples were dissolved in RNase-free water. The samples were incubated at 65 °C for 10 min to denature secondary structure of RNA, followed by stopping the reaction at 4 °C. RNA samples were diluted to get a concentration of 2 µg total RNA in 22.45 µl reaction. Then, the prepared master mix as follows were incubated at 42 °C for 120 min and 85 °C for 5 min, 4 °C for long-term storage.

Preparation master mix:

Master mix:	Volume (µl)
5x buffer	4.5
0.1M DTT	1
25 mM dNTPs	0.45
Rnasin and ribonuclease inhibitor (40 u/µl)	0.5

Acrylamide (15 µg/ml)	0.25
10x Hexanucleotide Mix	0.25
Superscript II (200 u/µl)	0.5
Sample (2 µg)	15
Total	22.45

---

### 3.12.3 Quantitative Real-time PCR

The quantitative real-time PCR was measured with the SYBR Green Dye Detection System on a Light Cycler 480. The cDNA samples were diluted at 1:100 for real-time PCR. The prepared master mix was incubated at the following settings with Light Cycler 480: Pre-incubation: 95 °C for 5 min. Amplification: 95 °C for 15 s, 60 °C for 15 s, 68 °C for 20 s, running 40 cycles. Melting curve: 95 °C for 5 s, 65 °C for 60 s. Cooling: 40 °C for 30 s. The CT values were calculated and the results were normalized with the reference gene (*18s rRNA*) for each sample.

Preparation master mix:

Master mix	Volume (µl)
Mix SybrGreen	10
Taq polymerase (5000 u/ml)	0.16
Forward primer (10 µM)	0.6
Reverse primer (10 µM)	0.6
cDNA	0.2
ddH <sub>2</sub> O	8.44
Total	20

---

### 3.12.4 Oligonucleotide primers used for endpoint PCR and quantitative RT-PCR

The following oligonucleotide primers were used in the study.

Gene	Sequence
Mouse <i>18s</i>	Forward: GCAATTATTCCCATGAACG Reverse: AGGGCCTCACTAAACCATCC
Mouse <i>Havcr1</i> ( <i>KIM1</i> )	Forward: TGGTTGCCTTCCGTGTCTCT Reverse: TCAGCTCGGGAATGCACAA
Mouse <i>Clu</i> ( <i>Clusterin</i> )	Forward: AAAAGCCGTGCGGAATGAGA Reverse: TCGCAAGGCGGCTTTTATTG
Mouse <i>TNF<math>\alpha</math></i>	Forward: AGGGTCTGGGCCATAGAACT Reverse: CCACCACGCTCTTCTGTCTAC
Mouse <i>Nos2</i> ( <i>iNos</i> )	Forward: AAACCCCTTGTGCTGTTCTCA Reverse: GAACATTCTGTGCTGTCCCAG
Mouse <i>Myd88</i>	Forward: ACCTGTGTCTGGTCCATTGCCA Reverse: GCTGAGTGCAAACCTGGTCTGG
Mouse <i>Plin4</i>	Forward: GCACTAAGGACACGGTGACCAC Reverse: GACCACAGACTTGGTAGTGTCC
Mouse <i>HMGB1</i>	Forward: TACTCGGAGAACTTCAGACCG Reverse: TAACGAGCCTTGTGAGCCTT
Mouse <i>Fabp1</i> ( <i>L-FABP</i> )	Forward: AGGAGTGCGAACTGGAGACCAT Reverse: GTCTCCATTGAGTTCAGTCACGG
Mouse <i>Prdx1</i>	Forward: TGCCAAGTGATTGGCGCTTCTG Reverse: AGCAATGGTGCGCTTGGGATCT
Mouse <i>Ins2</i>	Forward: CTAGGCCACAGAATTGAAAGATCT Reverse: GTAGGTGGAAATTCTAGCATCATCC
Mouse <i>Pax8_rTtA</i>	Forward: CCATGTCTAGACTGGACAAGA

	Reverse: CTCCAGGCCACATATGATTAG
Mouse <i>TetO_Cre</i>	Forward: TCGCTGCATTACCGGTCGATGC
<i>Cre8</i>	CCCAGAAATGCCAGATTACG
<i>MLys1</i>	CTTGGGCTGCCAGAATTTCTC
<i>MLys2</i>	TTACAGTCGGCCAGGCTGAC
<i>HMGB1 flox</i>	Forward: TGTCATGCCACCCTGAGCAGTT
	Reverse: TGTGCTCCCGGCAAGTT
<i>HNGB RV</i>	GCATTCTACAGGTTACAGCCAG

---

### 3.12.5 Endpoint PCR for LysMCre and HMGB1 transgene

Preparation master mix for MLysCre transgene:

Master mix	Volume (μl)
10x PE buffer	2.5
1.25 mM dNTP	4
5 x Optimizer	5
Cre8 (10 pmol/μ)	1
MLys1 (10 pmol/μ)	1
MLys2 (10 pmol/μ)	1
Taq DNA Polymerase (5000 u/ml)	0.2
H <sub>2</sub> O	9.3
DNA	1
Total	25

Preparation master mix for HMGB1 transgene:

Master mix	Volume (μl)
10x PE buffer	2.5
1.25 mM dNTP	4
5 x Optimizer	5
HMGB1 flox Forward (10 pmol/μ)	1
HMGB1 flox Reverse (10 pmol/μ)	1
HNGB RV (10 pmol/μ)	1
Taq DNA Polymerase (5000 u/ml)	0.2
H2O	9.3
DNA	1
Total	25

The master mix was prepared as above and incubated at the following settings with Eppendorf PCR cycler: Pre-denaturation: 94 °C for 3 min. Cycling: 94 °C for 40 s, 60 °C for 45 s, 72 °C for 60 s, running 35 cycles. Post extension: 72 °C for 5 min. Hold: 4 °C forever. Then, gel electrophoresis was performed on a 2% agarose gel.

MLysCre products: WT band 345 bp, knock-in band near 1 kb.

HMGB1 flox products: WT band 172 bp, flox-flox band 270 bp.

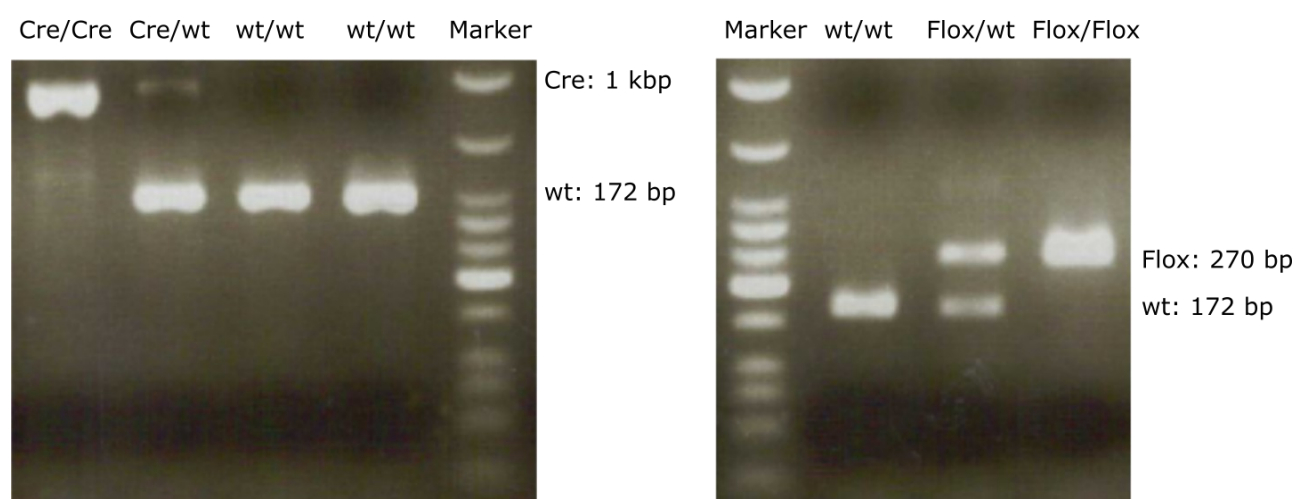


**Fig 6. Agarose gel electrophoresis for MLysCre gene and HMGB1 gene**



### 3.12.6 Pax8rtTA,TetOCre genotyping

Preparation of the master mix:

Master mix	Volume (μl)
Mix SybrGreen	10
Taq polymerase (5000 u/ml)	0.16
Forward primer (10 pmol/μ)	0.6
Reverse primer (10 pmol/μ)	0.6
DNA sample	0.2
ddH <sub>2</sub> O	8.44
Total	20

The prepared master mix were prepared as above and incubated at the following settings with Light Cycler 480: Pre-incubation: 95 °C for 10 min. Amplification: 95 °C for 15 s, 60 °C for 45 s, 72 °C for 60 s, running 40 cycle. Melting curve: 95 °C for 10 s, 65 °C for 60 s. Cooling: 40 °C for 30 s. The Light Cycler 480 was used to analyze the CT values and the results were normalized with the reference gene (*Ins2*) for all samples.

### 3.13 Bone marrow mononuclear cell isolation and cell culture

Mice were sacrificed by cervical dislocation. The femur and tibia were isolated from the mouse. The bones were placed in 75% ethanol for 1 min and moved to sterile PBS. The residual tissue was removed, and the tibia was separated from the femur by bending slightly at the knee joint. The terminals of the bones were removed with scissors, and a 25-G needle was applied to flush the bone marrow with the sterile medium, the needle was moved up and down until the bone becomes white. The flushed medium with bone marrow was collected into the Falcon and centrifuged at 1200 rpm for 5 min. Erythrocytes were lysed with 0.155 M NH<sub>4</sub>Cl for 10min on ice, followed by centrifuging for 5 min at 1200 rpm. The suspended cells were filtered through a 70 μM cell strainer. The filtered solution was collected and centrifuged at 1200 rpm for 5 min. The pellets were suspended with DMEM medium, and seeded in a plate supplemented with 50 ng/ml GM-CSF or 100 ng/ml M-CSF with additional 10%

FCS. New fresh medium was added supplemented with 50 ng/ml GM-CSF or 100 ng/ml M-CSF with additional 10% FCS at day 2, which was refreshed at day 5. Cells were harvested at day 7 for further experiment.

### 3.14 Renal primary murine tubule isolation and tubular cell culture

Mice were anesthetized by isoflurane with 20 % oxygen. The kidney was perfused by puncturing the left ventricle with cold PBS, then the kidney was harvested in 2 ml cold collagenase D (1.5 mg/ml) in a 6-well plate. The plate was kept with shaking at 120 rpm at 37 °C for 45 min. The kidney was squeezed through a 70 µm sieve with the sterile plunger of a 10 ml syringe and then centrifuged at 1200 rpm for 5 min at 4 °C. The pellets were resuspended with 2 ml cold PBS and layered onto 10 ml 31% Percoll solution, then centrifuged at 3000 rpm for 20 min without brake at 4 °C. The collected pellets were washed with PBS twice. The pellets were suspended with DMEM medium for culture supplemented with 10% FCS, 2.5% Hepes (1 M, PH=7.55), 1% hormone mix, 5 mg Insulin transferrin-sodium selenite supplement (ITSS), 25 ng/ml Epithelial growth factor (EGF), 1% Penicillin-streptomycin (PS).

Hormone mix	Volume (µl)
HBSS	50 ml
PGE1 (Prostaglandin E1, 125 ng/ml in ethanol)	12.5
T3 (Triiodothyronine, 3.4 ng/ml in ethanol)	50
Hydrocortisone (1.8 µg/ml in ethanol)	0.5 ml

### 3.15 Primary human kidney cell culture

Primary human kidney cells were cultured with endothelial cell basic medium supplemented with 20% hyclone FBS, huamn Epidermal Growth Factor (hEGF), Endothelial Cell Growth Supplement (ECGS), and hydrocortisone. Cells were cultured to 90% confluency and were harvested for further experimentation.

### 3.16 Preparation of kidney mononuclear cells for flow cytometry

Mice were anesthetized by isoflurane with 20 % oxygen. The kidney was harvested into a 6-well plate containing 2 ml cold collagenase A (1.5 mg/ml) + DNase I (40 U) solution. The plate was kept at 37 °C for 45 min with shaking at 120 rpm. The kidney

was squeezed to pieces through a sieve with the sterile plunger of a 10 ml syringe. The resuspended cell was centrifuged at 1200 rpm for 5 min at 4 °C. The pellets were washed with FACS buffer. Then the cell pellets were suspended in 8 ml of 40% Percoll, overlapping to 3 ml of 70% Percoll carefully, then centrifuged at 2000 rpm for 30 min without brake at room temperature. The interface layer cells were collected and washed with FACS buffer. (Option) To purify the mononuclear cells, the pellet can work through with CD45 microbeads (Miltenyibiotec, Germany). Fc block was administered to block non-specific Fc receptor. The antibody labeled with a fluorochrome was incubated for 30 min in the dark at 4 °C. The pellets were suspended with 500 µl of FACS buffer. After washing, the supernatant was discarded, and the pellets were resuspended with FACS buffer for running flow cytometry.

FACS buffer: 500 ml PBS, 1% BSA, 0.1% NaN<sub>3</sub>.

The following antibodies were used in this study:

Product	Clone	Company
APC anti-mouse F4/80 Antibody	BM8	Biolegend
APC/Fire™ 750 anti-mouse CD4 Antibody	RM4-4	Biolegend
APC anti-mouse CD45 Antibody	30-F11	Biolegend
APC anti-mouse Ly-6C Antibody	HK1.4	Biolegend
Brilliant Violet 510™ anti-mouse F4/80 Antibody	BM8	Biolegend
Brilliant Violet 510™ anti-mouse CD11b Antibody	M1/70	Biolegend
FITC anti-mouse I-A/I-E Antibody	M5/114.152	Biolegend
FITC anti-mouse CD192 (CCR2) Antibody	SA203G11	Biolegend
FITC anti-mouse CD3ε Antibody	145-2C11	Biolegend
PE/Cyanine7 anti-mouse/human CD11b Antibody	M1/70	Biolegend

PE anti-mouse CD8a Antibody	53-6.7	Biolegend
PE/Cyanine5 anti-mouse CD45 Antibody	30-F11	Biolegend
PE anti-mouse I-A/I-E Antibody	M5/114.152	Biolegend
PerCP/Cyanine5.5 anti-mouse CD45 Antibody	30-F11	Biolegend
PE/Cyanine7 anti-mouse CD11c Antibody	N418	Biolegend
V450 Hamster Anti-Mouse CD11c	HL3	BD Biosciences

---

### 3.17 Preparation of spleen B cells and T cells

Mice were sacrificed by cervical dislocation, then the spleen was isolated to fresh cold FACS buffer. The spleen CD19<sup>+</sup> B cells and CD3<sup>+</sup> T cells were collected by following the instrument of B cell isolation kit and T cell isolation kit II. The pelleted CD19<sup>+</sup> B cells and CD3<sup>+</sup> T cells were stored for further experiment.

### 3.18 Protein isolation and Western blot

The cell pellets were lysed with the cold RIPA buffer, supplemented with additional protease and phosphatase inhibitors, incubating for 30 min at 4 °C with shaking. The cell pellets were centrifuged at 16000 g for 20 min at 4 °C to collect the supernatant. The protein concentration was determined with the cell lysate. The cell lysate was heated at 95 °C for 5 min. Same amounts of protein were loaded into the 12 % SDS-PAGE gel wells, along with molecular weight markers. Run the gel for 1.5 h at 100 V. When the run has finished, the transfer “sandwich” was assembled for the semi-dry transfer: (bottom) 3 whatman papers + PCDF membrane + gel + 3 whatman papers (top), for 50 min at 10 V. The PVDF membrane was blocked in 5 % non-fatty milk (blocking buffer) for 1 h at room temperature with agitation, followed by incubating with the primary antibody diluted in blocking buffer overnight at 4 °C. After washing with TBST buffer, the PVDF membrane was incubated with the secondary antibody (in 5 % BSA blocking buffer) for 1 h at room temperature. Wash with TBST for three times, each for 5 min. ECL solution was applied with the membrane, and the chemiluminescent signals were captured in the dark. The image software was used to analyze the target protein with the reference protein ( $\beta$ -actin).

### **3.19 HMGB1 Elisa kits**

Mouse plasma was collected into 1.5 ml Eppendorf tubes containing heparin, then centrifuged at 1000 g at 4 °C for 15 min. The plasma samples were aliquoted and stored at – 80 °C for the long term. Reagents, working standards were prepared, and the plasma was diluted with sample diluent (1:200) as recommended. Assay procedures were followed by the instructions of the mouse HMGB1 ELISA kit (Cusabio, China).

### **3.20 Lactate dehydrogenase cell death assay and cell viability assay**

To determine cell cytotoxicity: a concentration of  $1 \times 10^4$  cells / well were seeded at in 96-well with 100  $\mu$ l without FCS culture medium and incubated overnight for the cell adhesion. The medium was changed with the stimulation group, negative group, and positive group (2% Tween). The 96-well plates were incubated for 3 h or 24 h. 50 $\mu$ l of the volume was taken from each well to the 96-well microplate, 50  $\mu$ l of prepared LDH reagent (4744934001, Roche) was added to each well. The absorbance was measured at 450 nm of the 96-well microplate immediately and an interval of 5 min for three times. The reference wavelength should be more than 650 nm. Analyze with the readout.

For determining cell viability or metabolic activity: a concentration of  $1 \times 10^4$  cells / well were seeded at in 96-well with 100  $\mu$ l without FCS culture medium and incubated overnight for the cell adhesion. The medium was changed with the stimulation group, negative group, and positive group. The 96-well plate was incubated for 3h or 24 h. Next, 10  $\mu$ l of MTT labeling reagent (CT01, Sigma-Aldrich) was added to each well and incubated 4 h for reaction. 100  $\mu$ l of the stop solution was added into each well and the 96-well plate was kept overnight in a humidified atmosphere. The absorbance of the samples was measured with the ELISA reader with a wavelength of 570 nm. The reference wavelength should be more than 650 nm.

### **3.21 Time-lapse imaging**

The passaged primary murine tubular cells or primary human renal cells were seeded in a 96-well plate with the treatment of 1 mM hydrogen peroxide (H<sub>2</sub>O<sub>2</sub>) for 24h and imaging every 30 min interval. Time-lapse imaging was performed by using a 10x objective of Nikon Eclipse Ti2 microcopy (NIKON, Japan) with an incubator chamber

of 37 °C, 5% CO<sub>2</sub>, and humidity control. Transmitted light and fluorescent images were obtained with Nikon DS-Qi2 camera (NIKON, Japan). Additional 1 µM Helix NP™ Green stain was applied to visualize the permeabilized cells with the color of green. Nec1f as a small molecule inhibitor was received from Andreas Linkermann, the University Hospital at Dresden University of Technology, Dresden, Germany [142].

### 3.22 Phagocytosis of monocyte-derived macrophages

Generation of Necrotic proteins-labeled phrodo (p35371, Thermo Fisher Scientific): The necrotic soup was collected from 10 million primary murine tubular cells in 1 ml PBS, then frozen and thaw for 5 times, followed by centrifuging at 500g for 5 min, and the supernatant was taken as necrotic proteins. 10 µl necrotic proteins mix with 1 µl phrodo dye were taken and incubated at 37 °C for 1 h.

Phagocytosis of monocyte-derived macrophages: 1 x 10<sup>4</sup> cells / well were seeded in a 96-well plate and incubated overnight in the incubator (37 °C, 5% CO<sub>2</sub>) for the macrophage adhesion. The medium was aspirated, and 11 µl of necrotic proteins-labeled phrodo was added in 100 µl culture medium with or without cytochalasin D (1 µg/ml) 45 min before. The cells were incubated for 1 h at 37 °C and washed with PBS for three times. The macrophage phagocytosis was determined under the fluorescence microscope. The mean fluorescence value was analyzed with Image J software (Imagej.nih.gov).

### 3.23 Statistics

All figures and statistical analyses were completed by using Prism 6 software (GraphPad Software, San Diego, CA). Data were checked for normal distribution before every statistical analysis. Normally distributed was used via unpaired T-test for two groups comparisons, one-way ANOVA followed by Fisher's LSD test for multiple comparisons. Not normally distributed data sets were compared by using Mann-Whitney test for two groups comparisons, Kruskal-Wallis test for multiple comparisons. Two-way ANOVA followed by Fisher's LSD test was used for multiple group comparisons. Data are presented as mean ± SD. A value of  $p < 0.05$  was considered to indicate statistical significance. \*  $p < 0.05$ , \*\*  $p < 0.01$ , \*\*\*  $p < 0.001$ , \*\*\*\*  $p < 0.0001$ .

## 4 Results

### 4.1 HMGB1 in myeloid cells mitigates postischemic kidney injury

The recruitment of bone marrow myeloid cell-derived immune cells contributes to the inflammatory response and kidney injury in the reperfusion phase after renal ischemia. Released HMGB1 as an inflammatory mediator triggers the migration of immune cells and inflammatory response during tissue injury. However, the role of endogenous HMGB1 from activated immune cells in AKI is elusive.

#### 4.1.1 Selective HMGB1 deletion in myeloid cells

To investigate how myeloid cell-derived HMGB1 plays a role in renal IRI, I established a transgenic MLys-HMGB1 mouse line (Fig 7). To confirm the deletion of HMGB1 in myeloid cells from MLys-HMGB1 mice, isolated bone marrow mononuclear cells were stimulated with M-CSF to differentiate to macrophages. B cells and CD3+T cells were isolated from murine spleen. Immunofluorescence staining of HMGB1 indicated the lack of nuclear HMGB1 in bone marrow-derived macrophages (Fig 8A). Western blot indicated the deletion of HMGB1 in bone marrow-derived macrophages, but not B cells and CD3+ T cells (Fig 8B). The purity of B cells and CD3+T cells were above 98% and 96%, respectively (Fig 9). The purity of bone marrow-derived macrophages was above 87% as shown by flow cytometry (Fig 9). Our results confirmed that MLys-HMGB1 mice were established successfully.

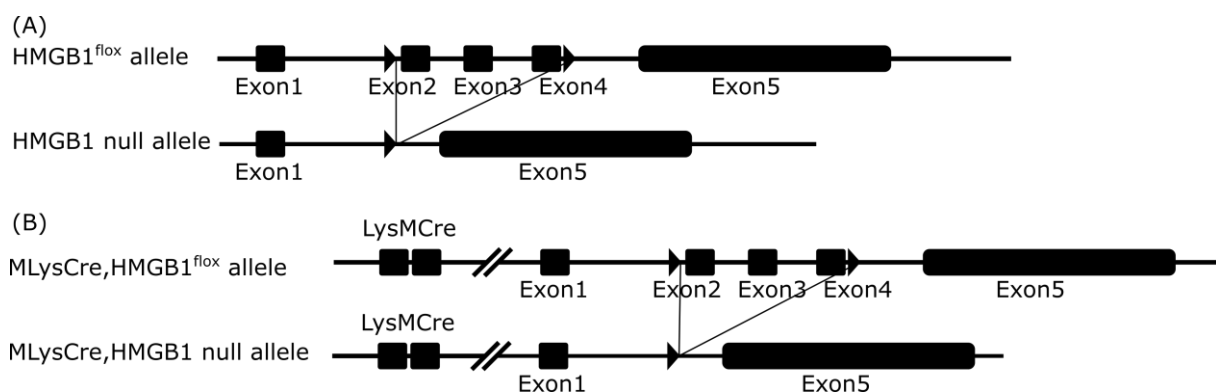


**Fig 7. Generation of myeloid cell-specific HMGB1 knockout mice.** (A) loxP was inserted to HMGB1 intron 1 and downstream of exon 4, HMGB1 null allele was the deletion of HMGB1 from exon 2 to exon 4, except for exon 1 and exon 5. (B) Cre recombinase was inserted to the promotor of lysozyme gene, MLysCre, HMGB1 null allele was deletion of HMGB1 in myeloid cells.

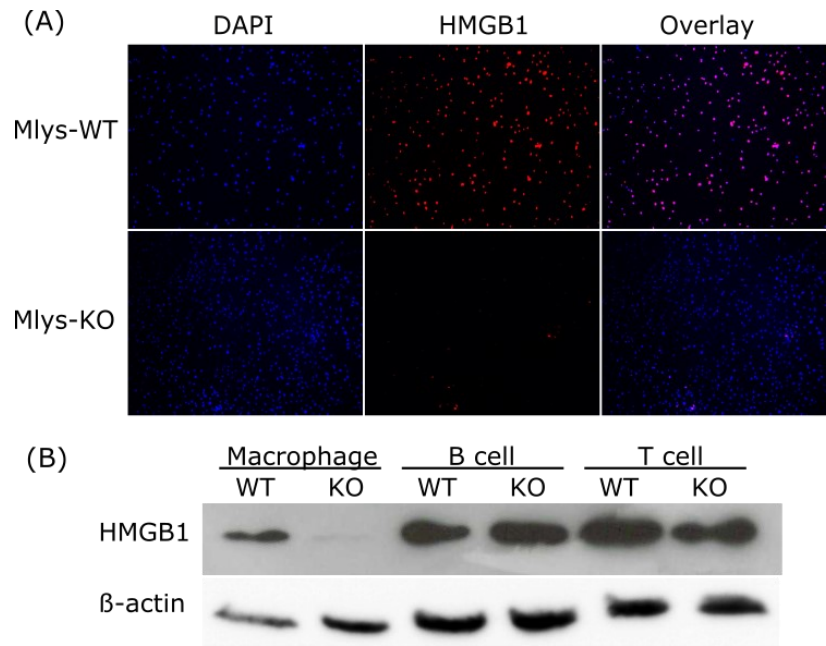


**Fig 8. The myeloid cell-derived HMGB1 deficiency.** (A) Monocytes were isolated from bone marrow and differentiated to macrophages with additional M-CSF. Immunofluorescence staining of HMGB1 in bone marrow-derived macrophages. Images were shown at the magnification of 100x. (B) Western blot was measured for HMGB1 protein.  $\beta$ -actin as reference protein. B cells and CD3+T cells were isolated from the spleen. MLys-WT or WT (MLys-HMGB1 WT mice) represent control group, MLys-KO or KO (MLys-HMGB1 KO mice) represent HMGB1 knockout group.

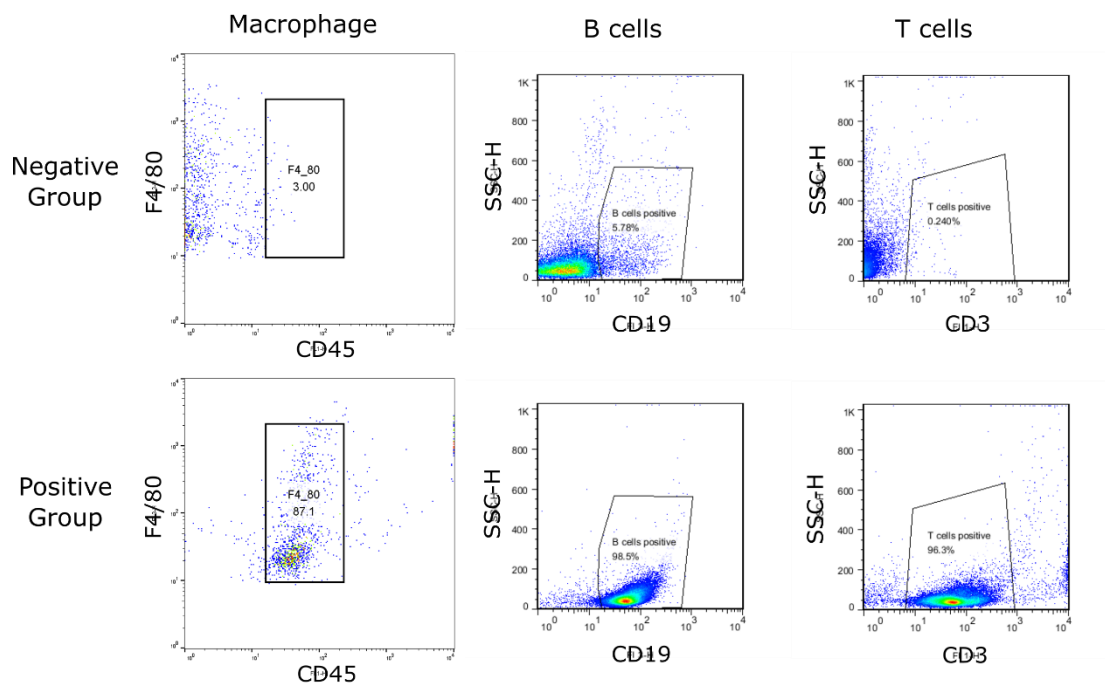


**Fig 9. The purity of different cell types.** B cell and T cell were isolated from mouse spleen. Flow cytometry indicated that 96.3% isolated T cells are CD3+ T cells, 98.5% isolated B cells are CD19+ B cells. The isolated bone marrow mononuclear cells were differentiated to macrophage with additional M-CSF. Flow cytometry demonstrated that 87.1% isolated cells are F4/80 positive cells.



#### 4.1.2 Myeloid cell-derived HMGB1 attenuates acute kidney injury

To investigate if myeloid cell-derived HMGB1 contributes to AKI after ischemia, Mlys-HMGB1 mice from 8- to 12-weeks-old were subjected to 17 min unilateral IRI. There was a reduction of GFR in HMGB1 knockout mice at day one after ischemia, compared with control mice (Fig 10). As shown in Fig 11, the plasma HMGB1 level in knockout mice was lower than control mice due to the deletion of endogenous HMGB1 in myeloid cells, which may result in less release of extracellular HMGB1 from activated monocytes and macrophages in AKI. HMGB1 knockout mice showed a higher level of plasma creatinine (Fig 11), severe tubular damage, and cell death than control mice (Fig 12A, 12C). In addition, HMGB1 knockout mice showed aggravated DNA damage in AKI in postischemic kidneys quantified by TUNEL staining (Fig 12B, 12D). However, there was no significant difference in neutrophil immigration at day one after ischemia (Fig 13). Thus, the deletion of endogenous HMGB1 in myeloid cells promoted amplified AKI in postischemic kidneys.

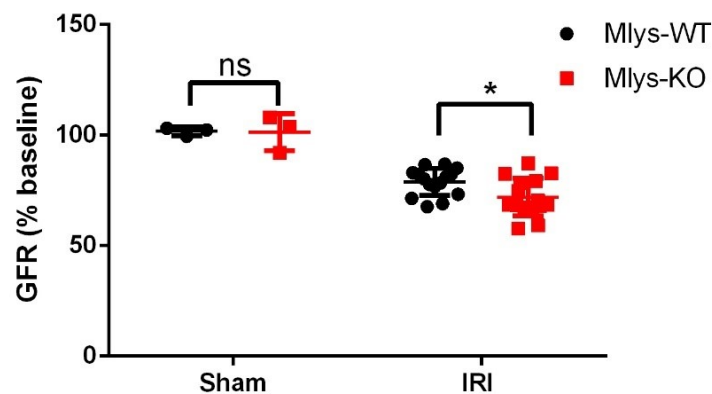


**Fig 10. The glomerular filtration rate (GFR) at day one in postischemic kidney injury.** The GFR level was measured at day one after ischemia. GFR changes were shown from the baseline GFR. Sham means no ischemic kidney injury, IRI represents ischemia-reperfusion injury.

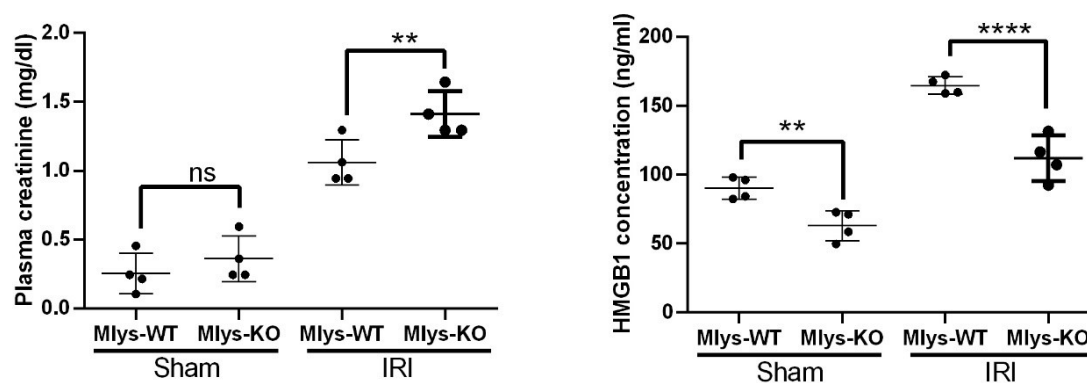


**Fig 11. Plasma creatinine and HMGB1 concentration in AKI.** Plasma was collected at day one after ischemia. Plasma HMGB1 concentrations were measured with murine HMGB1 ELISA kit.

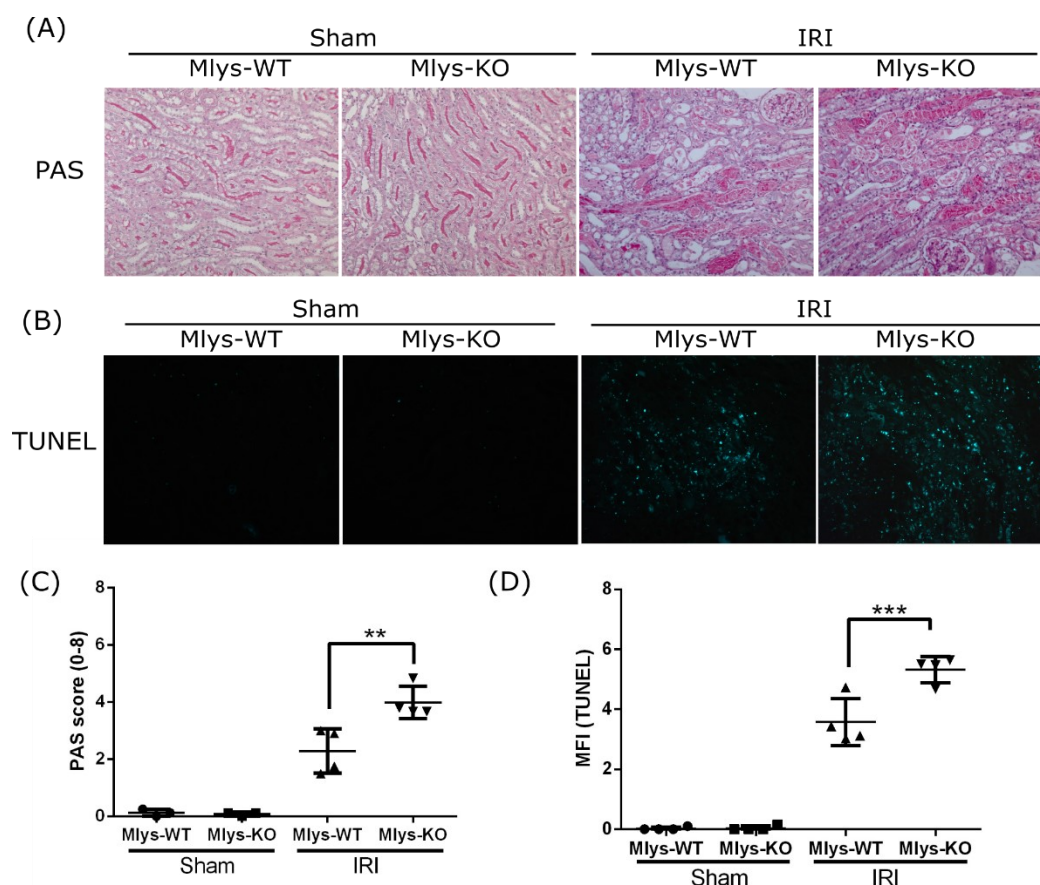


**Fig 12. The myeloid cell-derived HMGB1 deficiency accelerated ischemic AKI at day one.** (A) Periodic acid-Schiff (PAS) was applied for the quantification of renal tubular damage. (B) TUNEL staining represented DNA damage and tubular cell death. Images were shown at the magnification of 200x. (C, D) Quantification of PAS staining and TUNEL staining.

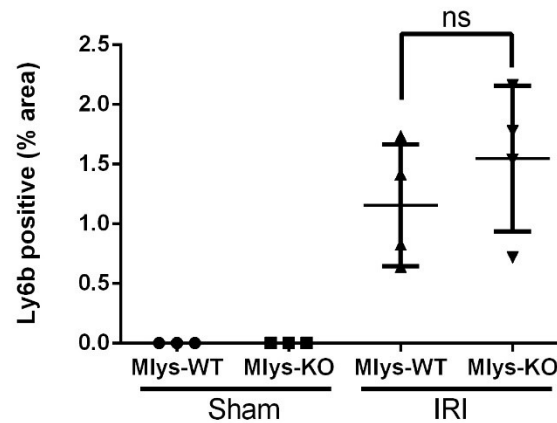


**Fig 13. Immigration of neutrophils at day one in AKI.** Neutrophils were quantified on ly6b-positive staining.

#### 4.1.3 Myeloid cell-derived HMGB1 protects resident dendritic cell from death

Infiltrating immune cells contribute to renal IRI. Kidney resident DCs initiate and propagate renal inflammatory response by enrolling the innate immune cells. To investigate how the mutation of endogenous HMGB1 in myeloid cells promoted additional AKI, I evaluated the resident DCs and infiltrated leukocytes in the postischemic kidneys. Flow cytometry revealed that myeloid cell-derived HMGB1 deficiency did not affect the amount of resident DCs in the sham group, but reduced the population of resident DCs with the markers of CD11c+MHCII+F4/80+ in renal IRI group (Fig 14B, 15). Also, more infiltration of monocyte-derived macrophages marked by Ly6c+CD11b++ was observed in Mlys-HMGB1 knockout group at day one in postischemic kidneys (Fig 14A, 15). Ablation of endogenous HMGB1 contributed to the infiltration of monocyte-derived macrophages and reduced the population of renal resident DCs in postischemic kidneys.

To investigate if the deletion of intracellular HMGB1 aggravates dendritic cell death, the isolated monocytes from bone marrow were differentiated into DCs with additional GM-CSF. The data showed that myeloid cell-derived HMGB1 deficiency had no effect on phagocytosis of DCs (Fig 16). However, stimulation of DCs with 10 mM H<sub>2</sub>O<sub>2</sub> induced more cell death in the Mlys-HMGB1 knockout group (Fig 16).

Overall, the ablation of intracellular HMGB1 in myeloid cells sensitized resident dendritic cells to oxidative stress-related death triggering additional infiltration of immune cells from the bone marrow, which promoted renal IRI in postischemic kidneys.

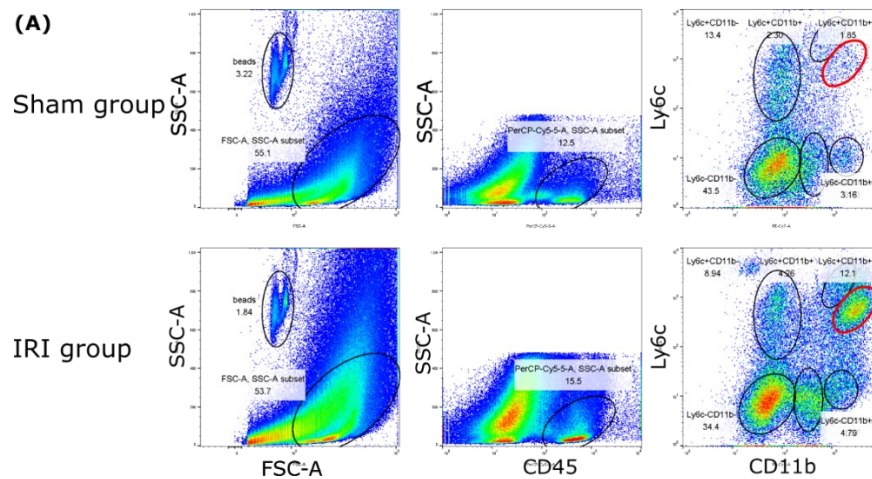


**Fig 14A. The gating strategy of monocyte-derived macrophages.** Kidney mononuclear cells were isolated from ischemic kidneys and sham group at day one in the reperfusion phase. CD45<sup>+</sup> leukocytes were gated and further split based on differential expression of ly6c and CD11b. Here I identified the population of monocyte-derived macrophages marked by Ly6c<sup>+</sup>CD11b<sup>++</sup> cells.

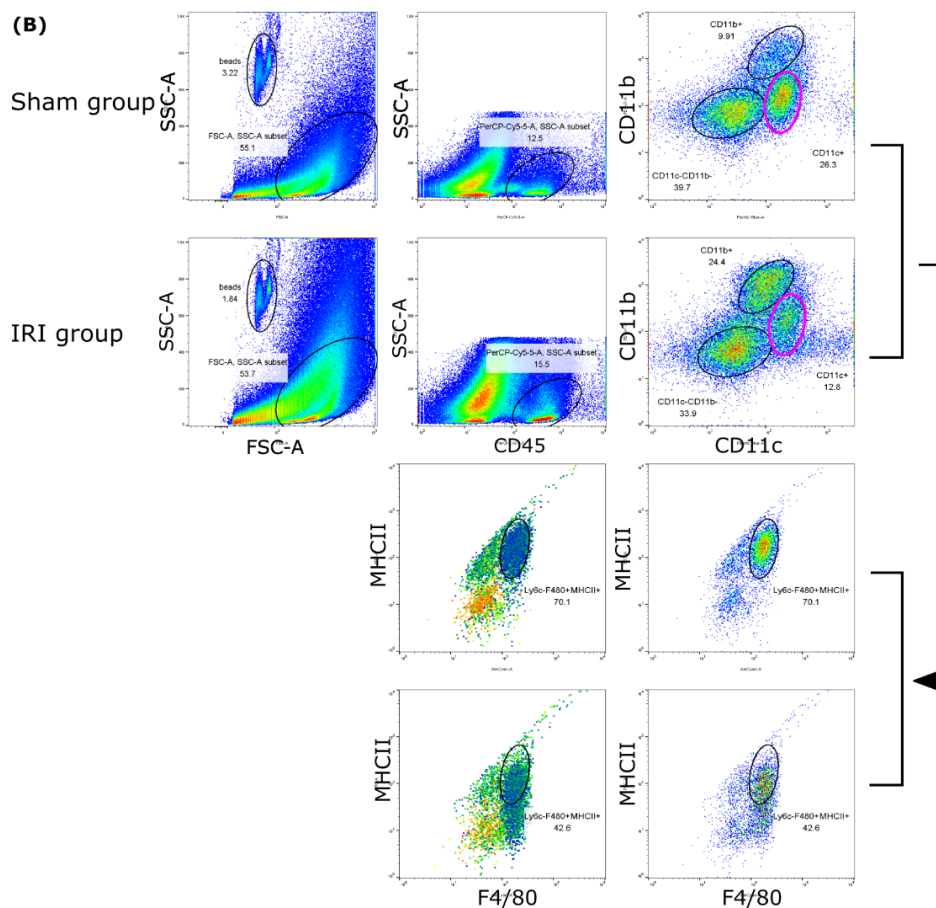


**Fig 14B. The gating strategy of renal resident DCs.** Kidney mononuclear cells were isolated, CD45<sup>+</sup> cells were gated and further subdivided with expression of CD11b and CD11c. The subpopulation of CD11c<sup>+</sup> cells was further divided into F4/80<sup>+</sup> and MHCII<sup>+</sup> cells, which were also shown Ly6c<sup>-</sup>. Here the identified Ly6c<sup>-</sup>F4/80<sup>+</sup>MHCII<sup>+</sup> cells are renal resident DCs.

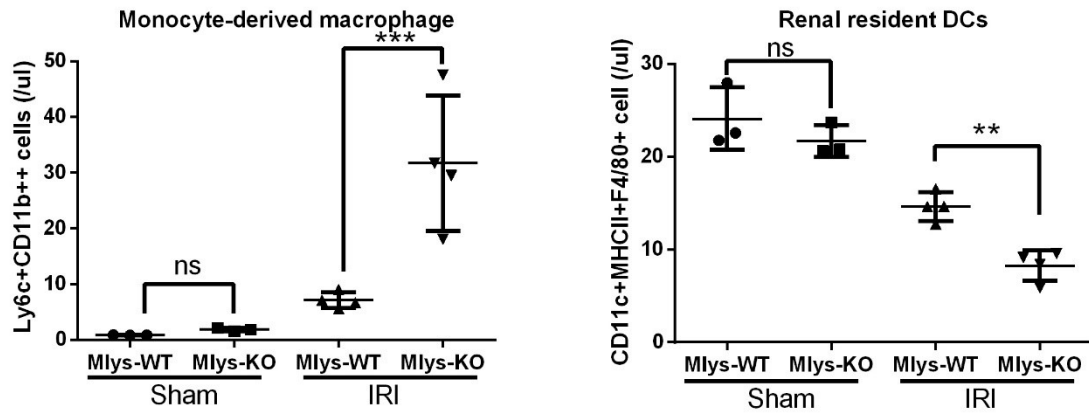


**Fig 15.** The quantification of monocyte-derived macrophages per microliter marked by Ly6c+CD11b++ and renal resident DCs marked by CD11c+MHCII+F4/80+. The Y-axis represents the population of cells per microliter.

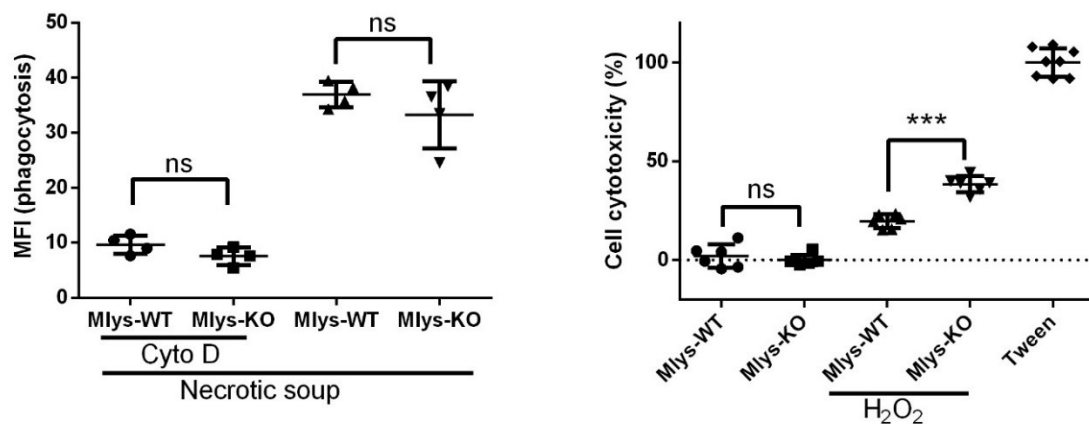


**Fig 16. Myeloid cell-derived HMGB1 deficiency aggravated hypoxia-induced dendritic cell death.** The isolated bone marrow-derived mononuclear cells were differentiated to macrophages or DCs with additional M-CSF or GM-CSF for 7 days, individually. The phagocytosis of macrophages to phrodo-labeled necrotic protein released by necrotic tubular cells. The data represented the mean fluorescence intensity (MFI) of macrophage phagocytosis. DCs challenged with 10 mM H<sub>2</sub>O<sub>2</sub> for 3 h, the cytotoxicity was measured by LDH assay.

#### 4.1.4 HMGB1 in myeloid cells determines the phenotype of infiltrating dendritic cells

At the late reperfusion phase, ischemic kidneys were infiltrated with diverse immune cells, such as monocyte-derived DCs, monocyte-derived macrophages, and T lymphocytes. To identify if HMGB1 deficiency in myeloid cells affected the phenotypes of infiltrated immune cells in the late reperfusion phase, Mlys-HMGB1 mice from 8- to

12-weeks old were subjected to 17 min unilateral IRI. At day 10 in the reperfusion phase, myeloid cell-derived HMGB1 deficiency contributed to the migration of monocyte-derived macrophages marked by CD11b<sup>++</sup>CCR2<sup>+</sup> cells (Fig 17B, 18). However, I identified less infiltrated dendritic cells marked by CCR2<sup>+</sup>F4/80<sup>+</sup>MHCII<sup>+</sup> population in MLys-HMGB1 knockout mice than control mice (Fig 17C, 18), which was compensated with more CD4<sup>+</sup>CD8<sup>+</sup> T cells (Fig 19-20). Thus, myeloid cell-derived HMGB1 deficiency modulated the phenotypes of infiltrating dendritic cells and macrophages in the late reperfusion phase.

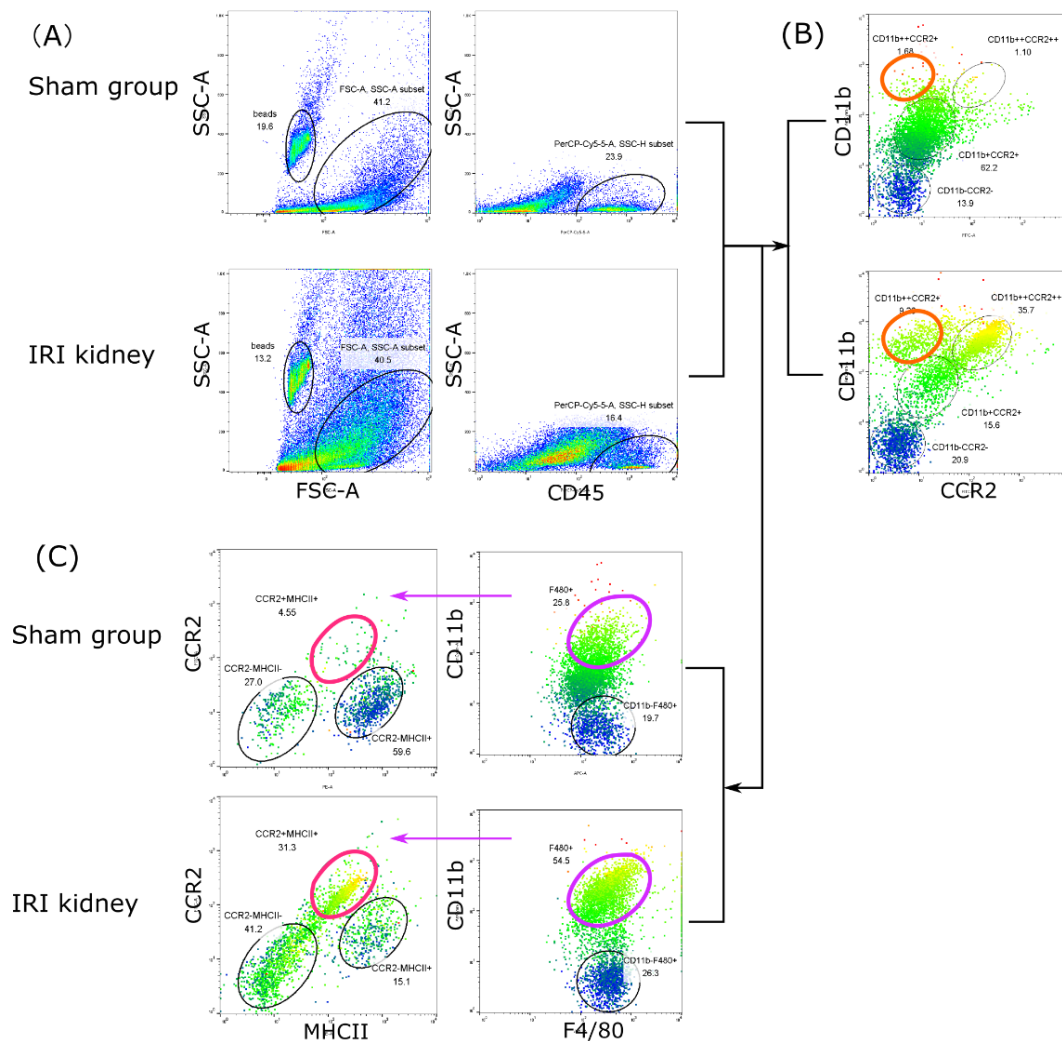


**Fig 17. The phenotypes of monocyte-derived DCs and monocyte-derived macrophages at day 10 in postischemic kidney injury.** (A) Kidney mononuclear cells were isolated from ischemic kidneys and sham group at day 10 in the reperfusion phase. CD45<sup>+</sup> leukocytes were gated. (B) In the other way, CD45<sup>+</sup> cells were subdivided into CCR2 and CD11b subpopulations. Here the population of CD11b<sup>++</sup>CCR2<sup>+</sup> cells represented monocyte-derived macrophages. (C) CD45<sup>+</sup> cells were analyzed with the expression of CD11b and F4/80 and the subpopulation of F4/80<sup>+</sup> cells were divided into CCR2 and MHCII subset. Here I identified infiltrated dendritic cells with the markers of CCR2<sup>+</sup>F4/80<sup>+</sup>MHCII<sup>+</sup>.



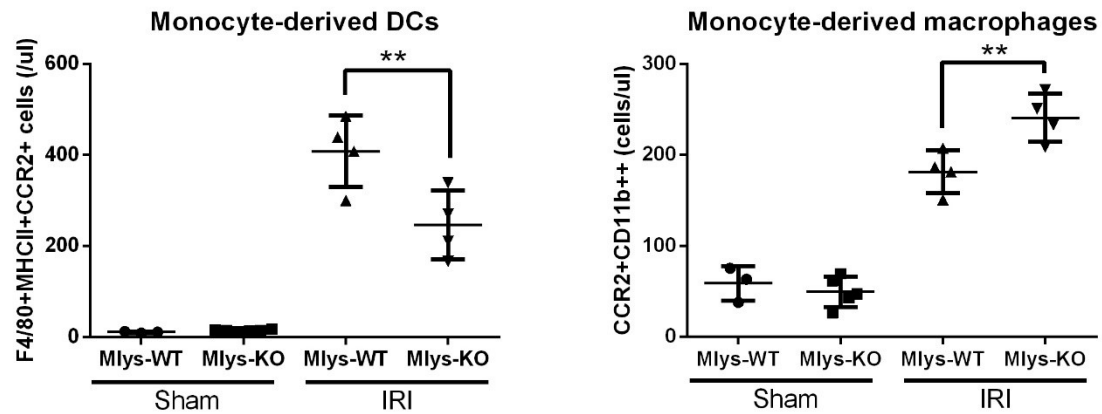


**Fig 18.** The quantification of monocyte-derived DCs marked by CCR2+F4/80+MHCII+ and monocyte-derived macrophages with the markers of CD11b++CCR2+. The Y-axis represents the population of cells per microliter.

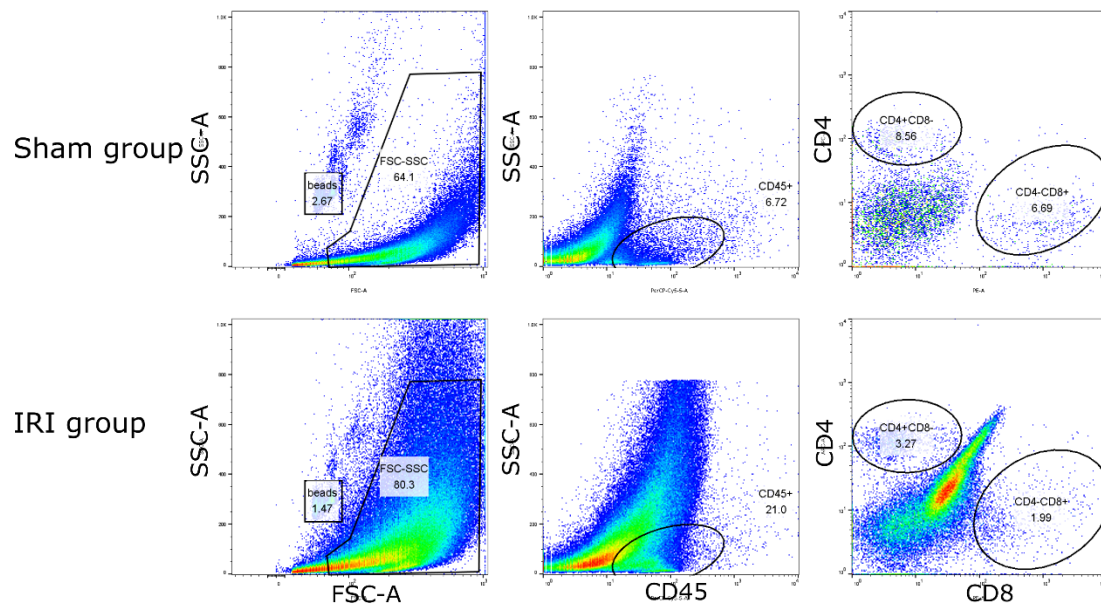


**Fig 19. T lymphocyte infiltration.** I isolated renal mononuclear cells from the kidney at day 10 in the reperfusion phase. CD45+ leukocytes were gated and divided into CD4-CD8+ T cells and CD4+CD8- T cells. Here I identified the population of CD4-CD8+ T cells by flow cytometry.

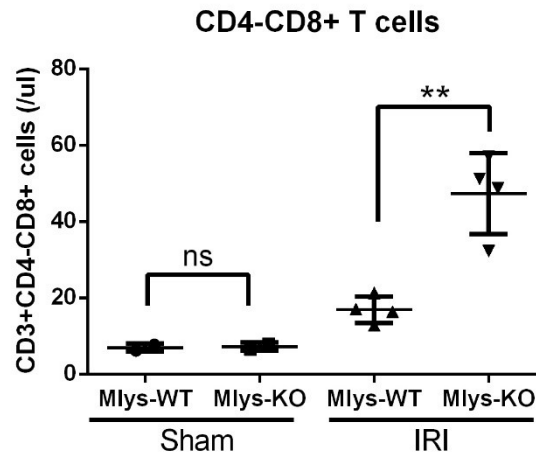


**Fig 20.** The quantification of CD4-CD8+ T lymphocytes. The Y-axis represents the population of cells per microliter.

#### 4.1.5 HMGB1 in myeloid cells ameliorates AKI-CKD transition

To evaluate the impact of myeloid cell-derived HMGB1 on the long-term outcomes, Mlys-HMGB1 mice were challenged with 17 min unilateral IRI, which resulted in CKD at 30 days of reperfusion. The data showed a consistent reduction of GFR in Mlys-HMGB1 knockout mice compared to control mice in postischemic kidney injury (Fig 21). Ischemic kidney function could not recover from the early kidney injury with severe tubular damage, more fibrosis, and less population of renal tubules marked by Lotus Tetragonolobus Lectin (proximal tubules) and Tamm-Horsfall protein (distal tubules) in Mlys-HMGB1 knockout mice (Fig 22-23). Thus, my data showed that ablation of intracellular HMGB1 in myeloid cells did not protect from the early kidney injury, but contributed to the progression of CKD on the long-term.

Altogether, myeloid cell-derived HMGB1 deficiency induced amplified cell death of renal resident DCs triggering more infiltration of monocyte-derived macrophages, which aggravated renal AKI in postischemic kidneys. In addition, myeloid cell-derived HMGB1 ablation modulated the phenotypes of infiltrated dendritic cells and diminished the infiltration of monocyte-derived DCs in the late reperfusion phase. The aggravated AKI and less infiltration of DCs may result in the progression of tissue damage and fibrosis in CKD.



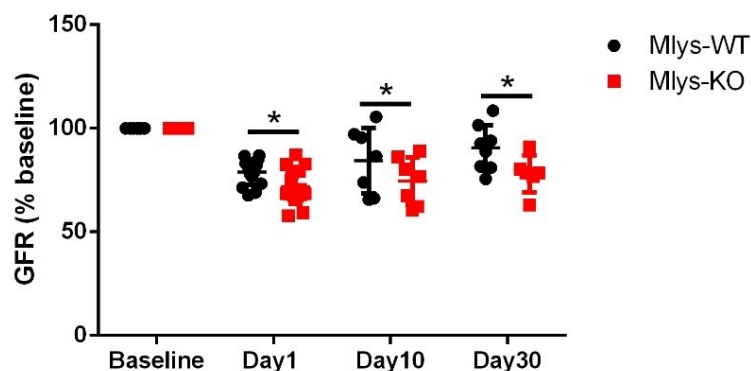


**Fig 21. The renal glomerular filtration rate (GFR) at the different time points in postischemic kidney injury.** The GFR was measured at the different reperfusion time points. GFR changes were shown from the baseline GFR.

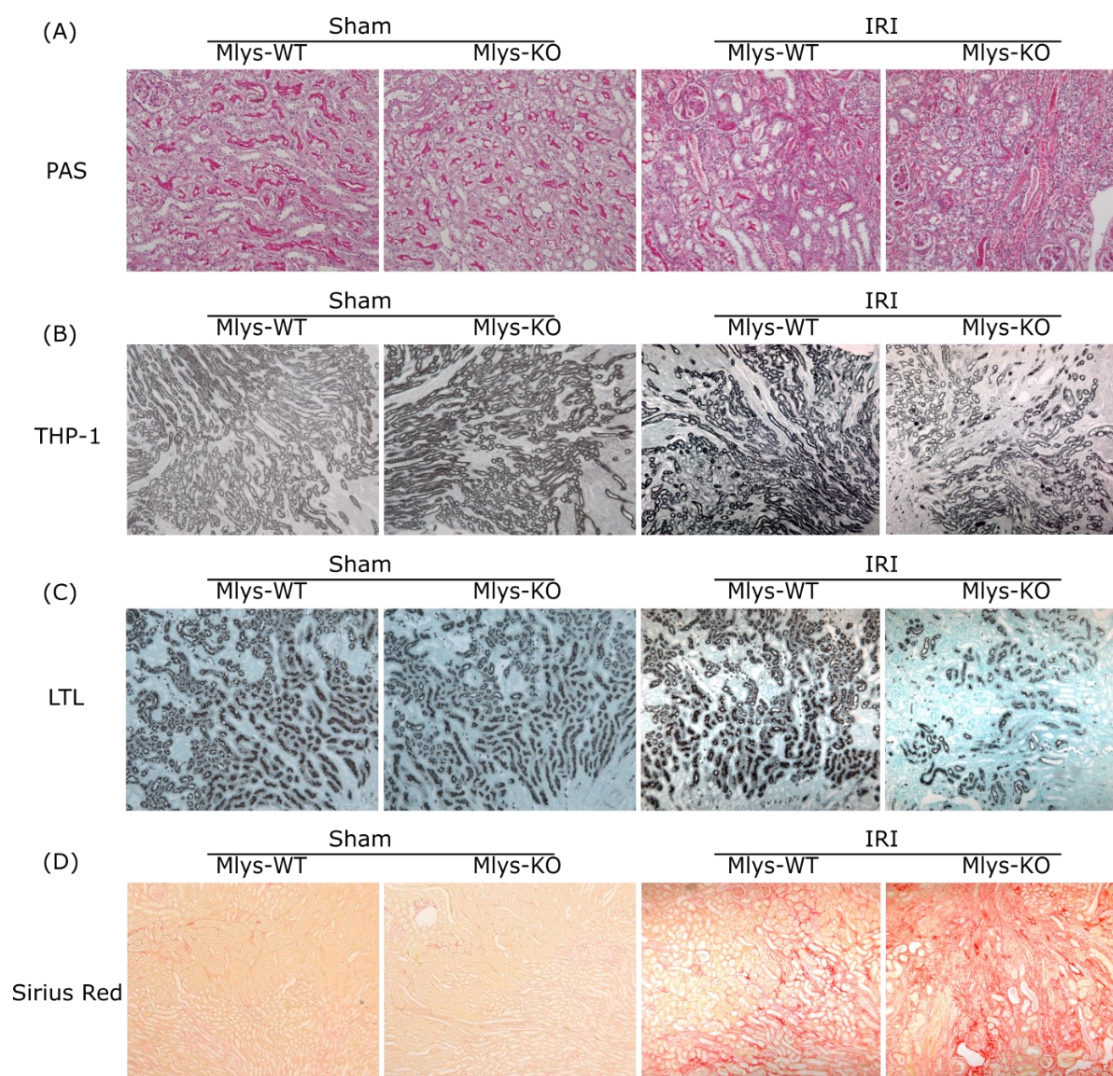


**Fig 22. Pathological histology in CKD.** (A) Periodic acid-Schiff (PAS) was applied for the quantification of renal tubular damage. (B) Tamm-Horsfall protein (THP-1) staining represents distal tubules. (C) Lotus tetragonolobus lectin (LTL) staining represents the proximal tubules. (D) Sirius red was used for the collagen or fibrosis level of renal tissue. Images were shown at the magnification of 200x.

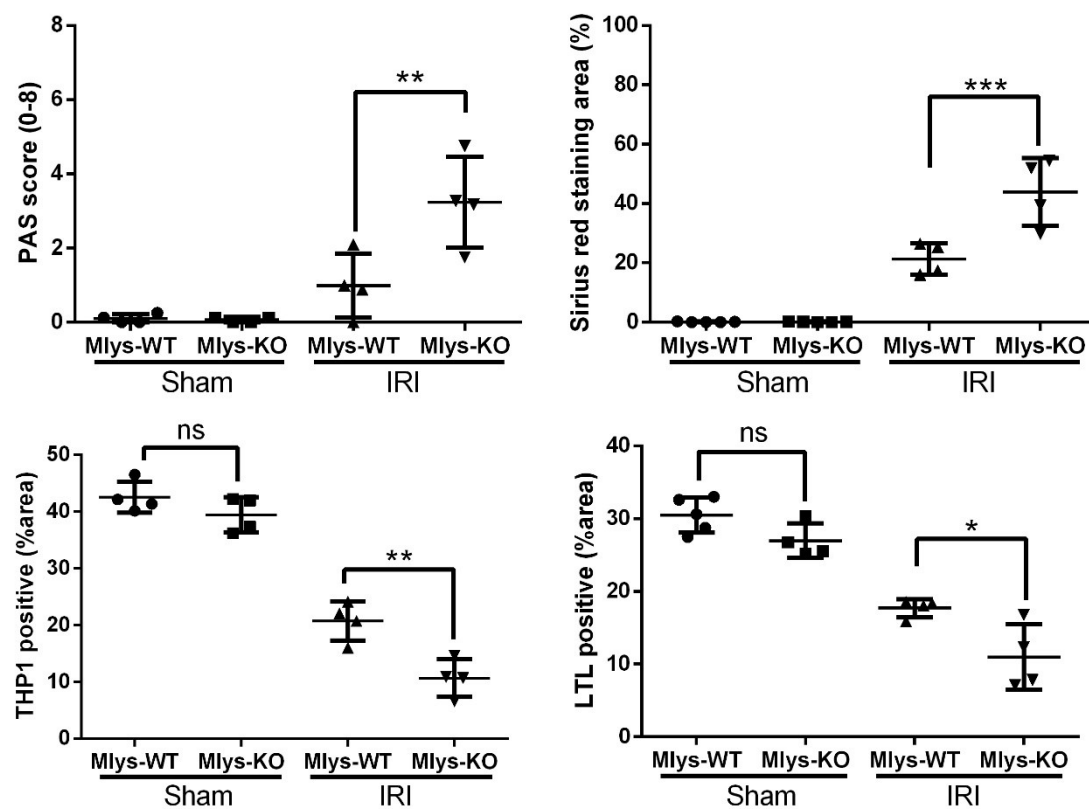


**Fig 23.** The quantification of histological staining. Mlys-WT (Mlys-HMGB1 WT mice) represent control group, Mlys-KO (Mlys-HMGB1 KO mice) represents HMGB1 knockout group. Sham means no ischemic kidney injury, IRI represents ischemia-reperfusion injury.

## 4.2 HMGB1 in tubular epithelial cells contributes to postischemic kidney injury

HMGB1 released from necrotic cells triggers the inflammatory response and amplifies kidney injury in renal IRI [73]. Thus, released HMGB1 may serve as a therapeutic target to protect from kidney injury. However, if and how renal tubular-derived endogenous HMGB1 contributes to kidney injury is elusive.

### 4.2.1 Ablation of HMGB1 in Pax8-positive tubular cells

To identify if renal tubular-derived HMGB1 contributes to kidney injury in ischemic kidneys, I established a transgenic mouse line with TetOCre recombinase activated by the transactivator of rTtA under the control of the Pax8 promotor (Fig 24). To prove the ablation of HMGB1 in renal Pax8-positive tubular cells, primary tubular cells were isolated from Pax8-HMGB1 mice. Immunofluorescence staining and western blot indicated that the ablation of HMGB1 in primary tubular epithelial cells, but not bone marrow-derived macrophages (Fig 25).

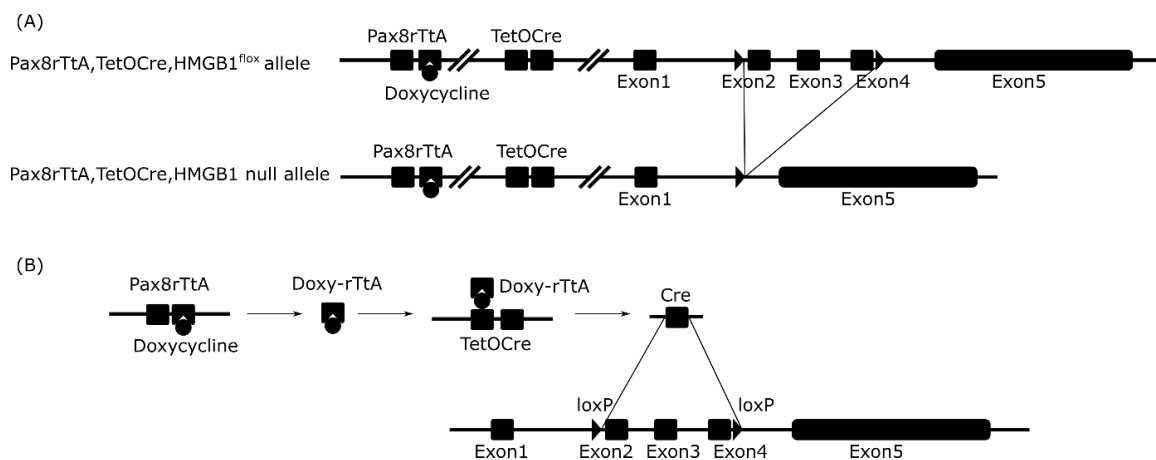


**Fig 24. Characterization of HMGB1 deficiency in renal Pax8-positive tubular cells.** (A) The transactivator rTtA was inserted into the promoter of the Pax8 gene, while TetOCre recombinase was under the control of Pax8rTtA promotor. Doxycycline induced rTtA transgene to activate TetOCre recombinase, which deletes the nuclear HMGB1 in Pax8-positive tubular epithelial cells. (B) Doxycycline-combined rTtA activates TetO-associated Cre activation, Cre cut the loxP site of HMGB1.

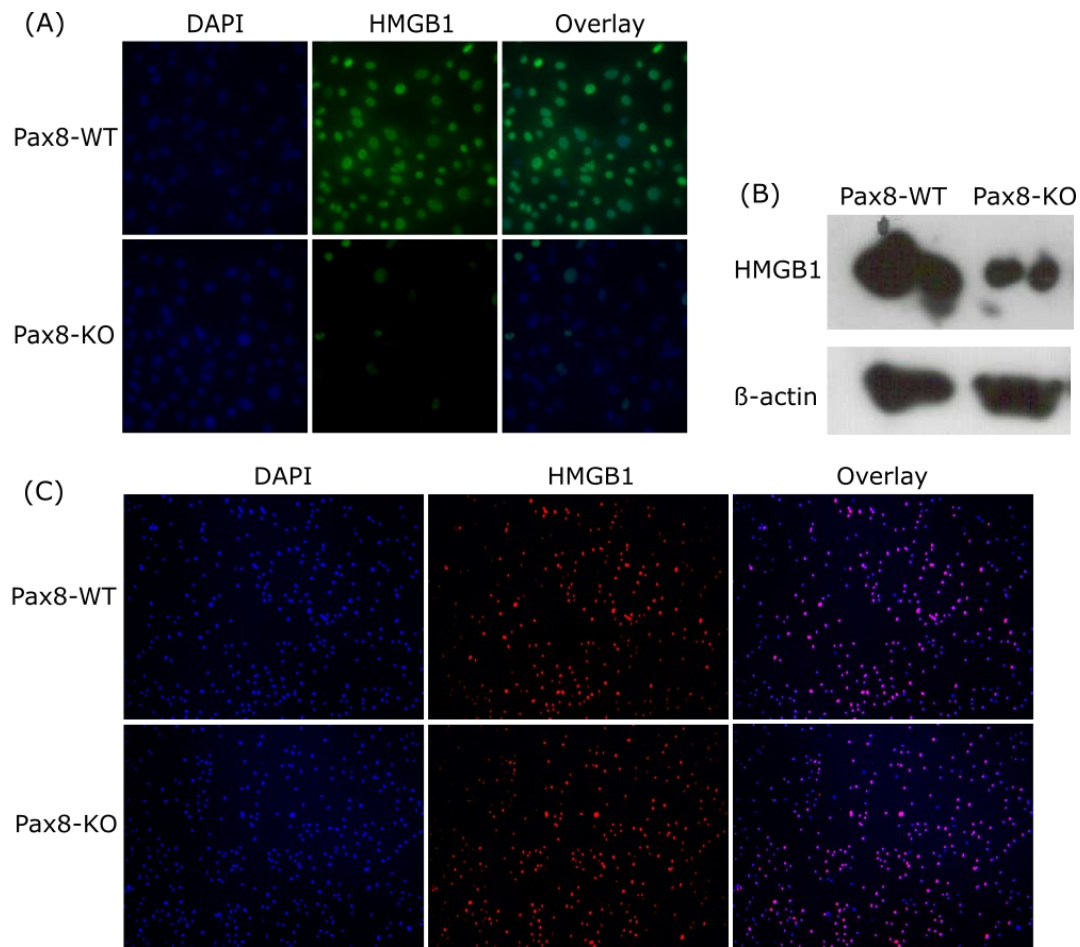


**Fig 25. The deletion of HMGB1 in renal Pax8-positive tubular cells.** A. Renal primary tubules were isolated from Pax8-HMGB1 mice. Immunofluorescence staining of HMGB1 in primary tubular cells were indicated. Images were shown at the magnification of 200x. B. Proteins were extracted from primary tubular cells. HMGB1 protein level was measured by western blot.  $\beta$ -actin as reference. C. Monocytes were isolated from bone marrow of Pax8-HMGB1 mice and differentiated to macrophages with additional M-CSF. Immunofluorescence staining of HMGB1. Images were shown at the magnification of 100x. Pax8-WT (Pax8-HMGB1 WT mice) represents control group. Pax8-KO (Pax8-HMGB1 KO mice) represents HMGB1 knockout group.

#### 4.2.2 Nuclear HMGB1 in Pax8-positive tubular cells has no substantial effect on postischemic acute kidney injury

To investigate the impact of HMGB1 deficiency in Pax8-positive cells on postischemic AKI, Pax8-HMGB1 mice from 8- to 12-weeks-old were subjected to 17 min unilateral IRI. My data showed that there was no significant difference in GFR decline at day 1 and day 7 in the reperfusion phase (Fig 26). There was no significant difference in tubular damage, the percentage of proximal tubules (marked by Lotus tetragonolobus lectin), and distal tubules (marked by Tamm-Horsfall protein) at day 7 in the reperfusion phase (Fig 27-28). Knockout HMGB1 in Pax8-positive tubular cells



has no significant effect on the mRNA level of gene expression correlated with inflammation (*TNF $\alpha$* , *iNOS*) and kidney injury (*KIM1*, *Clusterin*) (Fig 29). Thus, the deletion of intracellular HMGB1 in renal Pax8-positive cells did not significantly affect AKI in postischemic kidneys.

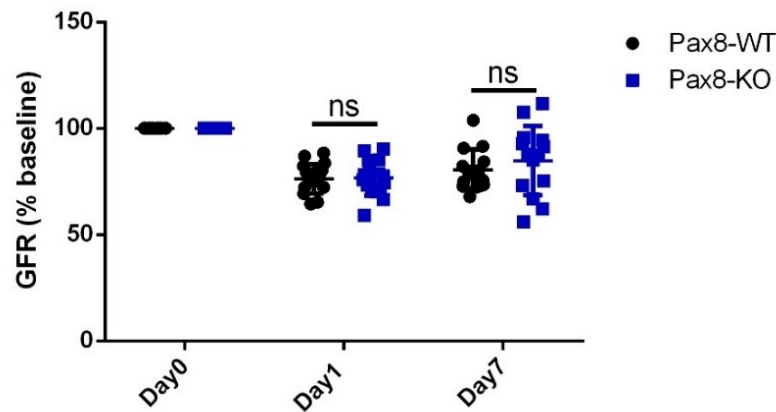


**Fig 26. The GFR level in postischemic kidney injury.** Pax8-HMGB1 mice were subjected to 17 min unilateral IRI with 1 day or 7 days reperfusion. GFR changes were shown from the baseline GFR.

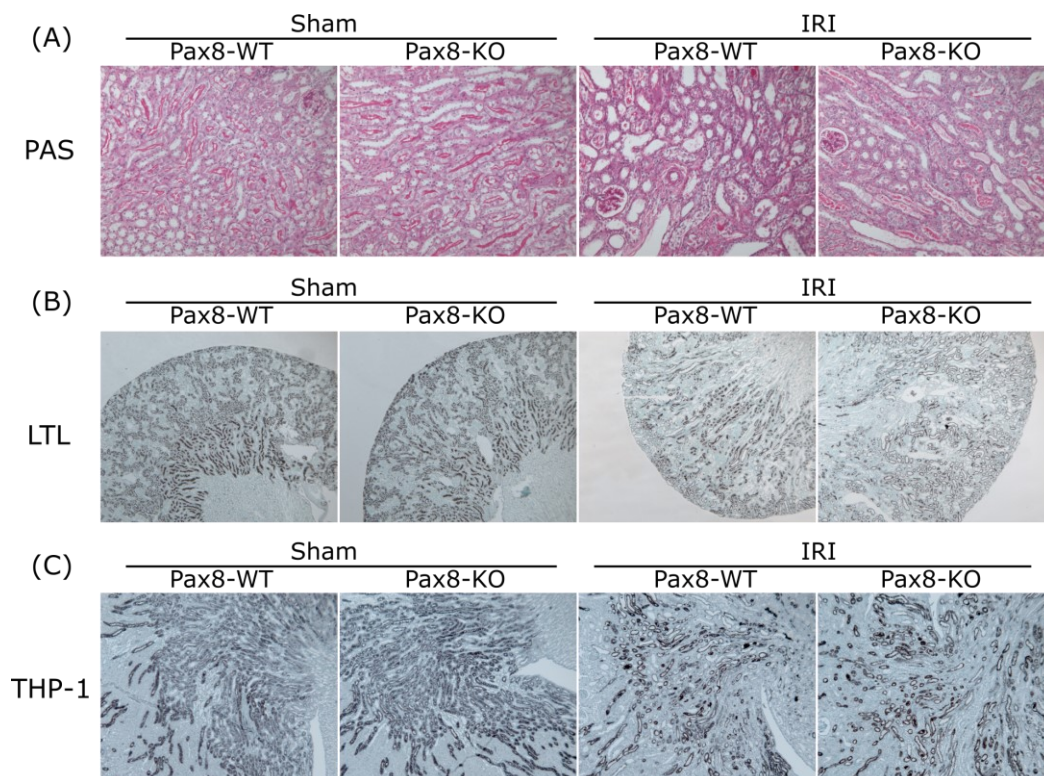


**Fig 27. Histological staining of kidney damage in postischemic kidney injury.** (A) Periodic acid-Schiff (PAS) was applied for the quantification of renal tubular damage. (B) Lotus tetragonolobus lectin (LTL) staining represents the proximal tubules. (C) Tamm-Horsfall protein (THP-1) staining represents distal tubules. Images were shown at the magnification of 200x. (LTL showed at magnification of 100x).

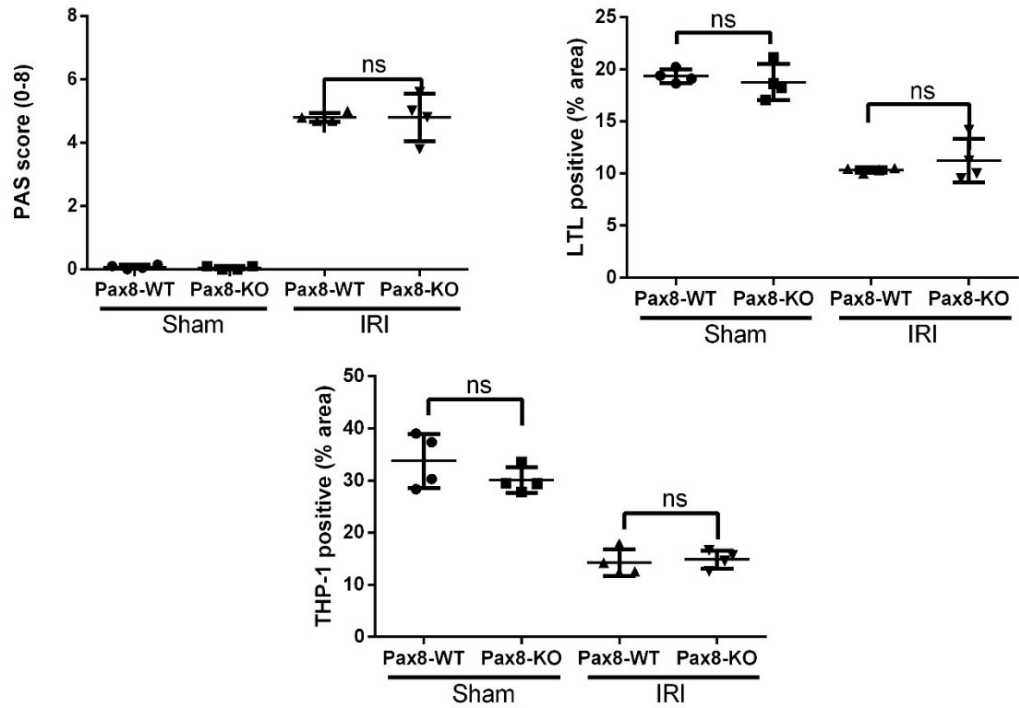


**Fig 28.** The quantification of histological staining. Sham means no ischemic kidney injury, IRI represents ischemia-reperfusion injury.

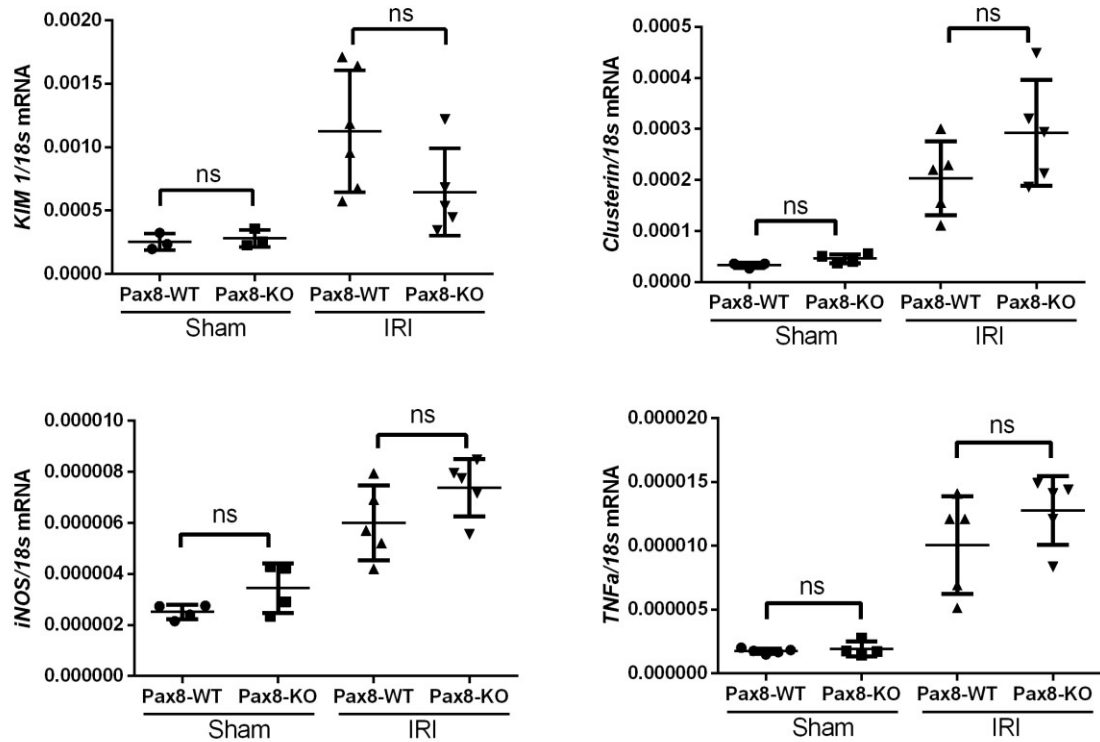


**Fig 29.** Total mRNA of kidney injury and inflammation at day 7 in postischemic kidney injury. The mRNA level of gene expression was determined for the indicated genes associated with kidney injury and inflammation at day 7 in postischemic kidneys.

#### **4.2.3 HMGB1 in Pax8-positive tubular cells contributes to AKI-CKD transition**

To investigate the impact of endogenous HMGB1 deficiency in renal Pax8-positive tubular cells on the transition from AKI to CKD progression in postischemic kidney injury, Pax8-HMGB1 mice were subjected to 17 min unilateral IRI with 30 days reperfusion. My data showed that HMGB1 deficiency mice increased GFR level at the late reperfusion phase after ischemia (Fig 30). The histological staining showed that postischemic kidneys had less tubular damage at day 30 in Pax8-HMGB1 KO mice. There was a higher percentage of tubules marked by Lotus tetragonolobus lectin (proximal tubules) and Tamm-Horsfall protein (distal tubules) in Pax8-HMGB1 KO mice at day 30. It also showed less fibrosis in Pax8-HMGB1 KO mice (Fig 31-32). In addition, it showed less delta kidney weight in Pax8-HMGB1 KO mice at day 30 (Fig 33).

Pax8-derived HMGB1 deficiency showed decreased level of HMGB1 expression. The mRNA level showed a higher level of fatty acid metabolic activity, and lower level of antioxidants in Pax8-HMGB1 KO mice at day 30 (Fig 34). Myeloid differentiation primary response 88 (Myd88) protein as an adaptor, connecting the signals from outside to inside the cells. Perilipin 4 (Plin4) as a regulator of lipid storage modulates free fatty acids for metabolic activation. Liver-type fatty acid-binding protein (L-FABP) protein involves in the metabolism of long-chain fatty acids. Peroxiredoxin 1 (Prdx1) and Peroxiredoxin 5 (Prdx5) play an antioxidant protective role in cells and may have a proliferative effect on cellular damage. Thus, the ablation of HMGB1 in Pax8-positive tubular cells may support the recovery of renal tubular cells in the late recovery phase. This implied that HMGB1 deficiency prevented the transition from AKI to CKD in postischemic kidneys.

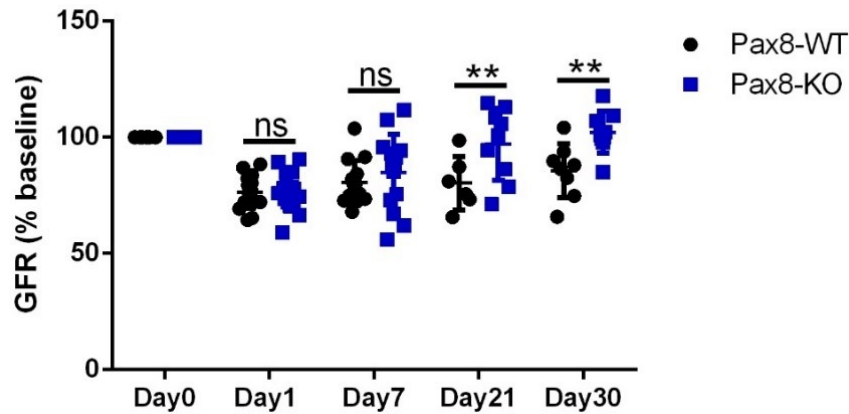


**Fig 30. The renal glomerular filtration rate (GFR) at the different time points in postischemic kidney injury.** Pax8-HMGB1 mice were subjected to 17 min unilateral IRI with 30 days reperfusion. GFR changes were shown from the baseline GFR.

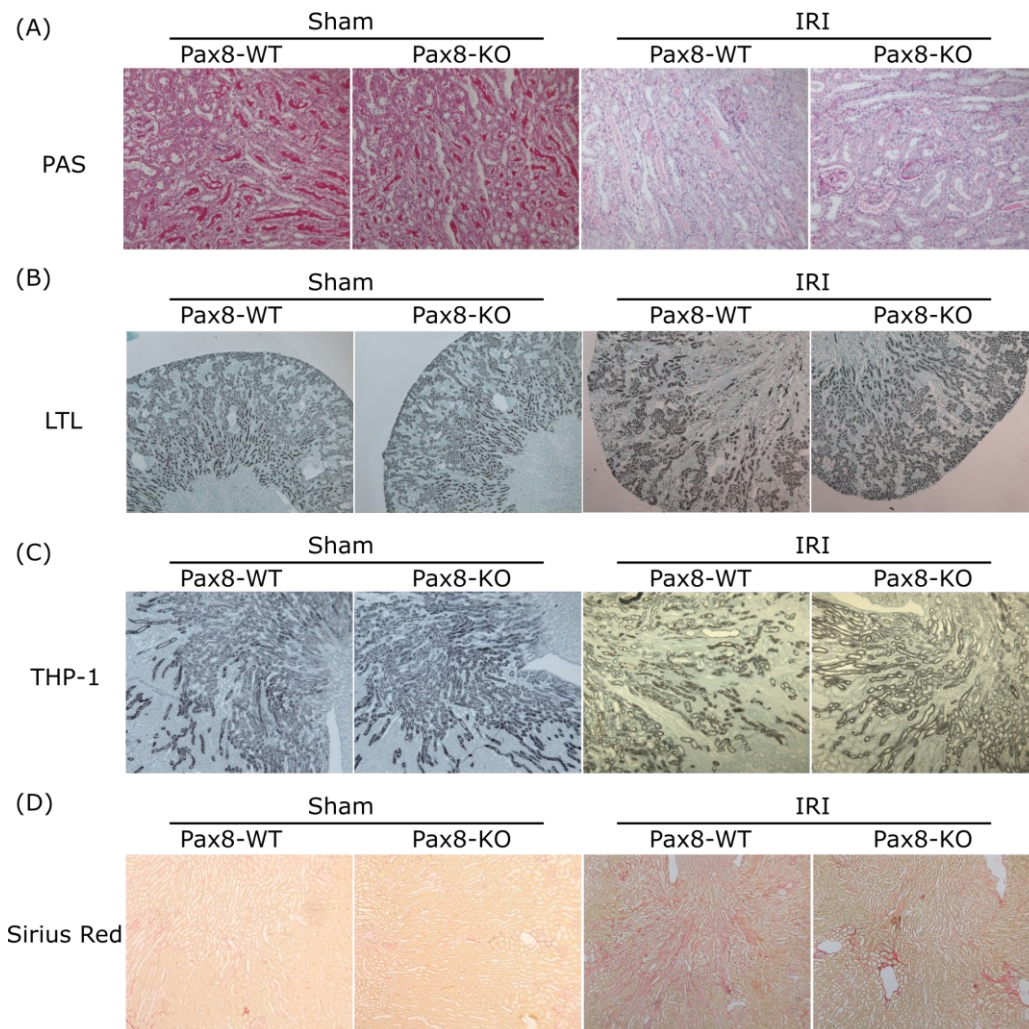


**Fig 31. Histology in CKD.** (A) Periodic acid-Schiff (PAS) was applied for the quantification of renal tubular damage. (B) Lotus tetragonolobus lectin (LTL) staining represents the proximal tubules. (C) Tamm-Horsfall protein (THP-1) staining represents distal tubules. (D) Sirius red was used for the collagen or fibrosis level of renal tissue. Images were shown at the magnification of 200x (LTL showed at magnification of 100x).



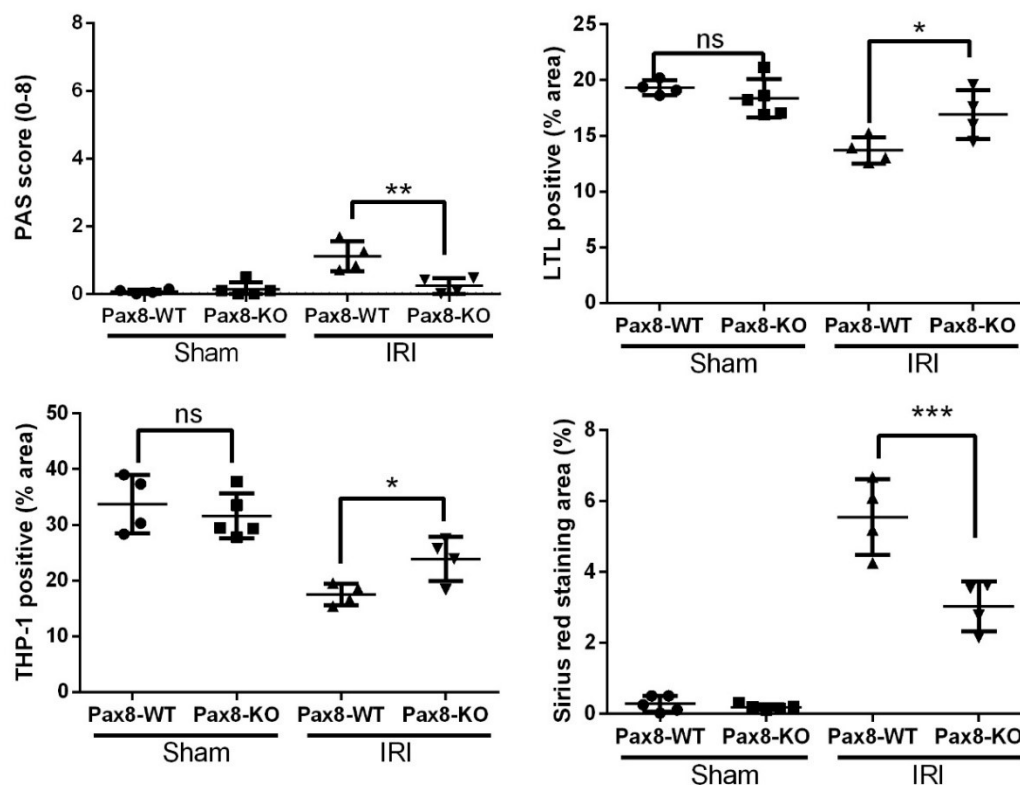


**Fig 32.** The quantification of histological staining at day 30 in postischemic kidneys.

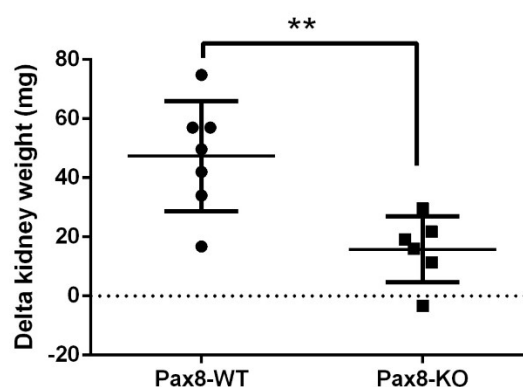
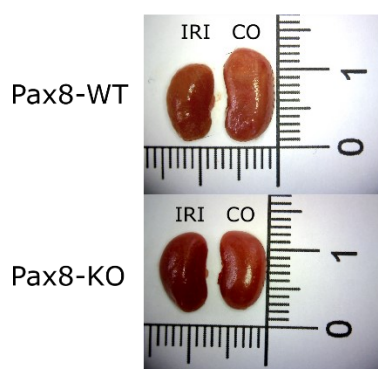


**Fig 33. Delta kidney weight at day 30 in postischemic kidney injury.** The delta kidney weight (contralateral kidney minus ischemic kidney weight) showed at day 30 in postischemic kidneys.

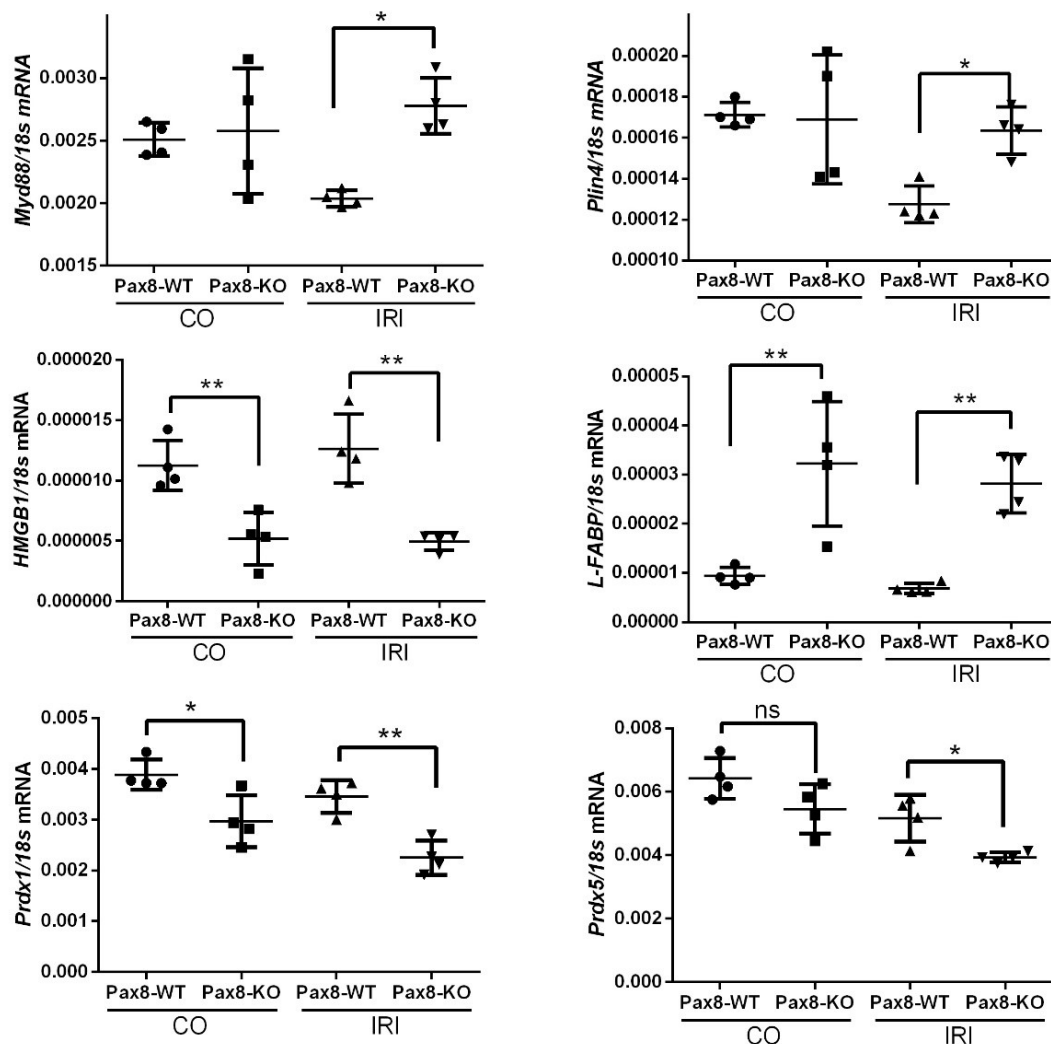


**Fig 34. Total mRNA of contralateral and ischemic kidneys at day 30 in postischemic kidney injury.** The mRNA level of gene expression was determined for the indicated genes. CO represents from contralateral kidneys, IRI represents from ischemic kidneys.

#### 4.2.4 Endogenous HMGB1 in Pax8-positive tubular cells as a late mediator contributes to tubular cell damage

To address the putative function of HMGB1 in tubular cells, murine primary tubular cells were isolated from Pax8-HMGB1 WT mice and Pax8-HMGB1 KO mice. *In vitro*, primary tubular cells were challenged with 1 mM  $H_2O_2$  to mimic hypoxia. The data showed that ablation of intracellular HMGB1 in Pax8-positive tubular cells protected from  $H_2O_2$ -induced cell death at the late time point (Fig 35).

To further verify that HMGB1 as a late mediator contributes to cell death, primary murine tubular epithelial cells were administrated with 1 mM  $H_2O_2$  and observed for 24

h using time-lapse imaging. The data showed HMGB1 deficiency protected against tubular cell death at the late time point (Fig 36).

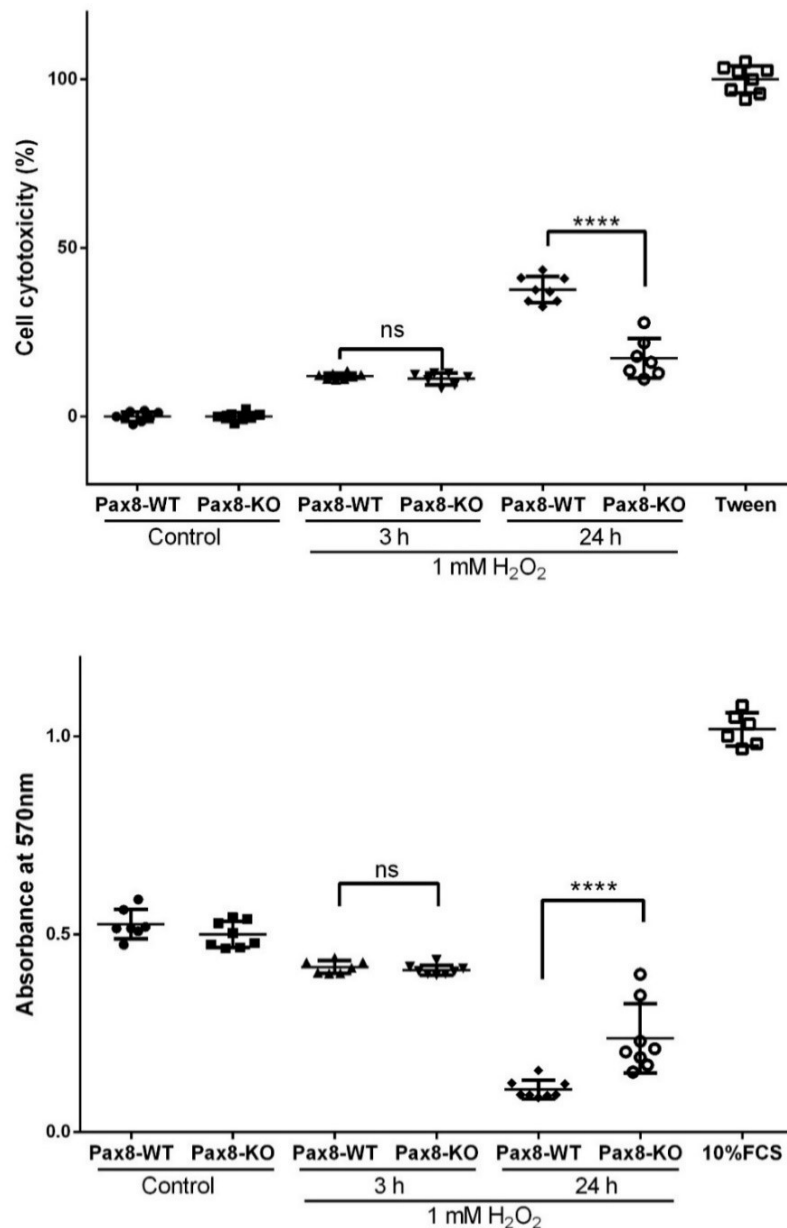


**Fig 35. The cell viability of renal primary tubular cells.** Renal murine primary tubular cells were isolated from Pax8-HMGB1 WT and Pax8-HMGB1 KO mice, individually. Both isolated primary tubular cells were treated with 1 mM H<sub>2</sub>O<sub>2</sub> for 3h and 24h, individually. The cytotoxicity was measured by LDH assay. The cell metabolic activity was measured by MTT assay. 2% Tween or 10 % FCS as positive control group.

Altogether, tubular cell-derived HMGB1 modulates late phenotype of kidney injury in renal IRI. Deleting endogenous HMGB1 in tubular cells may postpone the propagation of kidney injury and prevent AKI progression to CKD in postischemic

kidneys. This implied that endogenous HMGB1 in renal resident tubular cells might contribute to kidney damage and fibrosis in CKD.

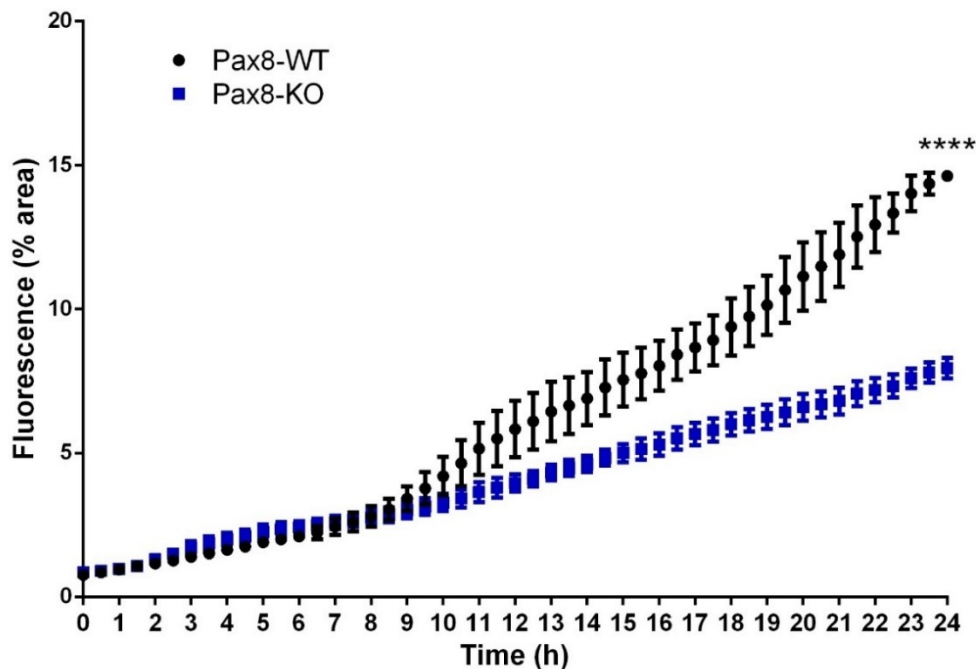


**Fig 36. Time lapse imaging.** Isolated renal primary tubular cells were treated with 1 mM  $H_2O_2$  to induce cell death. Time lapse images were obtained every 30 min for 24h. 1  $\mu$ M Helix NP Green nucleic acid stain was administrated to visualize the permeabilized cells. Fluorescence percentage represents the proportion of permeabilized damaged cells.

#### 4.3 Targeting HMGB1 with inhibitors attenuates kidney injury in postischemic kidneys

Extracellular HMGB1 as a danger signal elevates cellular damage and promotes inflammatory response, which contributes to necroinflammation and kidney injury [73, 143]. Data have reported that HMGB1 antagonists acts as therapeutic agents in HMGB1-related diseases [81, 99]. For example, glycyrrhizic acid impedes pro-inflammatory response by blocking HMGB1 phosphorylation and secretion in postischemic brain injury [81, 144]. In addition, ethyl pyruvate is a potent inhibitor of HMGB1 by preventing the shuttling from the nucleus to the cytoplasm, which reduces cytokines production and ameliorates inflammatory disease[81, 145]. However, the ability of HMGB1 antagonists protect from renal IRI has not been fully clarified.

### **4.3.1 Preemptive HMGB1 blockage with glycyrrhizic acid or ethyl pyruvate attenuates postischemic acute kidney injury**

To investigate if HMGB1 antagonists protect against renal tubular cell damage *in vitro*, the renal murine tubular cells were administrated with 1 mM H<sub>2</sub>O<sub>2</sub> to mimic hypoxia. Ethyl pyruvate can protect from cellular damage and cell death, while glycyrrhizic acid at a low concentration reduced renal tubular epithelial cell death (Fig 37A, 37B).

To validate the protective effect of HMGB1 inhibitors on human primary tubular cells under hypoxia, I did time-lapse imaging with primary human renal cells (RPCs) for cell death. RPCs were treated with different antagonists 30 min before administrating of 1 mM H<sub>2</sub>O<sub>2</sub> for 24 h. Z-VAD as a pan-caspase inhibitor blocks apoptosis [146]. Nec1f simultaneously targets necroptosis and ferroptosis. In addition, Helix NP Green was added to visualize the permeabilized damaged cells. The results showed that HMGB1 inhibitors could protect against H<sub>2</sub>O<sub>2</sub>-induced human renal cell death (Fig 38).

To investigate if the extracellular HMGB1 released from necrotic cells works as a therapeutic target in renal IRI, here I introduced two antagonists of HMGB1 to the renal IRI model. I performed 17 min unilateral IRI in C57BL6/J mouse with the intervention of HMGB1 inhibitors, glycyrrhizic acid (Gly), or ethyl pyruvate (EP) 1 h before IR surgery and daily treatment until day 7. The endpoint was kidney function at day 7 after ischemia. The intervention with HMGB1 inhibitors significantly increased the GFR level compared to control mice at day 7 after ischemia (Fig 39). Plasma creatinine level and HMGB1 concentration declined in the intervention group (Fig 40). Furthermore, HMGB1 inhibitors protected against tubular damage, which was demonstrated with PAS staining (Fig 41).

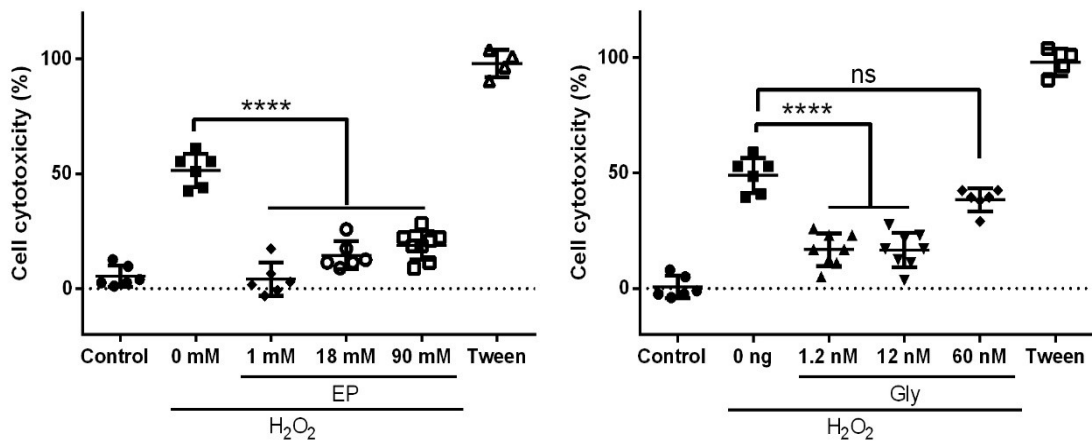


**Fig 37. Inhibition of HMGB1 with antagonists decreased tubular cell death in vitro.** Renal primary tubular epithelial cells were administrated with 1 mM H<sub>2</sub>O<sub>2</sub> for 3h to mimic hypoxia-induced cell death. Different concentrations of HMGB1 inhibitors were added 30 min before H<sub>2</sub>O<sub>2</sub> administration. The cell cytotoxicity was quantified by LDH assay.

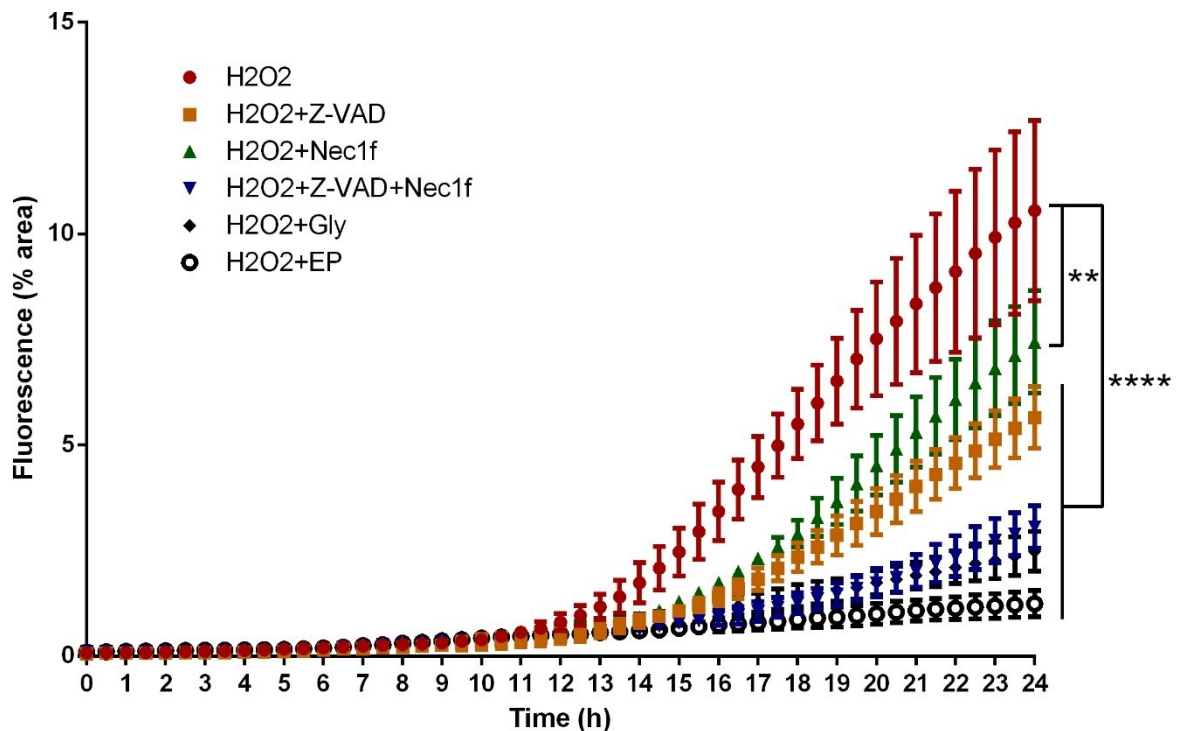


**Fig 38. HMGB1 antagonists attenuate primary renal cell (RPC) death in vitro.** RPCs were administrated with 1 mM H<sub>2</sub>O<sub>2</sub> for 24 h, pretreated with different antagonists (10  $\mu$ M Z-VAD or 20  $\mu$ M Nec1f or 10  $\mu$ M Z-VAD + 20  $\mu$ M Nec1f or 10 ng/ml Gly or 1 mM EP). Still images of a time lapse were recorded every 30 min for 24h. 1  $\mu$ M Helix NP Green nucleic acid stain was added to visualize the permeabilized cells. Fluorescence percentage represents the proportion of permeabilized damaged cells.

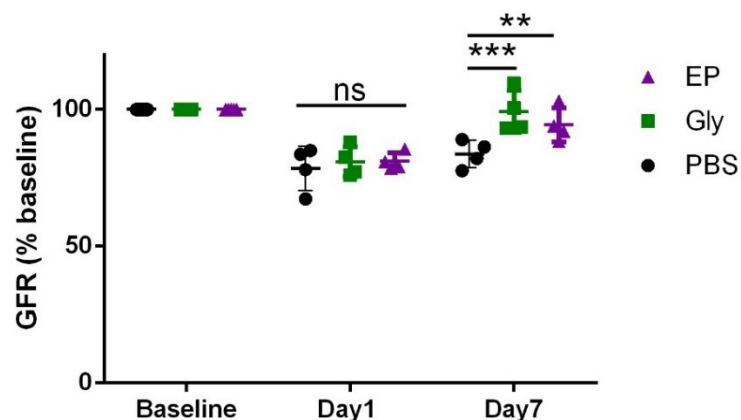


**Fig 39. Inhibition of extracellular HMGB1 with antagonists protected from acute kidney injury.** The GFR level at the different time points in postischemic kidney injury. GFR changes were shown from the baseline GFR. EP represents ethyl pyruvate, Gly represents glycyrrhizic acid, PBS as control group.

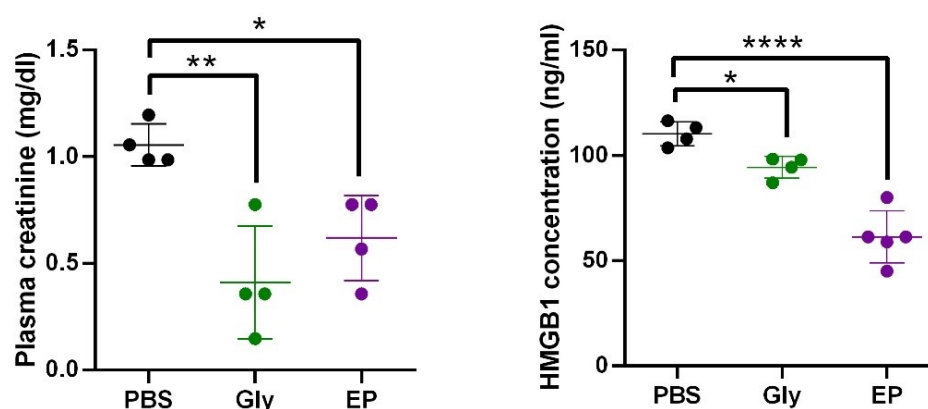


**Fig 40. Plasma creatinine and HMGB1 concentration in postischemic kidney injury.** The plasma creatinine level and HMGB1 concentration at day 7 in postischemic kidneys.

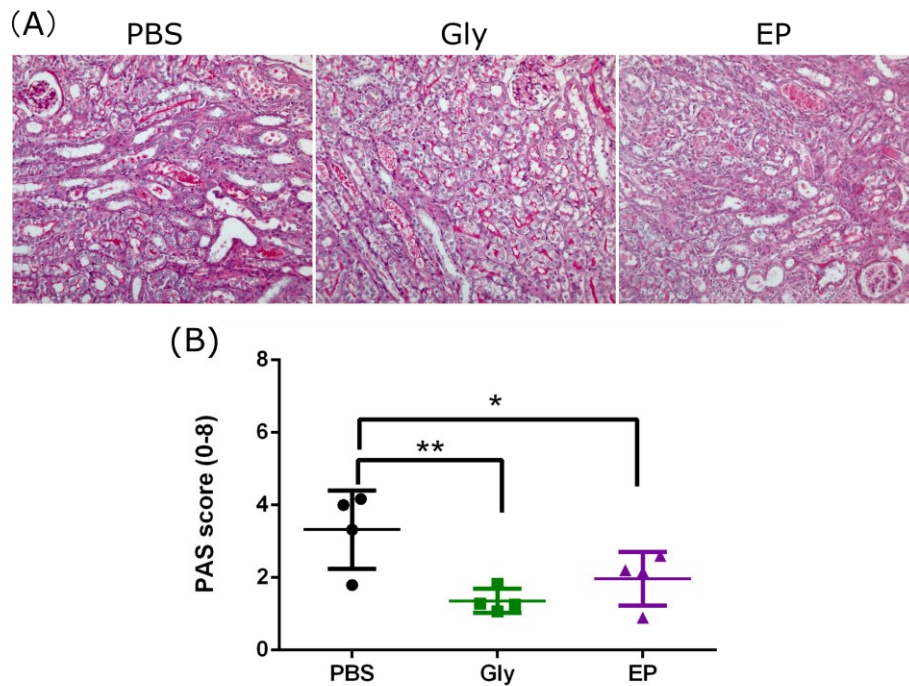


**Fig 41. HMGB1 inhibitors and postischemic kidney injury.** (A) Periodic acid-Schiff (PAS) was applied for the quantification of renal tubular damage. Images were shown at the magnification of 200x. (B) The quantification of PAS staining.

#### 4.3.2 Preemptive treatment with HMGB1 inhibitors attenuates chronic kidney disease in postischemic kidneys

To investigate if HMGB1 antagonists prevent the transition of AKI to CKD, we did 17 min unilateral IRI in C57BL6/J mouse with the intervention of HMGB1 inhibitors 1 h before IR surgery and daily treatment until day 14. The endpoints were GFR, delta kidney weight and tubular damage at day 30 after ischemia. Our data showed that HMGB1 inhibitors increased GFR level consistently (Fig 42). Intervention of HMGB1 antagonists reduced delta kidney weight compared with control group (Fig 43). HMGB1 antagonists group showed better outcomes of tubular damage and high proportion of proximal tubules (marked by Lotus Tetragonolobus Lectin), and distal tubules (marked by Tamm-Horsfall protein) in ischemic kidneys (Fig 44, 45). This implied that HMGB1 inhibitors prevented the transition of AKI to CKD, which may prevent tubular damage and contribute to tissue healing in postischemic kidney injury.



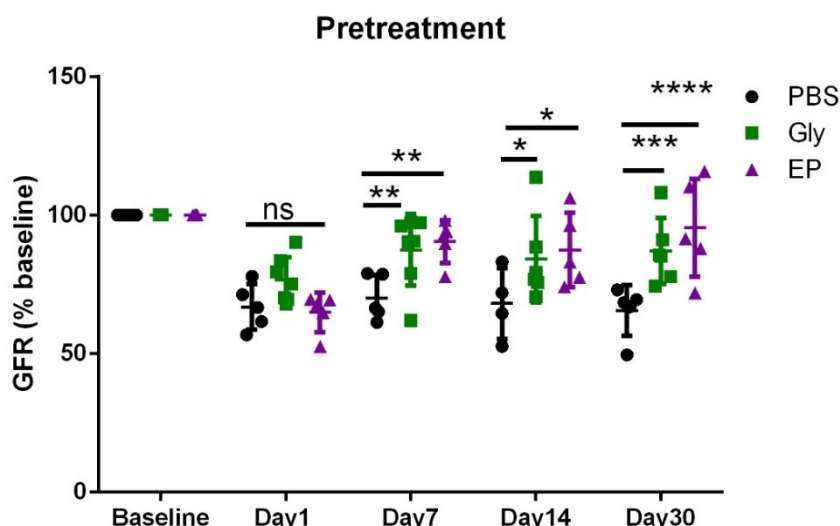


**Fig 42. Pretreatment of HMGB1 antagonists increased GFR level after ischemia.** The GFR level (from baseline) at the different time points in postischemic kidneys. GFR changes were shown from the baseline GFR. EP represents ethyl pyruvate, Gly represents glycyrrhizic acid, PBS as control group.

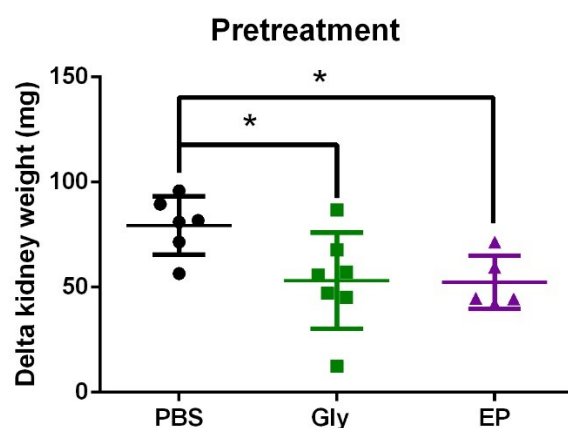


**Fig 43. Delta kidney weight at day 30 in postischemic kidney injury.** The delta kidney weight (contralateral kidney minus ischemic kidney weight) showed at day 30 in postischemic kidneys. EP represents ethyl pyruvate, Gly represents glycyrrhizic acid, PBS as control group.

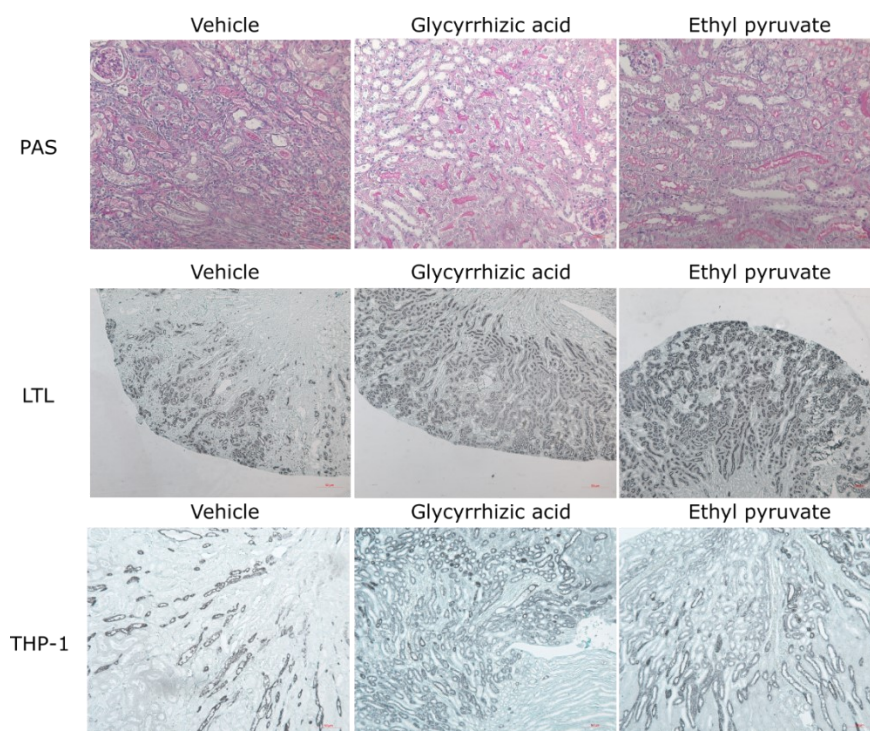


**Fig 44. Histology in CKD.** (A) Periodic acid-Schiff (PAS) was applied for the quantification of renal tubular damage. (B) Tamm-Horsfall protein (THP-1) staining represents distal tubules. (C) Lotus tetragonolobus lectin (LTL) staining represents the proximal tubules. (D) Sirius red was used for the collagen or fibrosis level of renal tissue. Images were shown at the magnification of 200x (LTL showed at magnification of 100x).

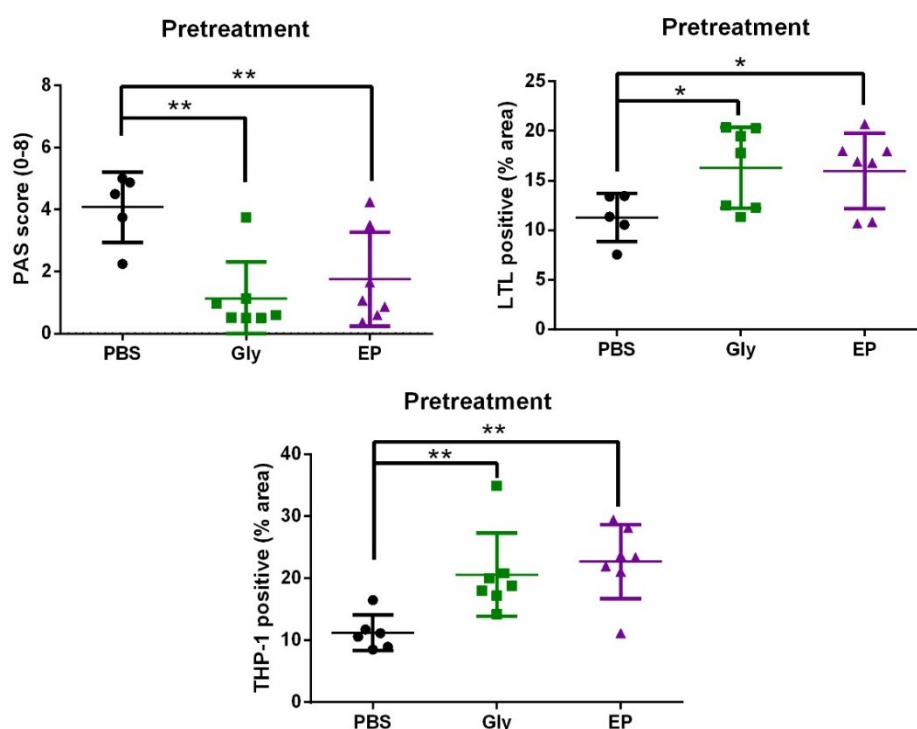


**Fig 45.** The quantification of histological staining at day 30 in postischemic kidneys. EP represents ethyl pyruvate, Gly represents glycyrrhizic acid, PBS as control group.

#### 4.3.3 Delayed treatment of HMGB1 inhibitors still contributes to tissue healing in the recovery phase after ischemia

Preemptive HMGB1 inhibitors attenuated tubular damage and prevented transition of AKI to CKD in ischemic kidneys. However, if HMGB1 inhibitors therapy started after the early injury phase of AKI still improves long-term outcome is elusive. To investigate if HMGB1 antagonists contribute to tissue healing in the recovery phase, we did 17 min unilateral-IRI with delayed treatment of HMGB1 inhibitors starting not before day 3 and continued up to day 17. The endpoints were GFR, delta kidney weight and tubular damage at day 30. Our data showed that delayed treatment of HMGB1 inhibitors still increased GFR at day 30 (Fig 46). Administration of delayed treatment had no effect on delta kidney weight (Fig 47). Delayed treatment with glycyrrhizic acid group showed less kidney damage, higher proportion of proximal tubules (marked by Lotus Tetragonolobus Lectin) and distal tubules (marked by Tamm-Horsfall protein) (Fig 48, 49). Delayed intervention of ethyl pyruvate reduced kidney damage, and showed higher proportion of distal tubules, but not proximal tubules (Fig 48, 49). This implied that delayed treatment of HMGB1 inhibitors may contribute to tubule healing in postischemic kidneys.

Together, HMGB1 antagonists may reduce extracellular HMGB1 release or compete with HMGB1 receptors, which decreased HMGB1-induced cell death. Targeting HMGB1 with inhibitors protected kidney injury and may contribute to tissue healing in postischemic kidney injury.

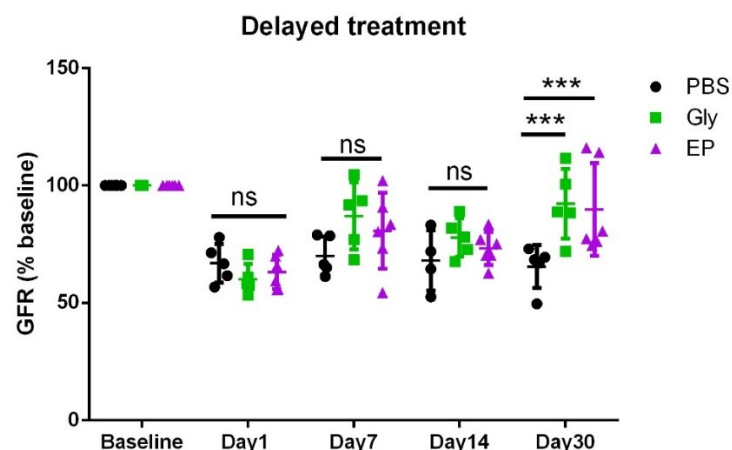


**Fig 46. Delayed treatment of HMGB1 antagonists protected from chronic kidney injury in postischemic kidneys.** The GFR level (from baseline) at the different time points in postischemic kidneys. GFR changes were shown from the baseline GFR. EP represents ethyl pyruvate, Gly represents glycyrrhizic acid, PBS as control group.

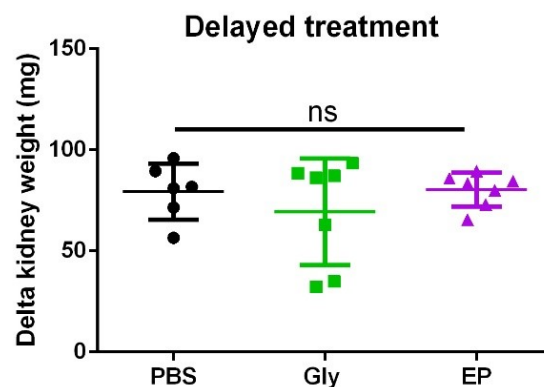


**Fig 47. Delta kidney weight at day 30 in postischemic kidney injury.** The delta kidney weight (contralateral kidney minus ischemic kidney weight) showed at day 30 in postischemic kidneys. EP represents ethyl pyruvate, Gly represents glycyrrhizic acid, PBS as control group.

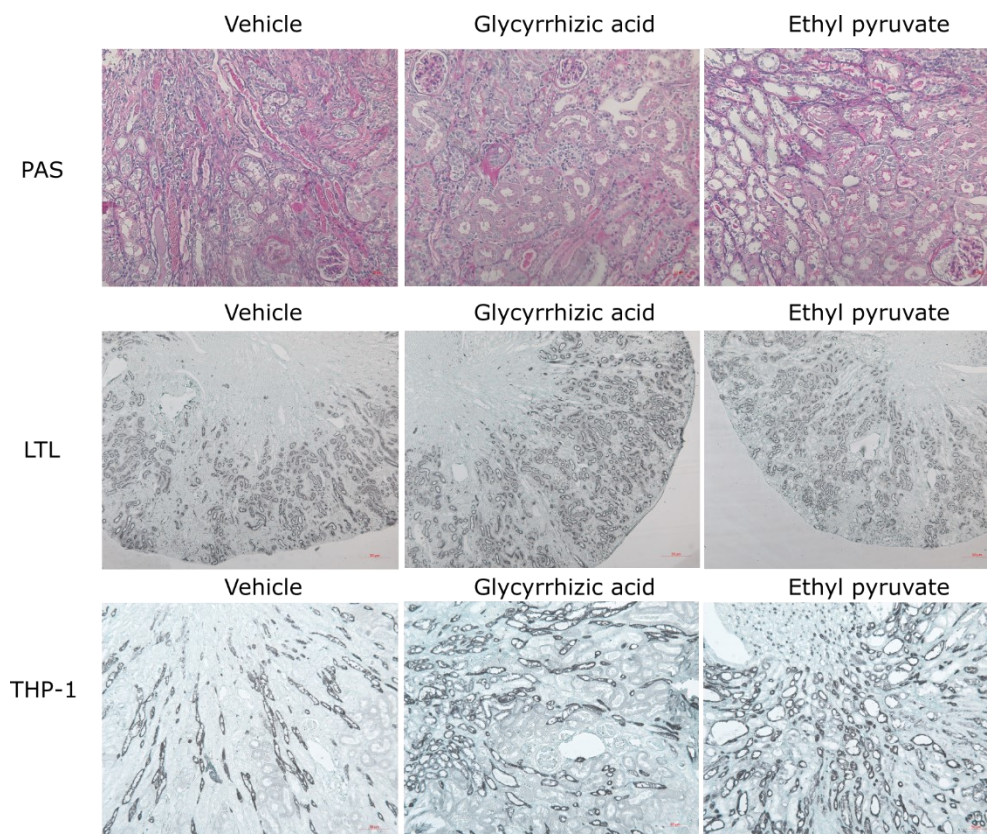


**Fig 48. Histology in CKD.** (A) Periodic acid-Schiff (PAS) was applied for the quantification of renal tubular damage. (B) Tamm-Horsfall protein (THP-1) staining represents distal tubules. (C) Lotus tetragonolobus lectin (LTL) staining represents the proximal tubules. (D) Sirius red was used for the collagen or fibrosis level of renal tissue. Images were shown at the magnification of 200x (LTL showed at magnification of 100x).

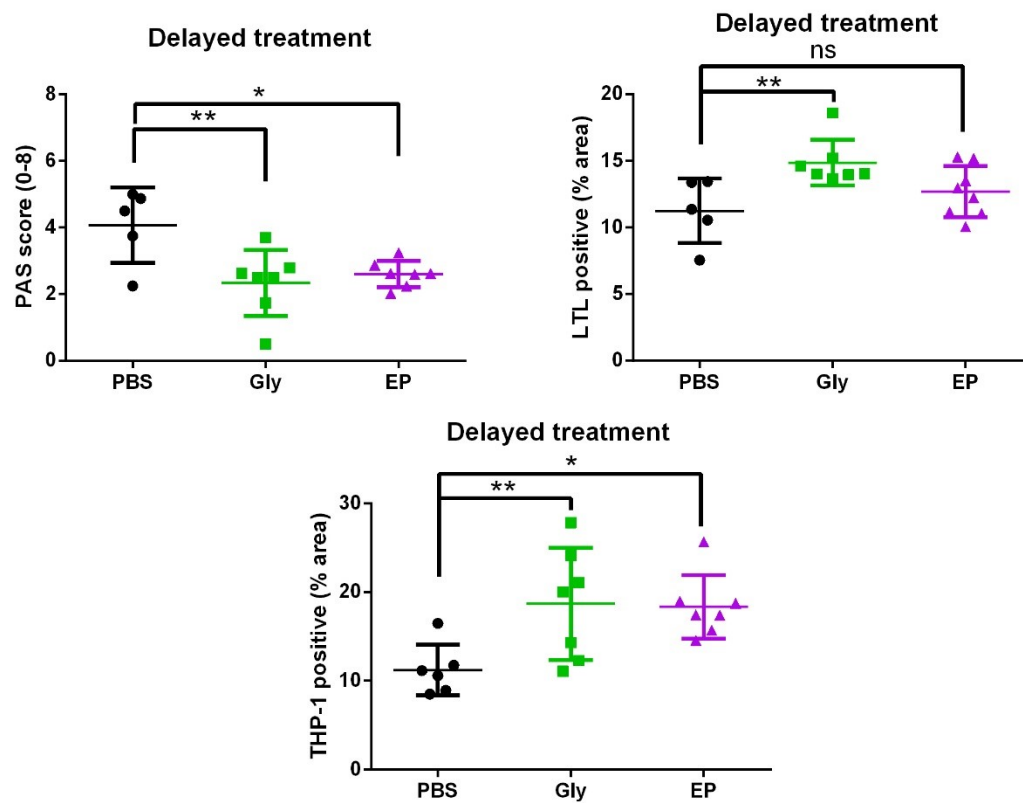


**Fig 49.** The quantification of histological staining at day 30 in postischemic kidneys. EP represents ethyl pyruvate, Gly represents glycyrrhizic acid, PBS as control group.



## 5 Discussion

### 5.1 Myeloid cell-derived HMGB1 attenuates kidney injury in renal IRI

HMGB1 is a known inflammatory mediator that contributes to leukocyte infiltration and tissue injury in inflammatory diseases. Therefore, we had hypothesized that myeloid cell-derived HMGB1 deficiency would ameliorate kidney injury by reducing infiltration of immune cells in postischemic kidneys. However, the finding of the present study is that endogenous HMGB1 in myeloid cells rather attenuates AKI in postischemic kidneys. Myeloid cell-derived HMGB1 deficiency decreased the population of renal resident DCs but promoted the infiltration of monocyte-derived pro-inflammatory macrophages, which resulted in more kidney damage in postischemic kidneys.

Previous data showed that conditional knockout of HMGB1 in myeloid cells renders them more sensitive to infection due to the release of nucleosomes and inhibition of autophagy and mitochondrial damage, leading to increased cell death [137]. HMGB1 binds to DNA similar to histone to maintain the nucleus homeostasis and functions, including DNA bending and regulating gene transcription. Cytosolic HMGB1 binds to beclin1 and ATG5 to protect from autophagy and to inhibit apoptosis in inflammatory bowel disease [147]. Inhibition of HMGB1 translocation to the cytoplasm by specific inhibitors decreases autophagy but increases apoptosis. Thus, the biological function of HMGB1 participates in sustaining autophagy to promote cell survival in response to cellular stress. The present study showed that myeloid cell-derived HMGB1 deficiency promoted resident DC death under ischemic conditions. Increased DC death triggered greater infiltration of pro-inflammatory immune cells, which amplified cellular damage and AKI. The aggravated cell death may be associated with the nuclear catastrophe and inhibition of autophagy in myeloid cell-derived HMGB1 deficiency cells.

Myeloid cell-derived endogenous HMGB1 determined the phenotype of infiltrated DCs, which was observed in the reperfusion phase. HMGB1 as an immune-stimulator induces DC maturation [128, 131], which facilitates infiltrated DC migration to lymph nodes and enhances the function of specific T cells [148]. HMGB1 triggers the infiltration of monocyte-derived immature DCs and the phenotypes changing of DCs responsiveness to the inflammatory response. The DC phenotype changing was associated with upregulation of DCs surface markers [130]. The deletion of

endogenous HMGB1 may decrease DC maturation and reduce the infiltration of peripheral DCs responsiveness to an innate immune response with less DCs surface markers expression in renal IRI. The present study showed that aggravated kidney injury enhanced the migration of monocytes-derived macrophages but not the peripheral infiltrated DCs, due to lack of endogenous HMGB1 in myeloid cells. The less migration of infiltrated DCs was compensated with T lymphocytes in renal IRI. Data showed that neutralization or blockade of HMGB1 decreased the pancreatic lymph nodes CD11c+CD11b+ DCs, but significantly increased pancreatic lymph nodes CD8+ T cells and higher proportion of CD8+IFN- $\gamma$ + (Th1) cells [149]. HMGB1 as an inflammatory mediator contributes to the migration of leukocytes and lymphocytes to the injured kidney. Ablation of myeloid cell-derived HMGB1 facilitates the migration of DCs and CD8+ T cells in ischemic kidneys.

In the present study, HMGB1 deficiency in myeloid cells resulted in the irreversible phenotype of CKD in postischemic kidneys, which was correlated with acute tubular damage and infiltration of immune cells in the early injury phase. Moreover, HMGB1-induced immigration of peripheral DCs also contributed to tissue healing and regeneration. HMGB1 contributes to kidney regeneration and healing in the late recovery phase. For example, HMGB1 accelerates tissue repair by homing endothelial stem cells, resident progenitor cells, and infiltrating immune cells [84, 150]. Also, post-translational modified HMGB1 released from necrotic cells promote infiltration of immune cells by forming the heterocomplex with CXCL12, which participates in tissue regeneration [89]. In addition, HMGB1 accelerates tissue regeneration via CXCR4 by increasing immune cell cycling and targeting exogenous stem cell migration to injured tissue [84, 151]. Infiltrating monocyte-derived macrophages and circulating DCs entering the injured tissue participate in tissue regeneration. Myeloid cell-derived HMGB1 deficiency reduces the maturation and migration of monocyte-derived DCs, resulting in the delay of kidney injury healing. In tissue disease model, extracellular HMGB1 activated the RAGE signaling pathway to promote the proliferation and expansion of progenitor cells in chronic liver disease [152, 153]. Myeloid cell-derived HMGB1 ablation decreased the infiltration of monocyte-derived DCs and less release of extracellular HMGB1, which may delay the homing of infiltrated stem cells and prevent the extension of resident progenitor cells in CKD.

## 5.2 Tubular cell-derived HMGB1 contributes to kidney injury

Extracellular HMGB1 released from necrotic tissue cells as a danger signal participates in cellular damage and triggers the inflammatory response, which contributes to amplified kidney injury under ischemia [143]. It was hypothesized that HMGB1 in tubular cells would contribute to kidney injury. Indeed, ablation of HMGB1 in Pax8-positive tubular cells ameliorated tubular damage in postischemic kidneys. In my study, ablation of endogenous HMGB1 in Pax8-positive tubular cells ameliorated H<sub>2</sub>O<sub>2</sub>-induced tubular cell death *in vitro*. Deletion of HMGB1 in tubular cells protected against kidney injury in postischemic kidneys also *in vivo*. Ablation of HMGB1 in tissue resident cells reduces the release of HMGB1 to extracellular space, which contributes to tubular damage and promotes the infiltration of immune cell-amplified kidney injury. In addition, previous data showed that knockout of nuclear HMGB1 modulates the elevated gene expression associated with hepatocyte glycolysis and lipid metabolic as well as downregulated gene response to hypoxia [94]. Thus, conditional HMGB1 knockout in Pax8-positive tubular cells may increase glucose production also in tubular epithelial cells of the kidney, which may contribute to cell viability under renal IRI.

However, the present study showed that HMGB1 from renal tubular cells does not contribute to AKI in the early injury phase but prevents the progression of AKI to CKD in postischemic kidneys.

The findings of the present study have the following implications:

First, previous studies reported that ablation of nuclear HMGB1 in the pancreas and liver promoted additional cellular damage due to the nuclear catastrophe in tissue injury [116, 154]. It can be assumed that deletion of intracellular HMGB1 in tissue cells aggravated cellular damage with nuclear DNA damage and reduced the release of extracellular HMGB1, which participated in the inflammatory response and tissue necrotic cell death [73]. The less inflammatory response balances HMGB1 deficiency-induced nuclear catastrophe. Thus, deletion of endogenous HMGB1 in tubular cells has no significant effect on the acute renal tubular damage and phenotypes of kidney injury.

Second, endogenous HMGB1 binds to beclin1, which promotes autophagic flux to protect from cellular damage under stress. Ablation of endogenous HMGB1 dissociates the binding to beclin1 and contributes to the binding of beclin1/Bcl2 junction,



which promotes apoptotic cell death but not tubular necrosis [147]. The retention of HMGB1 by apoptotic cells prohibits necrotic cell death by preventing HMGB1-induced inflammatory response. Therefore, released HMGB1 from necrotic cells may as a late mediator promotes inflammatory response [123].

Third, conditional transgenic Pax8-HMGB1 knockout mice are inducible to delete HMGB1 in Pax8-positive tubular epithelial cells. Pax8-HMGB1 knockout relies on the time of doxycycline induction. Therefore, the inducible Pax8-HMGB1 knockout mice model did not affect the development of embryonic renal Pax8-positive tubular cells. While released HMGB1 from necrotic cells as a late mediator contributes to tissue injury. Ablation of intracellular HMGB1 in tubular tissue cells protects against inflammatory-induced CKD in postischemic kidneys.

Thus, endogenous HMGB1 in tissue cells may be serve as a late mediator, which contributes to necrotic cell death. Deletion of intracellular HMGB1 prevents the recruitment of pro-inflammatory immune cells and necrotic cell death in the late injury phase, which may protect against CKD and support kidney healing in the late recovery phase.

### **5.3 Targeting HMGB1 as a danger signal protects against tissue injury**

Endogenous HMGB1 as a nuclear protein maintains the nucleosome structure and gene transcription [70]. Extracellular HMGB1 acts as a DAMP, which triggers the migration of immune cells and induces inflammation in sepsis, rheumatoid arthritis [82]. Released HMGB1 regards as a therapeutic object for agents to protect from kidney injury in renal IRI. Neutralization of extracellular HMGB1 by inhibiting HMGB1 shuttling from the nucleus to the cytoplasm, or agents interacting with receptors as competitive antagonists of HMGB1, that ameliorates HMGB1-induced inflammatory response and tissue injury.

It was reported that neutralization of HMGB1 with a neutralizing antibody either before or soon after ischemia-reperfusion protected from kidney injury [73, 80]. In addition, the study reported that the HMGB1 antagonists used also prevented extracellular HMGB1 release and pro-inflammatory response [99]. For example, glycyrrhizin inhibits the release of HMGB1 and impedes the interaction of HMGB1 with its receptors, especially the HMGB1-RAGE axis, which deactivates the inflammatory response and reduces the cytokines and chemokines released from damaged tissue

cells and immune cells [155, 156]. Glycyrrhizic acid attenuates HMGB1-induced tubular epithelial cell death and protects against kidney IRI [157]. In addition, ethyl pyruvate, a stable and simple lipophilic ester, can inhibit HMGB1 translocation from nucleus to cytoplasm under cellular stress [158]. Ethyl pyruvate attenuates HMGB1 secretion and reduces inflammatory response by targeting the HMGB1-RAGE signaling pathway [158-161]. In my study, glycyrrhizic acid and ethyl pyruvate as antagonists of HMGB1 ameliorated H<sub>2</sub>O<sub>2</sub>-induced tubular cell death. HMGB1 inhibitors prevented ischemic-induced kidney injury and may contribute to tissue healing after ischemic injury. Besides, targeting extracellular HMGB1 with antagonists have no functional effect on the cellular homeostasis in physiological and pathological condition. Thus, targeting extracellular HMGB1 with specific antagonists have a promptly protective effect on AKI in postischemic kidneys.

### **5.4 HMGB1 location and function**

In my study, ablation of endogenous HMGB1 in myeloid cell-derived or renal tubular cells mediates diverse phenotypes effects under renal IRI. Myeloid HMGB1 deficiency promotes DC death and aggravates AKI during renal IRI. However, conditional HMGB1 ablation in tubular cells reduces tubular cell death and prevents against postischemic kidney injury. Therefore, here I illustrate the main factors that determine the function of HMGB1, which are the cellular locations and cell types. There are three different states of HMGB1: normal location in nucleus, shuttling from nucleus to the cytoplasm, extracellular space (Fig 50).

First, HMGB1 as a DNA chaperone is localized in nucleus to maintain the nucleosome dynamics and chromosomal stability. HMGB1 regulates DNA duplication, gene transcription, and the interaction with other proteins [70]. In addition, HMGB1 can bind to damaged DNA, like cisplatin-modified DNA, to participate in DNA repair and telomere maintenance [162]. Deleting intracellular HMGB1 exacerbates DNA damage, nuclear catastrophe, oxidative stress, and mitochondrial instability, leading to more cell death and tissue injury in the liver and pancreas [116, 117].

Second, post-translational modified HMGB1 under cellular stress transports modified HMGB1 from nucleus to the cytoplasm [124]. Cytosolic HMGB1 regulates the processing of autophagy. For example, modified HMGB1, shuttling from nucleus to the cytoplasm, binds to beclin1 and ATG5, which disconnects the beclin1-Bcl2 junction and prevents apoptosis cell death. Meanwhile, HMGB1 interacts with beclin1 and

ATG5, which prevents the calpain-induced cleavage of these proteins and maintains the processing of autophagy [147]. In addition, HMGB1 modulates the expression of heat shock protein- $\beta$ -1, which prevents apoptotic signaling pathways and promotes autophagy and mitophagy [163]. However, the deletion of intracellular HMGB1 disrupts the mitochondrial stability and autophagic response under oxidative stress [164-166].

Third, HMGB1 is released to extracellular space from necrotic cells and activated immune cells where it acts as a danger signal, which initiates inflammatory response and amplifies cell death in tissue injury [167]. Modified HMGB1 shuttling from nucleus to cytoplasm, even released to extracellular space by lysosome-mediated exocytosis upon tissue injury, which contributes to tissue injury and inflammatory response by interacting with its receptors TLRs and RAGE [168, 169]. Extracellular HMGB1 induces pro-inflammatory cytokines from activated immune cells and necrotic tissue cells, which mediates inflammatory response, resulting in amplified cell death [39]. Blockage or neutralization extracellular HMGB1 release prevents HMGB1-induced tissue injury [73, 80, 157].

Finally, HMGB1 from different cell types exerts diverse functions in the regulation of cellular stress. HMGB1 from myeloid cells plays as a homeostatic protein in nucleus, which induces the maturation of DCs or regulates the antigen presentation of DCs [128, 129]. Ablation of HMGB1 in myeloid cells developed more sensitivity to endotoxin shock, accompanied by massive macrophage cell death [137]. Also, HMGB1 participates in kidney regeneration, which mainly comes from infiltrated hemopoietic stem cells and renal resident DCs. Previous data showed that released HMGB1 from myeloid cells participate in tissue healing and progenitor cell proliferation by interacting with RAGE or CXCR4 receptors and contributes to the migration of circulating dendritic cells to damaged tissue [84, 85, 88]. My data showed that HMGB1 contributes to the stability of resident DCs under ischemia. Myeloid cell-derived HMGB1 deficiency induces more DC death under oxidative stress. The additional DC death contribute to infiltration of immune cells and amplified AKI under ischemia. On the other hand, HMGB1 released from renal resident necrotic cells triggers the migration of immune cells and amplifies kidney injury. Reduced extracellular HMGB1 production ameliorates the inflammatory response and cellular damage. Deletion of endogenous HMGB1 in renal resident tubular cells reduce HMGB1-induced regulated cell death, resulting in the protective effect on postischemic kidneys. Thus, the altered cellular

phenotypes caused by the cross of HMGB1 with different Cre strains indicate diverse disease phenotype changing in different strains.

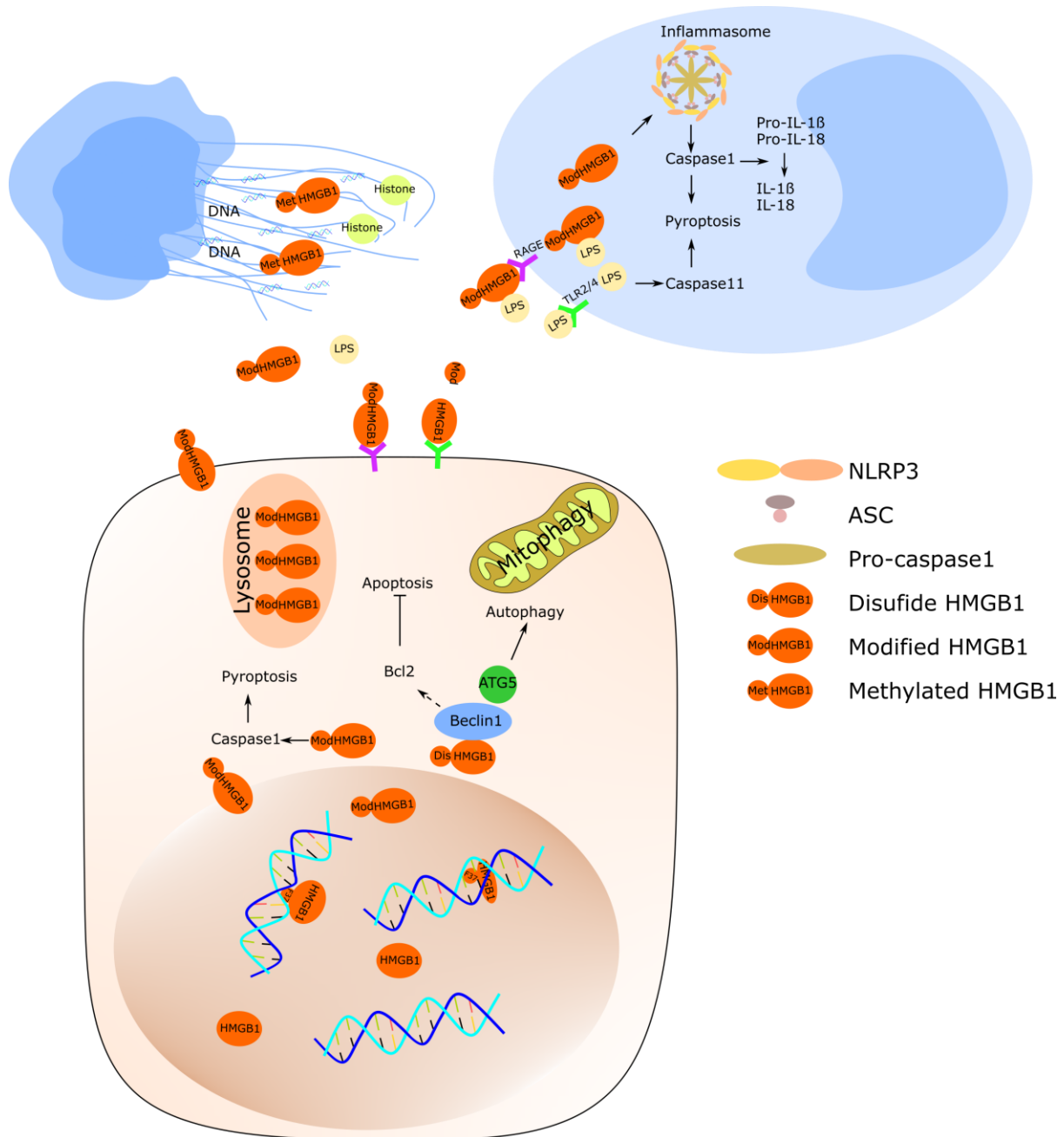


**Fig 50. Different locations of HMGB1 play diverse roles in physiological and pathological conditions.** In the nucleus, nuclear HMGB1 binds to linker DNA, to bend and kink DNA. HMGB1 can also bind to damaged DNA. Dissociation of HMGB1 from DNA exposes the binding region for transcriptional factors. In the cytoplasm, post-translational modified HMGB1 translocates from nucleus to the cytoplasm. Disulfide HMGB1 binds to beclin1, which promotes autophagic flux and inhibition of apoptosis. Modified HMGB1 can also modulate caspase1-induced pyroptosis. In the extracellular space, modified HMGB1 works as a danger signal of DAMPs, which participates in regulated necrotic cell death in tissue cells. From different cell types, HMGB1 participates in the formation of NETs in neutrophils. HMGB1 facilitates the delivery of LPS to the cytoplasm and contributes to the activation of inflammasome and pyroptosis in macrophages.

However, there are some limitations to the present study.

In the transgenic MLys-HMGB1 mice, HMGB1 depletion occurs at the beginning of life. This may affect myeloid cell development from their bone marrow progenitors. For instance, myeloid cell-derived HMGB1 deficiency may change the maturation or the expression of antigen-presentation under physiological and pathological conditions. While conditional knockout of HMGB1 in Pax8-positive tubular epithelial cells is an inducible transgenic mouse line. Induction of doxycycline at a specific time point induces the mutation of HMGB1 in Pax8-positive tubular cells.

Our animal model cannot mimic human diseases, especially the renal unilateral IRI model as AKI in humans usually affects both kidneys.

Here, I performed the unilateral version of the IRI model, but not bilateral-IRI or unilateral IRI with contralateral nephrectomy. During the ischemia and afterward reperfusion phase, the contralateral kidney undergoes functional changes to compensate for the blood flow after unilateral-IRI. While the ischemic kidney with aggravated cell death and kidney injury showed more renal fibrosis and reproducible CKD. However, unilateral-IRI makes it a more reliable model when investigating postischemic AKI-CKD transition [170]. Ischemic kidneys have less reperfusion due to kidney injury, while the contralateral kidneys functionally change and undergo hypertrophy.

Neutrophil infiltration occurs within 24 h after kidney ischemia. NET formation in the early injury phase contributes to AKI. While in the transgenic MLys-HMGB1 mice, there was no significant alteration of neutrophil infiltration in the early injury phase after ischemia between HMGB1 deficiency mice and wild type mice. However, I did not investigate this phenomenon in more detail. The phenotype may be associated with NET formation and NETosis of neutrophils in HMGB1 knockout mice. In the late injury phase, my data showed less infiltration of peripheral DCs with the compensation of CD4-CD8<sup>+</sup> T cells in ischemic kidneys. However, I did not investigate the T cell populations in regional lymph nodes, which may contribute to the recruitment of T cells.

Ablation of HMGB1 in Pax8-positive tubular cells ameliorate tubular cell death under ischemia. My data showed a better phenotype of kidney recovery in CKD but not AKI in HMGB1 knockout mice. However, the mechanism of how nuclear HMGB1

contributes to kidney injury in the early injury phase and the late injury phase remains elusive.

Pax8 is also expressed in some other tissue outside the kidney that may affect the results, but the type of AKI model is unlikely to be relevant.

In the intervention experiments, the HMGB1 antagonist glycyrrhizic acid ameliorated HMGB1 release to extracellular space with downregulating the plasma level of HMGB1 concentration. However, the agent of glycyrrhizic acid contributes to the translocation of HMGB1 from nucleus to extracellular space and also participates in the anti-inflammatory response during AKI. Glycyrrhizic acid not only serves as HMGB1 inhibitor but also participates in anti-inflammatory response, immune regulation, and other activities [171, 172]. Ethyl pyruvate inhibits HMGB1 translocation from nucleus to cytoplasm [158], and also regards as therapeutic agent for inflammatory diseases [173, 174].

*In vitro*, I isolated tubule segments, but the isolation process has a stressful injury to tubular segments, which may not be ignored. The following outgrowth of tubular segments spread to a monolayer of renal primary tubular cells. Then the outgrowth of primary tubular cells was used for the experiment.

In summary, ATN participates in the release of HMGB1 from tubular cells and activated immune cells, which promotes inflammatory response and kidney injury. However, the presented data shows that deletion of intracellular HMGB1 in myeloid cells has no benefit but exaggerates postischemic kidney injury. Myeloid cell-derived HMGB1 protects from ischemia-induced resident DC death. The aggravated cell death promotes infiltration of monocyte-derived macrophages, which further amplifies kidney injury. In addition, myeloid cell-derived HMGB1 modulates the phenotypes of infiltrating DCs and macrophages in the late recovery phase. HMGB1 deficiency in myeloid cells reduces the population of infiltrating DCs, which was compensated with CD4-CD8<sup>+</sup> T cells. The phenotype of resident DCs and infiltrating DCs regulated by myeloid cell-derived HMGB1 determine the outcome of CKD.

Tubular cell-derived HMGB1 works as another source of factor that participates in postischemic kidney injury. The data identify tubular cell-derived HMGB1 contributes to cellular damage and kidney injury. Ablation of HMGB1 in tubular cells ameliorates H<sub>2</sub>O<sub>2</sub>-induced cell death at a late time point. Tubular cell-derived HMGB1 modulates

the late phenotype of kidney injury and protects from the progression of AKI to CKD in postischemic kidneys.

Targeting extracellular HMGB1 with inhibitors reduces tubular cell death by decreasing the release of HMGB1 to extracellular space. Preemptive HMGB1 antagonists prevent postischemic AKI and the transition of AKI to CKD in postischemic kidneys. Delayed treatment of HMGB1 inhibitors still ameliorates CKD and may contribute to tissue healing in the recovery phase.

Therefore, the presented data confirm that extracellular HMGB1 acts as a danger signal contributing to ischemic kidney injury. It also implies the function of endogenous HMGB1 under pathological condition, which may depend on cell lineage and inducible knockout conditions.

## 6 References

1. Thomas, M.E., et al., *The definition of acute kidney injury and its use in practice*. Kidney international, 2015. **87**(1): p. 62-73.
2. Basile, D.P., M.D. Anderson, and T.A. Sutton, *Pathophysiology of acute kidney injury*. Comprehensive Physiology, 2011. **2**(2): p. 1303-1353.
3. Linkermann, A., et al., *Regulated cell death in AKI*. Journal of the American Society of Nephrology, 2014. **25**(12): p. 2689-2701.
4. de Boer, I.H., et al., *KDIGO 2020 Clinical Practice Guideline for Diabetes Management in Chronic Kidney Disease*. Kidney International, 2020. **98**(4): p. S1-S115.
5. Webster, A.C., et al., *Chronic kidney disease*. The lancet, 2017. **389**(10075): p. 1238-1252.
6. Linkermann, A., et al., *Two independent pathways of regulated necrosis mediate ischemia–reperfusion injury*. Proceedings of the National Academy of Sciences, 2013. **110**(29): p. 12024-12029.
7. Lau, A., et al., *RIPK3 - mediated necroptosis promotes donor kidney inflammatory injury and reduces allograft survival*. American Journal of Transplantation, 2013. **13**(11): p. 2805-2818.
8. Linkermann, A., et al., *The RIP1-kinase inhibitor necrostatin-1 prevents osmotic nephrosis and contrast-induced AKI in mice*. Journal of the American Society of Nephrology, 2013. **24**(10): p. 1545-1557.
9. Xu, Y., et al., *A role for tubular necroptosis in cisplatin-induced AKI*. Journal of the American Society of Nephrology, 2015. **26**(11): p. 2647-2658.
10. Orrenius, S., V. Gogvadze, and B. Zhivotovsky, *Mitochondrial oxidative stress: implications for cell death*. Annu. Rev. Pharmacol. Toxicol., 2007. **47**: p. 143-183.
11. Hosohata, K., *Role of oxidative stress in drug-induced kidney injury*. International journal of molecular sciences, 2016. **17**(11): p. 1826.
12. Vielhauer, V., et al. *Targeting the recruitment of monocytes and macrophages in renal disease*. in *Seminars in nephrology*. 2010. Elsevier.
13. Jang, H.R. and H. Rabb, *Immune cells in experimental acute kidney injury*. Nature Reviews Nephrology, 2015. **11**(2): p. 88.



14. Brodsky, S.V., et al., *Hyperglycemic switch from mitochondrial nitric oxide to superoxide production in endothelial cells*. American Journal of Physiology-Heart and Circulatory Physiology, 2002. **283**(5): p. H2130-H2139.
15. Zorov, D.B., M. Juhaszova, and S.J. Sollott, *Mitochondrial reactive oxygen species (ROS) and ROS-induced ROS release*. Physiological reviews, 2014. **94**(3): p. 909-950.
16. Ratliff, B.B., et al., *Oxidant mechanisms in renal injury and disease*. Antioxidants & redox signaling, 2016. **25**(3): p. 119-146.
17. Malek, M. and M. Nematbakhsh, *Renal ischemia/reperfusion injury; from pathophysiology to treatment*. Journal of renal injury prevention, 2015. **4**(2): p. 20.
18. Visarius, T.M., et al., *Pathways of glutathione metabolism and transport in isolated proximal tubular cells from rat kidney*. Biochemical pharmacology, 1996. **52**(2): p. 259-272.
19. Visarius, T.M., et al., *Pathways of glutathione metabolism and transport in isolated proximal tubular cells from rat kidney*. Biochem Pharmacol, 1996. **52**(2): p. 259-72.
20. Ratliff, B.B., et al., *Oxidant Mechanisms in Renal Injury and Disease*. Antioxid Redox Signal, 2016. **25**(3): p. 119-46.
21. Redza-Dutordoir, M. and D.A. Averill-Bates, *Activation of apoptosis signalling pathways by reactive oxygen species*. Biochimica et Biophysica Acta (BBA)-Molecular Cell Research, 2016. **1863**(12): p. 2977-2992.
22. Choi, K., et al., *Oxidative stress-induced necrotic cell death via mitochondria-dependent burst of reactive oxygen species*. Curr Neurovasc Res, 2009. **6**(4): p. 213-22.
23. Zhang, S., et al., *c-Jun N-terminal kinase mediates hydrogen peroxide-induced cell death via sustained poly (ADP-ribose) polymerase-1 activation*. Cell Death & Differentiation, 2007. **14**(5): p. 1001-1010.
24. Brodsky, S.V., et al., *Hyperglycemic switch from mitochondrial nitric oxide to superoxide production in endothelial cells*. Am J Physiol Heart Circ Physiol, 2002. **283**(5): p. H2130-9.
25. Anders, H.-J. and L. Schaefer, *Beyond tissue injury—damage-associated molecular patterns, Toll-like receptors, and inflammasomes also drive*

- regeneration and fibrosis*. Journal of the American Society of Nephrology, 2014. **25**(7): p. 1387-1400.
26. Mulay, S.R., et al. *How kidney cell death induces renal necroinflammation*. in *Seminars in nephrology*. 2016. Elsevier.
27. Allam, R., et al., *Histones from dying renal cells aggravate kidney injury via TLR2 and TLR4*. Journal of the American Society of Nephrology, 2012. **23**(8): p. 1375-1388.
28. Nakazawa, D., et al., *Histones and neutrophil extracellular traps enhance tubular necrosis and remote organ injury in ischemic AKI*. Journal of the American Society of Nephrology, 2017. **28**(6): p. 1753-1768.
29. Vanlangenakker, N., et al., *TNF-induced necroptosis in L929 cells is tightly regulated by multiple TNFR1 complex I and II members*. Cell death & disease, 2011. **2**(11): p. e230-e230.
30. Anders, H.-J., *Necroptosis in acute kidney injury*. Nephron, 2018. **139**: p. 342-348.
31. Kaczmarek, A., P. Vandenabeele, and D.V. Krysko, *Necroptosis: the release of damage-associated molecular patterns and its physiological relevance*. Immunity, 2013. **38**(2): p. 209-223.
32. Nakagawa, T., et al., *Cyclophilin D-dependent mitochondrial permeability transition regulates some necrotic but not apoptotic cell death*. Nature, 2005. **434**(7033): p. 652-658.
33. Choi, K., et al., *Oxidative stress-induced necrotic cell death via mitochondria-dependent burst of reactive oxygen species*. Current neurovascular research, 2009. **6**(4): p. 213-222.
34. Fritsch, M., et al., *Caspase-8 is the molecular switch for apoptosis, necroptosis and pyroptosis*. Nature, 2019. **575**(7784): p. 683-687.
35. Kezić, A., N. Stajic, and F. Thaiss, *Innate immune response in kidney ischemia/reperfusion injury: potential target for therapy*. Journal of immunology research, 2017. **2017**.
36. Kundert, F., et al., *Immune mechanisms in the different phases of acute tubular necrosis*. Kidney research and clinical practice, 2018. **37**(3): p. 185.
37. Schulz, C., et al., *A lineage of myeloid cells independent of Myb and hematopoietic stem cells*. Science, 2012. **336**(6077): p. 86-90.

38. Fogg, D.K., et al., *A clonogenic bone marrow progenitor specific for macrophages and dendritic cells*. Science, 2006. **311**(5757): p. 83-7.
39. Liu, K., et al., *In vivo analysis of dendritic cell development and homeostasis*. Science, 2009. **324**(5925): p. 392-7.
40. Kawakami, T., et al., *Resident renal mononuclear phagocytes comprise five discrete populations with distinct phenotypes and functions*. The Journal of Immunology, 2013. **191**(6): p. 3358-3372.
41. Soos, T.J., et al., *CX3CR1+ interstitial dendritic cells form a contiguous network throughout the entire kidney*. Kidney Int, 2006. **70**(3): p. 591-6.
42. Rogers, N.M., et al., *Dendritic cells and macrophages in the kidney: a spectrum of good and evil*. Nat Rev Nephrol, 2014. **10**(11): p. 625-43.
43. Lech, M., et al., *Macrophage phenotype controls long-term AKI outcomes—kidney regeneration versus atrophy*. Journal of the American Society of Nephrology, 2014. **25**(2): p. 292-304.
44. Kim, M.-G., et al., *Depletion of kidney CD11c+ F4/80+ cells impairs the recovery process in ischaemia/reperfusion-induced acute kidney injury*. Nephrology Dialysis Transplantation, 2010. **25**(9): p. 2908-2921.
45. Lin, S.-L., et al., *Macrophage Wnt7b is critical for kidney repair and regeneration*. Proceedings of the National Academy of Sciences, 2010. **107**(9): p. 4194-4199.
46. Kulkarni, O.P., et al., *Toll-like receptor 4–induced IL-22 accelerates kidney regeneration*. Journal of the American Society of Nephrology, 2014. **25**(5): p. 978-989.
47. Nakazawa, D., et al., *Extracellular traps in kidney disease*. Kidney international, 2018. **94**(6): p. 1087-1098.
48. Kinsey, G.R., L. Li, and M.D. Okusa, *Inflammation in acute kidney injury*. Nephron Experimental Nephrology, 2008. **109**(4): p. e102-e107.
49. Li, L., et al., *The chemokine receptors CCR2 and CX3CR1 mediate monocyte/macrophage trafficking in kidney ischemia–reperfusion injury*. Kidney international, 2008. **74**(12): p. 1526-1537.
50. Ricardo, S.D., H. van Goor, and A.A. Eddy, *Macrophage diversity in renal injury and repair*. J Clin Invest, 2008. **118**(11): p. 3522-30.
51. Lee, S., et al., *Distinct macrophage phenotypes contribute to kidney injury and repair*. Journal of the American Society of Nephrology, 2011. **22**(2): p. 317-326.

52. Deng, B., et al., *Plasmacytoid dendritic cells promote acute kidney injury by producing interferon- $\alpha$* . Cellular & molecular immunology, 2021. **18**(1): p. 219-229.
53. Burne, M.J., et al., *Identification of the CD4<sup>+</sup> T cell as a major pathogenic factor in ischemic acute renal failure*. The Journal of clinical investigation, 2001. **108**(9): p. 1283-1290.
54. Burne-Taney, M.J., N. Yokota-Ikeda, and H. Rabb, *Effects of combined T- and B-cell deficiency on murine ischemia reperfusion injury*. American Journal of Transplantation, 2005. **5**(6): p. 1186-1193.
55. Sallustio, F., et al., *Human renal stem/progenitor cells repair tubular epithelial cell injury through TLR2-driven inhibin-A and microvesicle-shuttled decorin*. Kidney International, 2013. **83**(3): p. 392-403.
56. Sallustio, F., et al., *TLR2 plays a role in the activation of human resident renal stem/progenitor cells*. The FASEB Journal, 2010. **24**(2): p. 514-525.
57. Zhao, M., et al., *Mitochondrial ROS promote mitochondrial dysfunction and inflammation in ischemic acute kidney injury by disrupting TFAM-mediated mtDNA maintenance*. Theranostics, 2021. **11**(4): p. 1845-1863.
58. Knight, S.F., et al., *Folate receptor-targeted antioxidant therapy ameliorates renal ischemia-reperfusion injury*. Journal of the American Society of Nephrology, 2012. **23**(5): p. 793-800.
59. Zhang, Q., et al., *Circulating mitochondrial DAMPs cause inflammatory responses to injury*. Nature, 2010. **464**(7285): p. 104-107.
60. Jang, H.R., et al., *The interaction between ischemia-reperfusion and immune responses in the kidney*. Journal of molecular medicine, 2009. **87**(9): p. 859-864.
61. Patel, N.S., et al., *Endogenous interleukin-6 enhances the renal injury, dysfunction, and inflammation caused by ischemia/reperfusion*. Journal of Pharmacology and Experimental Therapeutics, 2005. **312**(3): p. 1170-1178.
62. Donnahoo, K.K., et al., *Review article: the role of tumor necrosis factor in renal ischemia-reperfusion injury*. J Urol, 1999. **162**(1): p. 196-203.
63. Linas, S.L., et al., *Ischemia increases neutrophil retention and worsens acute renal failure: role of oxygen metabolites and ICAM 1*. Kidney Int, 1995. **48**(5): p. 1584-91.

64. Takada, M., et al., *The cytokine-adhesion molecule cascade in ischemia/reperfusion injury of the rat kidney. Inhibition by a soluble P-selectin ligand*. The Journal of clinical investigation, 1997. **99**(11): p. 2682-2690.
65. Andersson, U., H. Yang, and H. Harris, *Extracellular HMGB1 as a therapeutic target in inflammatory diseases*. Expert opinion on therapeutic targets, 2018. **22**(3): p. 263-277.
66. Rabadi, M.M., et al., *HMGB1 in renal ischemic injury*. American Journal of Physiology-Renal Physiology, 2012. **303**(6): p. F873-F885.
67. Sánchez-Giraldo, R., et al., *Two high-mobility group box domains act together to underwind and kink DNA*. Acta Crystallographica Section D: Biological Crystallography, 2015. **71**(7): p. 1423-1432.
68. Diener, K.R., et al., *The multifunctional alarmin HMGB1 with roles in the pathophysiology of sepsis and cancer*. Immunology and cell biology, 2013. **91**(7): p. 443-450.
69. Li, J., et al., *Structural basis for the proinflammatory cytokine activity of high mobility group box 1*. Mol Med, 2003. **9**(1-2): p. 37-45.
70. Štros, M., *HMGB proteins: interactions with DNA and chromatin*. Biochimica et Biophysica Acta (BBA)-Gene Regulatory Mechanisms, 2010. **1799**(1-2): p. 101-113.
71. Ge, Y., M. Huang, and Y.-m. Yao, *The Effect and Regulatory Mechanism of High Mobility Group Box-1 Protein on Immune Cells in Inflammatory Diseases*. Cells, 2021. **10**(5): p. 1044.
72. Ni, Y.A., et al., *HMGB1: An overview of its roles in the pathogenesis of liver disease*. Journal of Leukocyte Biology, 2021.
73. Wu, H., et al., *HMGB1 contributes to kidney ischemia reperfusion injury*. J Am Soc Nephrol, 2010. **21**(11): p. 1878-90.
74. Huang, H., et al., *Damage-associated molecular pattern-activated neutrophil extracellular trap exacerbates sterile inflammatory liver injury*. Hepatology, 2015. **62**(2): p. 600-614.
75. Tadie, J.-M., et al., *HMGB1 promotes neutrophil extracellular trap formation through interactions with Toll-like receptor 4*. American Journal of Physiology-Lung Cellular and Molecular Physiology, 2013. **304**(5): p. L342-L349.

76. Jia, C., et al., *Endothelial cell pyroptosis plays an important role in Kawasaki disease via HMGB1/RAGE/cathespins B signaling pathway and NLRP3 inflammasome activation*. Cell death & disease, 2019. **10**(10): p. 1-16.
77. Wang, Y., et al., *TNF- $\alpha$ /HMGB1 inflammation signalling pathway regulates pyroptosis during liver failure and acute kidney injury*. Cell Proliferation, 2020. **53**(6): p. e12829.
78. Andersson, U. and K. Tracey, *HMGB1, a pro-inflammatory cytokine of clinical interest: introduction*. Journal of internal medicine, 2004. **255**(3): p. 318-319.
79. Treutiger, C., et al., *High mobility group 1 B-box mediates activation of human endothelium*. Journal of internal medicine, 2003. **254**(4): p. 375-385.
80. Li, J., et al., *Neutralization of the extracellular HMGB1 released by ischaemic-damaged renal cells protects against renal ischaemia–reperfusion injury*. Nephrology Dialysis Transplantation, 2011. **26**(2): p. 469-478.
81. Kang, R., et al., *HMGB1 in health and disease*. Mol Aspects Med, 2014. **40**: p. 1-116.
82. Goldstein, R.S., et al., *Cholinergic anti-inflammatory pathway activity and High Mobility Group Box-1 (HMGB1) serum levels in patients with rheumatoid arthritis*. Molecular medicine, 2007. **13**(3): p. 210-215.
83. De Leo, F., et al., *Diflunisal targets the HMGB1/CXCL12 heterocomplex and blocks immune cell recruitment*. EMBO reports, 2019. **20**(10): p. e47788.
84. Tirone, M., et al., *High mobility group box 1 orchestrates tissue regeneration via CXCR4*. Journal of Experimental Medicine, 2018. **215**(1): p. 303-318.
85. Bianchi, M.E. and R. Mezzapelle, *The chemokine receptor CXCR4 in cell proliferation and tissue regeneration*. Frontiers in Immunology, 2020. **11**: p. 2109.
86. Hori, O., et al., *The receptor for advanced glycation end products (RAGE) is a cellular binding site for amphotericin: mediation of neurite outgrowth and co-expression of RAGE and amphotericin in the developing nervous system*. Journal of biological chemistry, 1995. **270**(43): p. 25752-25761.
87. Miyata, T., et al., *The receptor for advanced glycation end products (RAGE) is a central mediator of the interaction of AGE-beta2microglobulin with human mononuclear phagocytes via an oxidant-sensitive pathway. Implications for the pathogenesis of dialysis-related amyloidosis*. The Journal of clinical investigation, 1996. **98**(5): p. 1088-1094.

88. Palumbo, R., et al., *Extracellular HMGB1, a signal of tissue damage, induces mesoangioblast migration and proliferation*. J Cell Biol, 2004. **164**(3): p. 441-9.
89. Bianchi, M.E., et al., *High-mobility group box 1 protein orchestrates responses to tissue damage via inflammation, innate and adaptive immunity, and tissue repair*. Immunological reviews, 2017. **280**(1): p. 74-82.
90. Lange, S.S. and K.M. Vasquez, *HMGB1: The jack-of-all-trades protein is a master DNA repair mechanic*. Molecular Carcinogenesis: Published in cooperation with the University of Texas MD Anderson Cancer Center, 2009. **48**(7): p. 571-580.
91. Imamura, T., et al., *Interaction with p53 enhances binding of cisplatin-modified DNA by high mobility group 1 protein*. Journal of Biological Chemistry, 2001. **276**(10): p. 7534-7540.
92. Roemer, S.C., et al., *Mechanism of high-mobility group protein B enhancement of progesterone receptor sequence-specific DNA binding*. Nucleic Acids Res, 2008. **36**(11): p. 3655-66.
93. Zappavigna, V., et al., *HMG1 interacts with HOX proteins and enhances their DNA binding and transcriptional activation*. The EMBO Journal, 1996. **15**(18): p. 4981-4991.
94. Yu, P., et al., *Cardiomyocyte-restricted high-mobility group box 1 (HMGB1) deletion leads to small heart and glycolipid metabolic disorder through GR/PGC-1 $\alpha$  signalling*. Cell death discovery, 2020. **6**(1): p. 1-11.
95. Wang, H., et al., *HMG-1 as a late mediator of endotoxin lethality in mice*. Science, 1999. **285**(5425): p. 248-251.
96. Wei, S., et al., *SIRT1-mediated HMGB1 deacetylation suppresses sepsis-associated acute kidney injury*. American Journal of Physiology-Renal Physiology, 2019. **316**(1): p. F20-F31.
97. Zhang, C., et al., *High-mobility group box 1 inhibition alleviates lupus-like disease in BXSB mice*. Scandinavian journal of immunology, 2014. **79**(5): p. 333-337.
98. Wirestam, L., et al., *Antibodies against High Mobility Group Box protein-1 (HMGB1) versus other anti-nuclear antibody fine-specificities and disease activity in systemic lupus erythematosus*. Arthritis Res Ther, 2015. **17**(1): p. 338.

99. Musumeci, D., G.N. Roviello, and D. Montesarchio, *An overview on HMGB1 inhibitors as potential therapeutic agents in HMGB1-related pathologies*. Pharmacology & therapeutics, 2014. **141**(3): p. 347-357.
100. Bonventre, J.V. and L. Yang, *Cellular pathophysiology of ischemic acute kidney injury*. The Journal of clinical investigation, 2011. **121**(11): p. 4210-4221.
101. Sutton, T.A., *Alteration of microvascular permeability in acute kidney injury*. Microvasc Res, 2009. **77**(1): p. 4-7.
102. Verma, S.K. and B.A. Molitoris. *Renal endothelial injury and microvascular dysfunction in acute kidney injury*. in *Seminars in nephrology*. 2015. Elsevier.
103. Kikuchi, K., et al., *Minocycline attenuates both OGD-induced HMGB1 release and HMGB1-induced cell death in ischemic neuronal injury in PC12 cells*. Biochemical and biophysical research communications, 2009. **385**(2): p. 132-136.
104. Minsart, C., et al., *New insights in acetaminophen toxicity: HMGB1 contributes by itself to amplify hepatocyte necrosis in vitro through the TLR4-TRIF-RIPK3 axis*. Scientific reports, 2020. **10**(1): p. 1-15.
105. Yu, Y., D. Tang, and R. Kang, *Oxidative stress-mediated HMGB1 biology*. Front Physiol, 2015. **6**: p. 93.
106. Abdulmahdi, W., et al., *HMGB1 redox during sepsis*. Redox Biol, 2017. **13**: p. 600-607.
107. Mi, L., et al., *HMGB1/RAGE pro-inflammatory axis promotes vascular endothelial cell apoptosis in limb ischemia/reperfusion injury*. Biomed Pharmacother, 2019. **116**: p. 109005.
108. Fiuza, C., et al., *Inflammation-promoting activity of HMGB1 on human microvascular endothelial cells*. Blood, 2003. **101**(7): p. 2652-60.
109. He, M., et al., *The role of the receptor for advanced glycation end-products in lung fibrosis*. Am J Physiol Lung Cell Mol Physiol, 2007. **293**(6): p. L1427-36.
110. Tian, S., et al., *HMGB1 exacerbates renal tubulointerstitial fibrosis through facilitating M1 macrophage phenotype at the early stage of obstructive injury*. American Journal of Physiology-Renal Physiology, 2015. **308**(1): p. F69-F75.
111. Lynch, J., et al., *High-mobility group box protein 1: a novel mediator of inflammatory-induced renal epithelial-mesenchymal transition*. Am J Nephrol, 2010. **32**(6): p. 590-602.



112. Huebener, P., et al., *The HMGB1/RAGE axis triggers neutrophil-mediated injury amplification following necrosis*. The Journal of clinical investigation, 2019. **125**(2): p. 539-550.
113. Calogero, S., et al., *The lack of chromosomal protein Hmg1 does not disrupt cell growth but causes lethal hypoglycaemia in newborn mice*. Nature genetics, 1999. **22**(3): p. 276-280.
114. Cui, X.S., X.H. Shen, and N.H. Kim, *High mobility group box 1 (HMGB1) is implicated in preimplantation embryo development in the mouse*. Molecular Reproduction and Development: Incorporating Gamete Research, 2008. **75**(8): p. 1290-1299.
115. Huebener, P., et al., *High-mobility group box 1 is dispensable for autophagy, mitochondrial quality control, and organ function in vivo*. Cell metabolism, 2014. **19**(3): p. 539-547.
116. Kang, R., et al., *Intracellular Hmgb1 inhibits inflammatory nucleosome release and limits acute pancreatitis in mice*. Gastroenterology, 2014. **146**(4): p. 1097-1107. e8.
117. Huang, H., et al., *Hepatocyte -specific high -mobility group box 1 deletion worsens the injury in liver ischemia/reperfusion: a role for intracellular high -mobility group box 1 in cellular protection*. Hepatology, 2014. **59**(5): p. 1984-1997.
118. Zhao, G., et al., *Down-regulation of nuclear HMGB1 reduces ischemia-induced HMGB1 translocation and release and protects against liver ischemia-reperfusion injury*. Scientific reports, 2017. **7**(1): p. 1-11.
119. Kawamoto, H. and N. Minato, *Myeloid cells*. The international journal of biochemistry & cell biology, 2004. **36**(8): p. 1374-1379.
120. Nelson, P.J., et al., *The renal mononuclear phagocytic system*. Journal of the American Society of Nephrology, 2012. **23**(2): p. 194-203.
121. Hoste, E., et al., *Epithelial HMGB1 Delays Skin Wound Healing and Drives Tumor Initiation by Priming Neutrophils for NET Formation*. Cell Rep, 2019. **29**(9): p. 2689-2701 e4.
122. Wang, Y., et al., *Neutrophil extracellular trap -microparticle complexes trigger neutrophil recruitment via high -mobility group protein 1 (HMGB1) -toll -like receptors (TLR2)/TLR4 signalling*. British journal of pharmacology, 2019. **176**(17): p. 3350-3363.

123. Scaffidi, P., T. Misteli, and M.E. Bianchi, *Release of chromatin protein HMGB1 by necrotic cells triggers inflammation*. Nature, 2002. **418**(6894): p. 191-5.
124. Tang, Y., et al., *Regulation of Posttranslational Modifications of HMGB1 During Immune Responses*. Antioxid Redox Signal, 2016. **24**(12): p. 620-34.
125. Deng, M., et al., *The Endotoxin Delivery Protein HMGB1 Mediates Caspase-11-Dependent Lethality in Sepsis*. Immunity, 2018. **49**(4): p. 740-753 e7.
126. Zou, G.M. and Y.K. Tam, *Cytokines in the generation and maturation of dendritic cells: recent advances*. European cytokine network, 2002. **13**(2): p. 186-99.
127. Blander, J.M. and R. Medzhitov, *On regulation of phagosome maturation and antigen presentation*. Nature immunology, 2006. **7**(10): p. 1029-1035.
128. Rovere-Querini, P., et al., *HMGB1 is an endogenous immune adjuvant released by necrotic cells*. EMBO reports, 2004. **5**(8): p. 825-830.
129. Chen, X., et al., *Effects of mimicked acetylated HMGB1 on macrophages and dendritic cells*. Mol Med Rep, 2018. **18**(6): p. 5527-5535.
130. Yang, D., et al., *High mobility group box -1 protein induces the migration and activation of human dendritic cells and acts as an alarmin*. Journal of leukocyte biology, 2007. **81**(1): p. 59-66.
131. Messmer, D., et al., *High mobility group box protein 1: an endogenous signal for dendritic cell maturation and Th1 polarization*. J Immunol, 2004. **173**(1): p. 307-13.
132. Macconi, D., et al., *Proteasomal processing of albumin by renal dendritic cells generates antigenic peptides*. J Am Soc Nephrol, 2009. **20**(1): p. 123-30.
133. Dumitriu, I.E., et al., *Release of high mobility group box 1 by dendritic cells controls T cell activation via the receptor for advanced glycation end products*. J Immunol, 2005. **174**(12): p. 7506-15.
134. Jo, S.-K., et al., *Macrophages contribute to the initiation of ischaemic acute renal failure in rats*. Nephrology Dialysis Transplantation, 2006. **21**(5): p. 1231-1239.
135. Ko, G.J., et al., *Macrophages contribute to the development of renal fibrosis following ischaemia/reperfusion-induced acute kidney injury*. Nephrology Dialysis Transplantation, 2008. **23**(3): p. 842-852.
136. Rogers, N.M., et al., *Dendritic cells and macrophages in the kidney: a spectrum of good and evil*. Nature Reviews Nephrology, 2014. **10**(11): p. 625.

137. Yanai, H., et al., *Conditional ablation of HMGB1 in mice reveals its protective function against endotoxemia and bacterial infection*. Proceedings of the National Academy of Sciences, 2013. **110**(51): p. 20699-20704.
138. Deng, M., et al., *Location is the key to function: HMGB1 in sepsis and trauma - induced inflammation*. Journal of leukocyte biology, 2019. **106**(1): p. 161-169.
139. Cecchinato, V., et al., *Redox-Mediated Mechanisms Fuel Monocyte Responses to CXCL12/HMGB1 in Active Rheumatoid Arthritis*. Front Immunol, 2018. **9**: p. 2118.
140. Marschner, J.A., et al., *Optimizing mouse surgery with online rectal temperature monitoring and preoperative heat supply. Effects on post-ischemic acute kidney injury*. PLoS One, 2016. **11**(2): p. e0149489.
141. Scarfe, L., et al., *Transdermal Measurement of Glomerular Filtration Rate in Mice*. J Vis Exp, 2018(140): p. e58520.
142. Tonnus, W., et al., *Dysfunction of the key ferroptosis-surveilling systems hypersensitizes mice to tubular necrosis during acute kidney injury*. Nature Communications, 2021. **12**(1): p. 1-14.
143. Chen, Q., et al., *The role of high mobility group box 1 (HMGB1) in the pathogenesis of kidney diseases*. Acta Pharm Sin B, 2016. **6**(3): p. 183-8.
144. Kim, S.-W., et al., *Glycyrrhizic acid affords robust neuroprotection in the postischemic brain via anti-inflammatory effect by inhibiting HMGB1 phosphorylation and secretion*. Neurobiology of disease, 2012. **46**(1): p. 147-156.
145. Davé, S.H., et al., *Ethyl pyruvate decreases HMGB1 release and ameliorates murine colitis*. Journal of leukocyte biology, 2009. **86**(3): p. 633-643.
146. Van Noorden, C.J., *The history of Z-VAD-FMK, a tool for understanding the significance of caspase inhibition*. 2001, Elsevier.
147. Zhu, X., et al., *Cytosolic HMGB1 controls the cellular autophagy/apoptosis checkpoint during inflammation*. J Clin Invest, 2015. **125**(3): p. 1098-110.
148. Bianchi, M.E. and A.A. Manfredi, *High -mobility group box 1 (HMGB1) protein at the crossroads between innate and adaptive immunity*. Immunological reviews, 2007. **220**(1): p. 35-46.
149. Han, J., et al., *Extracellular high-mobility group box 1 acts as an innate immune mediator to enhance autoimmune progression and diabetes onset in NOD mice*. Diabetes, 2008. **57**(8): p. 2118-2127.

150. Chavakis, E., et al., *High-mobility group box 1 activates integrin-dependent homing of endothelial progenitor cells*. Circ Res, 2007. **100**(2): p. 204-12.
151. Lee, G., et al., *Fully reduced HMGB1 accelerates the regeneration of multiple tissues by transitioning stem cells to GAlert*. Proc Natl Acad Sci U S A, 2018. **115**(19): p. E4463-E4472.
152. Khambu, B., et al., *HMGB1 promotes ductular reaction and tumorigenesis in autophagy-deficient livers*. The Journal of clinical investigation, 2019. **128**(6): p. 2419-2435.
153. Hernandez, C., et al., *HMGB1 links chronic liver injury to progenitor responses and hepatocarcinogenesis*. The Journal of clinical investigation, 2019. **128**(6): p. 2436-2450.
154. Huang, H., et al., *Hepatocyte-specific high-mobility group box 1 deletion worsens the injury in liver ischemia/reperfusion: a role for intracellular high-mobility group box 1 in cellular protection*. Hepatology, 2014. **59**(5): p. 1984-1997.
155. Chen, D., et al., *Glycyrrhetic acid suppressed hmgb1 release by up-regulation of Sirt6 in nasal inflammation*. J Biol Regul Homeost Agents, 2017. **31**(2): p. 269-277.
156. Okuma, Y., et al., *Glycyrrhizin inhibits traumatic brain injury by reducing HMGB1–RAGE interaction*. Neuropharmacology, 2014. **85**: p. 18-26.
157. Lau, A., et al., *Glycyrrhizic acid ameliorates HMGB1-mediated cell death and inflammation after renal ischemia reperfusion injury*. Am J Nephrol, 2014. **40**(1): p. 84-95.
158. Shen, M., et al., *Ethyl pyruvate ameliorates hepatic ischemia-reperfusion injury by inhibiting intrinsic pathway of apoptosis and autophagy*. Mediators Inflamm, 2013. **2013**: p. 461536.
159. Zhao, J., et al., *Ethyl Pyruvate Attenuates CaCl<sub>2</sub>-Induced Tubular Epithelial Cell Injury by Inhibiting Autophagy and Inflammatory Responses*. Kidney Blood Press Res, 2018. **43**(5): p. 1585-1595.
160. Bhat, S.M., et al., *Ethyl pyruvate reduces organic dust-induced airway inflammation by targeting HMGB1-RAGE signaling*. Respir Res, 2019. **20**(1): p. 27.

161. Seo, M.S., et al., *Ethyl Pyruvate Directly Attenuates Active Secretion of HMGB1 in Proximal Tubular Cells via Induction of Heme Oxygenase-1*. J Clin Med, 2019. **8**(5): p. 629.
162. Ohndorf, U.M., et al., *Basis for recognition of cisplatin-modified DNA by high-mobility-group proteins*. Nature, 1999. **399**(6737): p. 708-12.
163. Livesey, K.M., et al., *Direct molecular interactions between HMGB1 and TP53 in colorectal cancer*. Autophagy, 2012. **8**(5): p. 846-848.
164. Tang, D., et al., *High-mobility group box 1 is essential for mitochondrial quality control*. Cell metabolism, 2011. **13**(6): p. 701-711.
165. Tang, D., et al., *High mobility group box 1 (HMGB1) activates an autophagic response to oxidative stress*. Antioxid Redox Signal, 2011. **15**(8): p. 2185-95.
166. Tang, D., et al., *Endogenous HMGB1 regulates autophagy*. Journal of Cell Biology, 2010. **190**(5): p. 881-892.
167. Andersson, U., D. Antoine, and K. Tracey, *Expression of Concern: The functions of HMGB 1 depend on molecular localization and post-translational modifications*. Journal of internal medicine, 2014. **276**(5): p. 420-424.
168. Bonaldi, T., et al., *Monocytic cells hyperacetylate chromatin protein HMGB1 to redirect it towards secretion*. EMBO J, 2003. **22**(20): p. 5551-60.
169. Gardella, S., et al., *The nuclear protein HMGB1 is secreted by monocytes via a non-classical, vesicle-mediated secretory pathway*. EMBO reports, 2002. **3**(10): p. 995-1001.
170. Fu, Y., et al., *Rodent models of AKI-CKD transition*. Am J Physiol Renal Physiol, 2018. **315**(4): p. F1098-F1106.
171. Chen, K., et al., *Advances in pharmacological activities and mechanisms of glycyrrhizic acid*. Current medicinal chemistry, 2020. **27**(36): p. 6219-6243.
172. Rehman, M.U., et al., *Preclinical Evidence for the Pharmacological Actions of Glycyrrhizic Acid: A Comprehensive Review*. Current drug metabolism, 2020. **21**(6): p. 436-465.
173. Jung, S.M., et al., *Ethyl pyruvate ameliorates inflammatory arthritis in mice*. International immunopharmacology, 2017. **52**: p. 333-341.
174. Yao, L., et al., *Ethyl pyruvate and analogs as potential treatments for acute pancreatitis: A review of in vitro and in vivo studies*. Pancreatology, 2019. **19**(2): p. 209-216.

## 7 Acknowledgement

I would like to delivery my gratitude to everyone who support me during my doctoral study.

Firstly, I would like to thank **my family, my mother, my father and my brother** to support and encourage me through my life and my doctoral study process.

I have the opportunity to study and work on my doctoral degree under the support of my tutor: **Prof. Hans-Joachim Anders**. He provide the guide, knowledge, and suggestion to proceed the final doctoral program. Thank you for giving me the opportunity to study and work as a team at Nephrological Centre, LMU hospital. I would also like to thank Dr. Volker Vielhauer, Dr. Bruno Luckow and Dr. Peter Nelson for their constructive advice during my doctoral study.

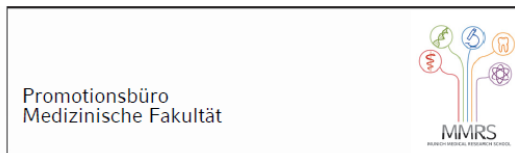
I thank my **lab members**, Julian, Taka, Chenyu, Steffi, Manga for their support to process the project. Especially to **Julian**, for sharing his skill and knowledge and **Taka**. We work as a team to complete the project. I would also thank Jana, Dan, Anna for the technical assistance to carry out the research work. I would also like to thank for other buddies, Lidia, Mohsen, Qiuyue, Yutian, ShiShi, Lina, Wenkai, Luying and all medical students for the lab memories. Thank you for my girlfriend, Dandan. Thank you for my friends Xing, Zhimin, Yazhou and others for the wonderful time.

Thanks for the China Scholarship Council to support my doctoral study for 48 months.

It is my duty to express my tearful acknowledgement to the animals, which have been sacrificed for the betterment of human being.

Date:

Signature: Zhibo Zhao



### Affidavit

Zhao Zhibo

Surname, first name

Munich

Street

Germany

Zip code, town, country

I hereby declare, that the submitted thesis entitled:

Differential roles of HMGB1 in myeloid cells versus tubular epithelial cells in the healthy or postischemic kidney

is my own work. I have only used the sources indicated and have not made unauthorized use of services of a third party. Where the work of others has been quoted or reproduced, the source is always given.

I further declare that the dissertation presented here has not been submitted in the same or similar form to any other institution for the purpose of obtaining an academic degree.

Munich, 14.07.2022  
place, date

Zhibo Zhao  
Signature doctoral candidate